UNIVERSIDADE FEDERAL DO RIO GRANDE

INSTITUTO DE CIÊNCIAS BIOLÓGICAS - ICB

PROGRAMA DE PÓS- GRADUAÇÃO EM CIÊNCIAS FISIOLÓGICAS

Estratégias para minimizar a toxicidade das saxitoxinas na linhagem hipocampal HT-22: Da modelagem *in silico* à bioensaios *in vitro*

MSc. Patrícia Baptista Ramos

Tese submetida ao Programa de Pós Graduação em Ciências Fisiológicas, como parte dos requisitos para a obtenção do título de DOUTOR em Ciências Fisiológicas

Orientador: Prof. Dr. José Maria Monserrat

Rio Grande

2017

"Aprender é a única coisa de que a mente nunca se cansa, nunca tem medo e nunca se arrepende"

(Leonardo da Vinci)

AGRADECIMENTOS

Meu especial agradecimento ao meu orientador, José Maria Monserrat, por ter me dado a oportunidade de estudar e trabalhar no que mais amo. Sempre pronto para contribuir com a construção do meu conhecimento. É uma imensa honra e orgulho tê-lo como orientador durante toda a minha formação acadêmica. Não esquecerei nunca dos teus ensinamentos, teus conselhos e tua inestimável confiança;

Aos meus pais, Rudimar e Margarida, que sempre me deram amor e apoio incondicional, sempre batalharam muito para me proporcionar o melhor;

Ao meu marido, Guilherme, meu companheiro de todas as horas, que SEMPRE esteve comigo, pela força, amor e por apostar em mim em todos os momentos;

À minha família, em especial minha irmã Carol, minha madrasta Claúdia, e não menos importante, minhas tias Jaqueline e Simone, e minha prima Laura, que sempre foram presente em todos os grandes momentos da minha vida, e sempre me acompanharam com muito carinho.

À família do meu marido, e em especial aos meus sogros, Rosângela e Jarbas, sempre muito presentes e preocupados com o nosso bem estar, sempre prontos a me ajudar em qualquer situação e sempre muito carinhosos comigo.

Às minhas amigas que a Biologia e vida me deram: Kati, Thais, Roberta, Cris, Dédi e Lili. Muito obrigada por estarem sempre do meu lado e muito presentes na minha vida;

À equipe diretiva da escola Silvério da Costa Novo, especialmente Márcia e Joel, que sempre compreenderam os motivos pelos quais eu precisei faltar na escola; A ajuda de vocês foi muito importante!

Às minhas colegas da pós-graduação, obrigada por sempre estarem dispostas a ajudar.

Às gurias da salinha 3, e ao chaveirinho da sala 2 Samuel, pela companhia e pela amizade. Ao longo dos últimos dois anos, foram meus fiéis companheiros de café, almoço, de conversas, de risadas diariamente;

À professora Ana Paula Votto, pela atenção e constante disponibilidade em discutir os resultados e contribuir para o desenvolvimento do meu trabalho;

À minha amiga e fiel companheira de laboratório Aline. Muito obrigada por toda a tua ajuda nos experimentos do segundo manuscrito;

Aos ICs Darling, Sibele e Josué. A ajuda de vocês foi muito importante, na construção desta tese;

Ao Marcos, IC e colega. Fostes de um coração sem igual. Sempre companheiro no laboratório me ajudando nas análises.

Ao professor João Sarkis, por proporcionar a continuidade do meu trabalho com cianotoxinas e por liberar o Marcos em muitos momentos que precisei;

À Inês, porteira do ICB, sempre muito carinhosa e preocupada comigo, além de minha companheira nos dias em que ficava até de madrugada na FURG.

À minha amiga Roberta Klein e ao Paulo, por me ajudarem na revisão do inglês do manuscrito, estruturação e formatação desta tese;

Ao programa de Pós graduação da Universidade Federal do Rio Grande;

Às agências de fomento CAPES e CNPq que viabilizaram a realização deste trabalho.

À todos, muito obrigada!!!!

SUMÁRIO

LISTA DE FIGURAS

LISTA DE TABELAS

LISTA DE ABREVIATURAS

AL: Ácido lipóico

ARE: Elemento de resposta antioxidante

ATP: Adenosina trifosfato

BHE: Barreira hemato encefálica

CAT: Catalase

Cys: Cisteína

CySS: Cístina

dc-STX: Dc-saxitoxina

DFT: Teoria funcional da densidade

DHLA: Ácido dihidrolipóico

DMSO: Dimetilsulfóxido

EAO: Espécies ativas de oxigênio

Eq.STX: Equivalentes de saxitoxina

FEB: Energia de ligação livre

GCL: Glutamato-cisteína-ligase

GPx: Glutationa peroxidade

GR: Glutationa redutase

GSSG: Glutationa oxidada

GSH: Glutationa reduzida

GST: Glutationa-S-transferase

GTX: Goniautoxinas

HOMO: Highest occupied molecular orbital (orbital molecular mais alto).

Keap1: Kelch-like ECH-associated protein 1

LPO: Lipoperoxidação lipídica

LUMO: Lowest unoccupied molecular orbital (orbital molecular mais baixo não ocupado)

MDR: Resistência a múltiplos fármacos

MO: Matéria orgânica

MWCNT: Nanotubos de parede múltipla

NBD: Domínio de ligação de nucleotídeos

Neo-STX : Neo-Saxitoxina

Nrf2: Nuclear factor (erythroid-derived 2)-like 2 (fator transcriptacional)

NTCs: Nanotubos de carbono

P-gp: Glicoproteína-P

PST: Toxina paralisante de molusco

Rho 123: Rodamina

SDA: Sistema de defesa antioxidante

SOD: Superóxido dismutase

STX_AL 1: Interação saxitoxina e acido lipóico (conformação 1)

STX_AL 2: Interação saxitoxina e acido lipóico (conformação 2)

STX_AL 3: Interação saxitoxina e acido lipóico (conformação 3)

STXs : Saxitoxinas

SWCNT: Nanotubos de parede simples

TMD: Domínio transmembranar

Trx: Tioredoxina reduzida

TrxSS: Tioredoxina oxidada

VP: Verapamil

RESUMO GERAL

Saxitoxinas (STXs) são neurotoxinas que toxicologicamente bloqueiam canais iônicos dependentes de voltagem em neurônios. Podem ser prejudiciais aos componentes celulares através da formação de espécies ativas de oxigênio (EAO) e diminuição das defesas antioxidantes, conduzindo a uma situação de estresse oxidativo. Os nanotubos de carbono (NTC) são nanoestruturas cilíndricas com grande razão comprimento/diâmetro. Podem apresentar funcionalização e são classificados como nanotubos de parede única (SWCNT) e nanotubos de parede múltipla (MWCNT). Possuem capacidade de adsorção com contaminantes ambientais, promovendo o efeito "Cavalo de Tróia". Frente a uma situação pró-oxidante, a utilização de antioxidantes não enzimáticos, como o ácido lipóico (AL), supõe-se importante para atenuar os efeitos deletérios induzidos por STXs. A presente tese tem como objetivo avaliar mecanismos envolvidos na redução dos efeitos tóxicos das STXs e suas interações físico-químicas e biológicas com NTCs e AL na linhagem hipocampal HT-22. Nesta perspectiva, foram utilizados simulações *ab initio* e docking molecular associadas a bioensaios *in vitro* de viabilidade celular e estresse oxidativo. Os resultados de *ab initio* demostraram que a interação de STXs tanto com SWCNTs quanto com AL ocorrem por fisisorção. A interação de STXs com SWCNTs mostraram um padrão claramente diferente nos ensaios *in vitro*, ora capaz de induzir efeito sinérgico ora capaz de induzir um efeito antagônico de STX e SWCNTs. O AL foi capaz de minimizar os efeitos citotóxicos induzidos pelas STXs. A atenuação dos efeitos tóxicos provocados pelas STXs pode estar relacionada com a presença da glicoproteína-P (P-gp) mostrados pela primeira vez, estarem presentes na linhagem hipocampal HT-22. De fato, ensaios *in vitro* e de docking molecular demonstraram claramente que as STXs atuam como um substrato para a

P-gp, induzindo sua atividade de extrusão na linhagem hipocampal HT-22, e o AL pode atuar como um modulador da P-gp estabelecendo respostas de quimioproteção a curto e longo prazo.

Palavras chave: nanotubos de carbono, ácido lipóico, Glicoproteína-P, estresse oxidativo, viabilidade celular, docking molecular

ABSTRACT

Saxitoxins (STXs) are neurotoxins that act blocking voltage-gated ion channels in neurons. STXs can also negatively affect the cellular components through the generation of reactive oxygen species (ROS) and by reducing antioxidant defenses, which can lead to a situation of oxidative stress. Carbon nanotubes (CNTs) are cylindrical nanostructures with great length/diameter ratio. It can present functionalization and are classified as single-walled carbon nanotubes (SWCNTs) and multiwalled carbon nanotubes (MWCNTs). Nanomaterials have adsorption capacity with environmental contaminants thus promoting the “Trojan horse effect”. In pro-oxidant situations, the use of non-enzymatic antioxidants, as lipoic acid (LA), is considered important to attenuate the deleterious effects induced by STXs. Taking these facts account, the objective of this thesis was to evaluate mechanisms involved in reducing the toxic effects of STXs and its biological and physical-chemical interaction with CNTs and LA using the hippocampal HT-22 cell line. In this regard, *ab initio* simulations and *molecular docking* associated with *in vitro* bioassays of cell viability and oxidative stress were used. The *ab initio* results demonstrated that the interaction of STXs with both SWCNTs and LA occurs by physisorption. The STXs interaction with SWCNTs presented a marked different pattern in the in vitro assays, sometimes capable of inducing a synergistic effect, sometimes capable of inducing an antagonistic effect of STX and SWCNTs. LA interaction was able to minimize the cytotoxic effects induced by STXs. Attenuation of the toxic effects caused by STXs may be related to the presence of the P-glycoprotein (P-gp), showed for the first time, are present in the HT-22 hippocampal cell line. In fact, the *in vitro* and *molecular docking* assays have clearly evidenced that STXs act as a substrate for P-gp, inducing its extrusion activity in the hippocampal HT-22 cell line,

and the LA can act as a modulator of P-gp by establishing short and long-term chemoprotective responses.

Kay words: Carbon nanotube, lipoic acid, oxidative stress, P-glycoprotein, cell viability, molecular docking

1. INTRODUÇÃO

1.1.Florações de cianobactérias e cianotoxinas

A formação de florações de cianobactérias está associada ao processo de eutrofização e poluição em ambientes aquáticos. São consideradas um perigo potencial ao ambiente, já que algumas espécies produzem toxinas que são prejudiciais aos organismos vivos, incluindo os seres humanos (GOLUBIC et al., 2010; WOOD, 2016). O aumento da frequência e da prevalência de florações de cianobactérias tornou-se um problema crescente no mundo e especialmente no Brasil (ZABAGLO et al., 2016), configurando um risco potencialmente grave à saúde pública e ambiental (PEARSON et al., 2016; TAKSER et al., 2016).

A proliferação maciça de cianobactérias ocorre em virtude da oferta excessiva de nutrientes (principalmente nitrogênio e fósforo) associado à condições ideais de pH, temperatura, turbulência e luz solar nos ambientes aquáticos, com consequente alterações na qualidade de água (cor, odor e sabor) e depleção do oxigênio dissolvido (GRATTAN; HOLOBAUGH; MORRIS, 2016; PEARSON et al., 2016; WANG et al., 2015).

As cianotoxinas, toxinas produzidas por cianobactérias, são liberadas pelo rompimento da célula bacteriana e constituem uma grande fonte de produtos naturais tóxicos, em geral, resistentes à degradação química e biológica (FERRÃO-FILHO; KOZLOWSKY-SUZUKI, 2011). Cianotoxinas são produtos do metabolismo secundário de cianobactérias, e sua síntese pode estar associada: (1) ao mecanismo de defesa, (2) a melhor captação da luz solar e/ou (3) a comunicação entre as cianobactérias (ARÁOZ; MOLGÓ; TANDEAU DE MARSAC, 2010; ETHERIDGE, 2010; WANG et al., 2016).

As cianotoxinas podem ser classificadas quanto ao seu mecanismo de ação em hepatoxinas (fígado), dermatotoxinas (pele), neurotoxinas (sistema nervoso), citotoxinas e lipopolissacarídeos (ARÁOZ; MOLGÓ; TANDEAU DE MARSAC, 2010; CORBEL; MOUGIN; BOUAÏCHA, 2014; ZHENG et al., 2015). De maneira geral, as cianotoxinas são consideradas potentes toxinas ambientais que podem ser bioacumuladas ao longo da cadeia trófica, causando graves injúrias nos organismos aquáticos e terrestres, além de intoxicação humana atribuída ao consumo oral de água e alimentos contaminados ou através de atividades recreacionais (WANG et al., 2016; WOOD, 2016). No Brasil destacam-se gêneros potencialmente nocivos, como *Microcystis*, *Anabaena*, *Cylindrospermopsis*, *Oscillatoria*, *Trichodesmium* (CORBEL; MOUGIN; BOUAÏCHA, 2014).

É comum a ocorrência de florações nocivas ao longo da costa brasileira encontradas em águas superficiais, as quais comumente são utilizadas para o abastecimento de água potável (CHATZIEFTHIMIOU et al., 2016). Por exemplo, a Reserva de Alagados (Paraná) é uma fonte importante para o abastecimento de água, recreação e pesca, e desde 2002 tem sido reportada a ocorrência de florações de cianobactérias produtoras de neurotoxinas (CLEMENTE et al., 2010). Infelizmente, no Brasil, o gerenciamento do risco de cianotoxinas emergentes em fontes de água está comprometido devido à insuficiência de dados experimentais. Além disso, atuais diretrizes de qualidade da água, que se concentram em toxinas individuais, não consideram os potenciais efeitos combinados ou sinérgicos de misturas de toxinas (TAKSER et al 2016).

1.2.Saxitoxinas

Dentre as neurotoxinas, as saxitoxinas (STXs) compreendem um grupo de alcalóides neurotóxicos de diferentes isoformas, popularmente identificadas como toxinas paralíticas dos bivalves marinhos (‘paralytic shellfish toxins’, PSTs) (CORBEL; MOUGIN; BOUAÏCHA, 2014; ETHERIDGE, 2010). Em ambientes marinhos são produzidas por cianobactérias do gênero *Cylindrospermopsis*, *Anabaena*, *Aphanizomenon* e *Planktothrix,* e por dinoflagelados responsáveis pela ocorrência de maré vermelha pertencentes ao gênero *Trichodesmium*, *Alexandrium*, e *Gymnodinium* (ARÁOZ; MOLGÓ; TANDEAU DE MARSAC, 2010; CORBEL; MOUGIN; BOUAÏCHA, 2014; ETHERIDGE, 2010).

As STXs constituem um grupo de mais de 57 análogos, que compartilham um esqueleto de 3,4,6-trialquil-tetra-hidropurina com dois grupos guadinina (O’NEILL; MUSGRAVE; HUMPAGE, 2016). As STXs possuem variação em relação à toxicidade de acordo com o resíduo da cadeia lateral (**Figura 1**). As toxinas mais potentes são pertencentes ao grupo carbamato toxinas, que incluem a saxitoxina (STX), Neo-saxitoxina (Neo-STX), goniautoxina (GTX) e dc-saxitoxina (dc-STX) (WIESE et al., 2010). As variações das cadeias laterais dão aos análogos diferentes níveis de toxicidade. A variante mais tóxica é a STX propriamente dita, assim a toxicidade das outras variantes pertencentes a esse grupo de toxinas é expressa em termos de “toxicidade relativa”, que se refere ao grau de toxicidade em relação à STX, que tem 1 como toxicidade relativa (**Tabela 1**).

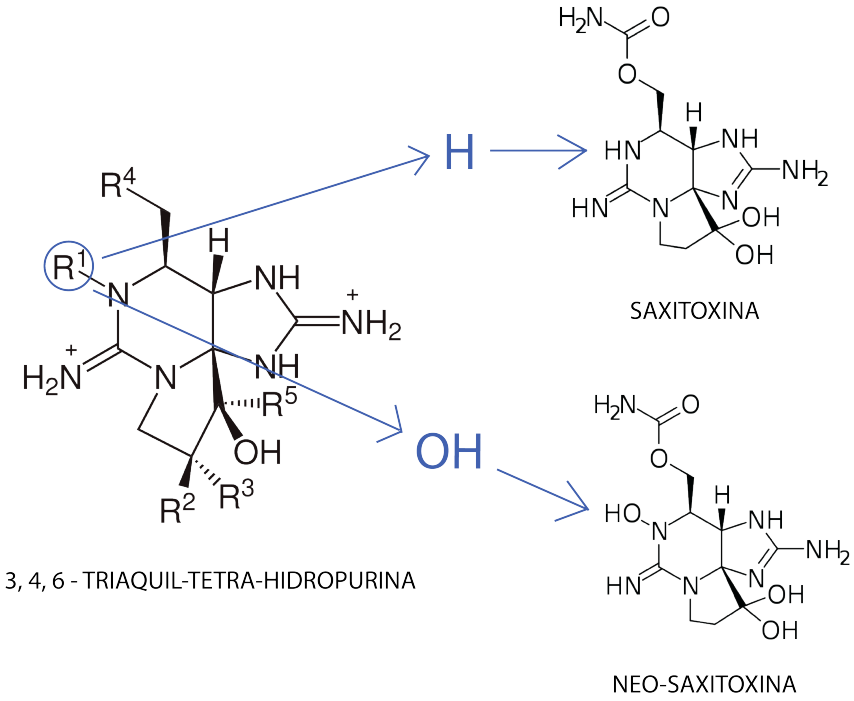

Figura 1: Estrutura química das saxitoxinas e os radicais que determinam suas possíveis variações. Alcalóides carbamatos não sulfatados: Saxitoxina e Neo-saxitoxina. Obtido de (ARÁOZ; MOLGÓ; TANDEAU DE MARSAC, 2010).

A toxicidade das PSTs é determinada através de métodos químicos e expressa como equivalente de saxitoxina (Eq.STX), que representa o somatório das concentrações de todas as variantes de STX (ETHERIDGE, 2010). Em decorrência de diversos eventos envolvendo STXs, o Ministério da Saúde por meio da portaria 2914/2011 tornou obrigatória a análise de STXs na água potável, com o limite máximo aceitável de 3,0 µg/L Eq.STX.

Tabela 1: Toxicidade relativa das Saxitoxinas: Saxitoxinas (STX); Neo-Saxitoxinas (Neo-STX); Goniautoxinas (GTX 1-4). (Adaptado de ETHERIDGE, 2010).

Carbamato toxinas	
Toxina	**Toxicidade relativa (Eq.STX)**
STX	1.00
NEO STX	0.99
GTX 1	0.92
GTX 2	0.73
GTX 3	0.64
GTX 4	0.36

As STXs são carbamatos que agem especificamente como bloqueador de canais de sódio dependentes de voltagem presentes nas membranas excitáveis dos neurônios, impedindo a liberação do neurotransmissor acetilcolina e a propagação da despolarização e transmissão do impulso nervoso, além de alterar a permeabilidade seletiva da membrana e consequentemente o fluxo iônico, causando danos à homeostasia celular (CORBEL; MOUGIN; BOUAÏCHA, 2014; O'NEILL; MUSGRAVE; HUMPAGE, 2016; ZHENG et al., 2015) conforme ilustrado na **Figura 2**.

No sistema nervoso central, as saxitoxinas apresentam especificidade aos canais de sódio voltagem-dependentes do tipo NaV1-9 (ONDRUS et al., 2012b). As STXs bloqueiam a transmissão do impulso nervoso por meio da ligação ao sítio 1 da sub-unidade α de receptores dos canais de sódio, impedindo assim a propagação da despolarização e transmissão do impulso nervoso, induzindo a paralisia neuromuscular e morte por parada respiratória (ARÁOZ; MOLGÓ; TANDEAU DE MARSAC, 2010). Além disso, as toxinas STXs podem ser bioacumuladas ao longo

da cadeia trófica que pode se estender desde zooplâncton até seres humanos, representando um risco para a saúde pública (ARAOZ; MOLGO; MARSAC, 2010; WANG et al., 2016). Mexilhões de água doce tendem acumular saxitoxinas quando alimentados com cianobactérias tóxicas (NICOLAS et al., 2015a; O'NEILL; MUSGRAVE; HUMPAGE, 2016)

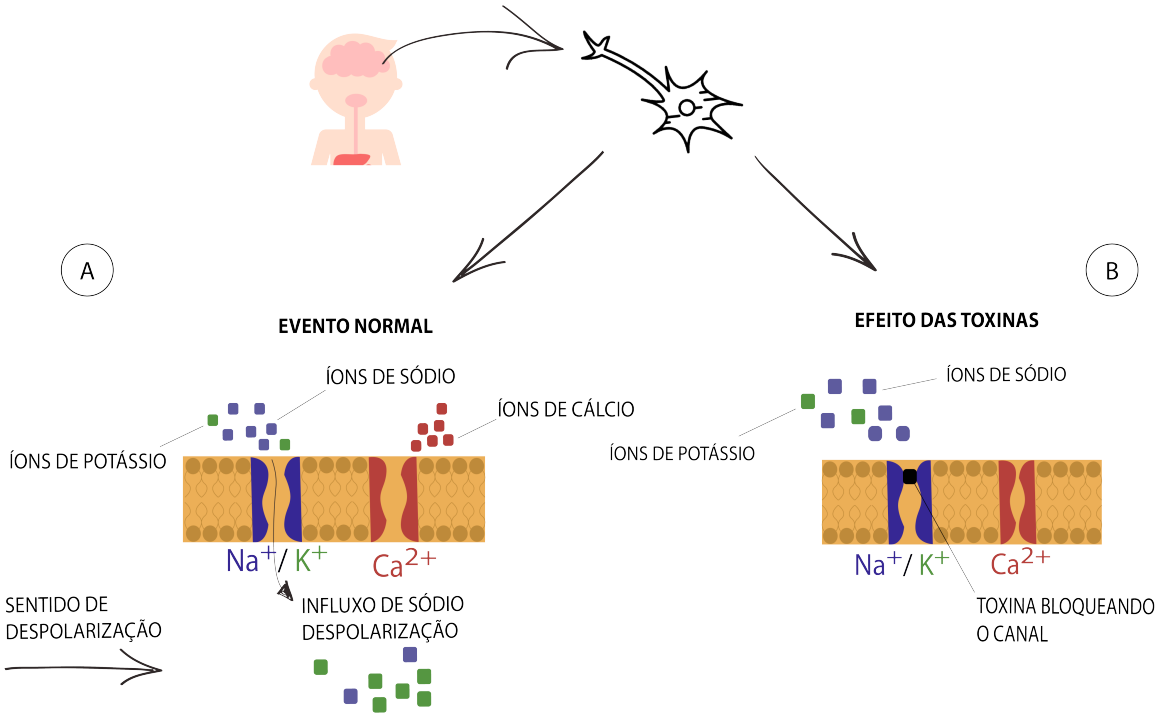

Figura 2: Mecanismo de ação das Saxitoxinas. A) representação esquemática do fluxo iônico durante o evento normal de propagação da despolarização e transmissão do impulso nervoso (canais de Na^+, K^+ e de Ca^+) B) representação esquemática do efeito das STXs, bloqueando os canais de sódio e potássio, durante a propagação da despolarização e transmissão do impulso nervoso

Trabalhos recentes demonstraram que STXs também podem se ligar aos canais de cálcio e potássio, interferindo na velocidade de abertura e fechamento desses canais, que por sua vez, podem levar à alteração do influxo destes íons para a célula (CORBEL; MOUGIN; BOUAÏCHA, 2014; NICOLAS et al., 2015a). Além

disso, a exposição a baixas doses de STXs pode induzir a apoptose e altas doses pode causar necrose no tecido cerebral do peixe-zebra (ZHANG et al., 2013). O consumo oral e prolongado de STXs foi capaz de alterar padrões comportamentais de memória e aprendizagem em *Rattus norvegicus*. (DIEHL et al., 2016). Além disso, evidências indicam que o estresse oxidativo tem papel significativo na toxicidade das STXs (MELEGARI et al., 2012; NICOLAS et al., 2015b; RAMOS et al., 2014; SILVA et al., 2014), aspecto que é tratado na próxima seção.

1.3. Estresse oxidativo e Saxitoxinas

Durante o metabolismo aeróbico normal são produzidas espécies ativas de oxigênio (EAO), devido ao escape de elétrons da cadeira respiratória mitocondrial durante a redução do oxigênio no processo de fosforilação oxidativa e por outros processos bioquímicos como a resposta imune, que geram também o radical ânion superóxido ($O_2^{\bullet-}$) (HANSEN; GO; JONES, 2006; HELLOU; ROSS; MOON, 2012a; PAMPLONA; COSTANTINI, 2011a). Outros intermediários reativos são o peróxido de hidrogênio (H_2O_2) e o mais reativo, o radical hidroxila ($^{\bullet}OH$), que quando em elevadas concentrações são capazes de danificar a maioria dos componentes celulares, e disparar sistemas de sinalização celular que ativam vias intrínsecas de apoptose (JONES, 2006; PAMPLONA; COSTANTINI, 2011b). Quando a produção de EAO ultrapassa a capacidade de proteção fornecida pelo sistema de defesa antioxidante (SDA) é estabelecido uma condição de estresse oxidativo, entendido como um desequilíbrio entre pró-oxidantes e antioxidantes em favor do primeiro, que pode afetar processos de sinalização redox (JONES, 2006; PAMPLONA; COSTANTINI, 2011b) como pode ser observado na **Figura 3**.

Os principais efeitos tóxicos das STXs são encontrados no cérebro, já que elas são capazes de atravessar a barreira hemato-encefálica (BHE), pois já foi reportada a acumulação de STX no sistema nervoso central. No entanto o mecanismo de transporte das STXs na BHE ainda permanece desconhecido (CERVANTES CIANCA et al., 2011; D'MELLO et al., 2017). De fato, a exposição às STXs pode causar tanto uma produção excessiva de espécies ativas de oxigênio (EAO) como também alterar os níveis de antioxidantes, afetando processos de sinalização celular e causando danos em macromoléculas, processo gerado por vários tipos de cianotoxinas, incluindo as STXs (**Figura 3**) (COSTA et al., 2012; D'MELLO et al., 2017; DA SILVA et al., 2011; ESTRADA et al., 2007; MELEGARI et al., 2012; RAMOS et al., 2014; SILVA et al., 2014).

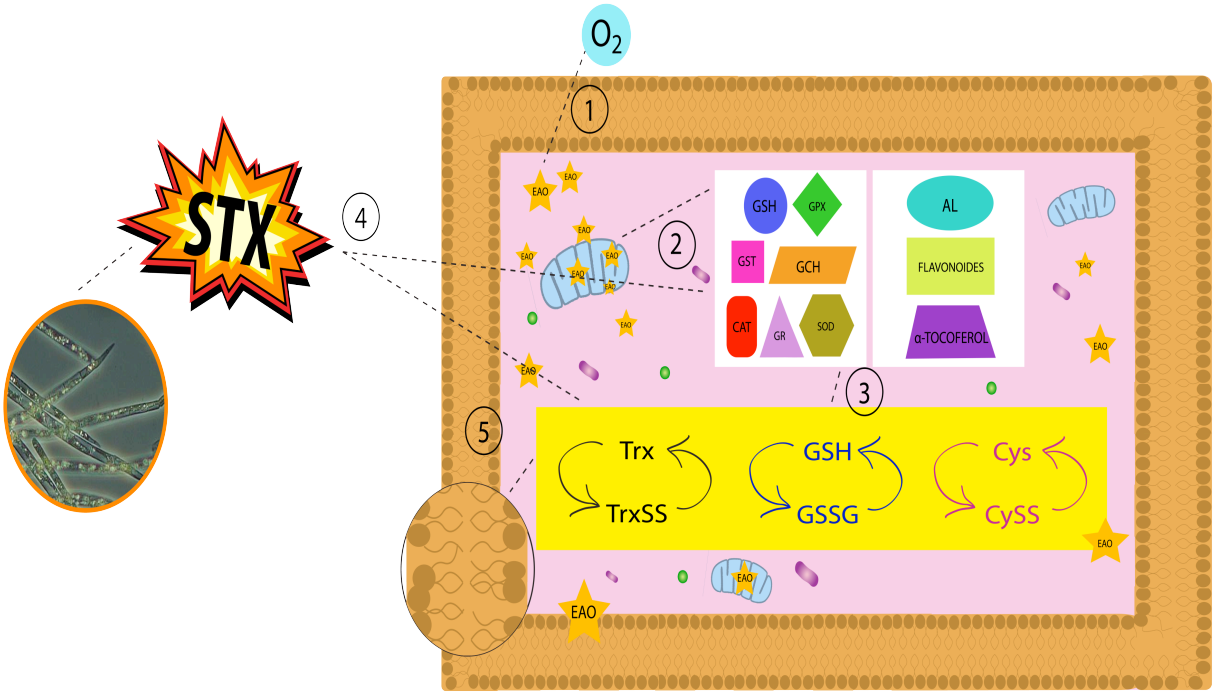

Figura 3: Geração de estresse oxidativo como um dos mecanismos da toxicidade das saxitoxinas.1) Metabolismo aeróbico normal produz EAO; 2) Sistema de Defesa antioxidante (SDA) constituído por antioxidantes enzimáticos e não enzimáticos têm

a função de interceptar, atenuar e reparar as EAO; 3) A produção excessiva de EAO pode também alterar a sinalização de pares redox, tais como: Tioredoxina reduzida (Trx) e Tioredoxina oxidada (TrxSS); Glutationa reduzida (GSH) e Glutationa oxidada (GSSG); Cisteína (Cys) e Cistina (cySS); 4) STXs induz a produção excessiva de EAO, capaz de alterar o SDA afetando processos de sinalização celular e 5) causando danos em macromoléculas, como lipídios presentes nas membranas celulares.

Vários trabalhos reportam indução de estresse oxidativo por STXs. Por exemplo, no trabalho de Silva et al. (2011) foi constatado que as STXs podem ser bioacumuladas ao longo da cadeia trófica, provocando uma diminuição da atividade das enzimas antioxidantes superóxido dismutase (SOD), glutationa-S-transferase (GST) e glutationa peroxidase (GPx), gerando estresse oxidativo no cérebro do peixe *Hoplias malabaricus*. No trabalho de Melegari et al. (2012) foi evidenciado que as STXs induzem estresse oxidativo através da lipoperoxidação lipídica (LPO) e diminuem a atividade de algumas enzimas antioxidantes na linhagem celular Neuro-2A.

De Assis et al. (2013) demonstraram aumento da produção de EAO e dos níveis de LPO e glutationa reduzida (GSH) associado à maior atividade de GPx e menor atividade da SOD no sangue do peixe *Hoplias malabaricus* após exposição às STXs, e embora os efeitos de STXs sejam conhecidos como neurotóxicos, alterações bioquímicas hepáticas relevantes foram observadas. Ramos et al. (2014) demonstraram que o consumo por 30 dias de água contaminada com STX é capaz de alterar a atividade de enzimas antioxidantes como a glutamato cisteína-ligase (GCL) e GST, assim como alterar a concentração do antioxidante GSH, tanto no encéfalo como no fígado de ratos. D`Mello et al. (2017) demonstraram que as STXs são capazes de causar alterações fisiológicas consistentes com neurodegeneração

em células gliais, pela geração de estresse oxidativo e excitotoxicidade, levando a uma redução na proliferação celular que culmina na morte celular.

Dentro de um contexto pró-oxidante induzido pelas STXs, a perturbação da sinalização redox afeta importantes processos celulares (JONES, 2006; PAMPLONA; COSTANTINI, 2011b). De fato, danos causados em biomoléculas pela exposição às STXs, certamente afetam a produção de ATP, alterando assim todos os processos que envolvem esta molécula como a síntese de GSH, principal antioxidante não enzimático do SDA.

A GSH é um tripeptídeo localizado no citoplasma e mitocôndrias das células, desempenhando um papel crítico na defesa contra a geração de estresse oxidativo por xenobiótiocos, como as cianotoxinas (AMADO; MONSERRAT, 2010) mais notavelmente no sistema nervoso central (VALDOVINOS-FLORES; GONSEBATT, 2012). Além disso, o par GSH (glutationa reduzida)/GSSG (glutationa oxidada) atua na manutenção do ambiente redox da célula (HELLOU; ROSS; MOON, 2012).

O mecanismo de defesa e de detoxificação das cianotoxinas envolve a GSH e ocorre através de duas vias distintas: (1) pela interação direta com as EAO e servindo como substrato para a reação catalisada pela enzima glutationa peroxidase (GPx) na redução do peróxido de hidrogênio e hidroperóxidos lipídicos; e/ou (2) pela conjugação com cianotoxinas através de uma reação catalisada pela enzima glutationa S-transferase (GST), sendo vista como um processo de biotransformação que resultará na formação de um derivado mais solúvel em água, facilitando o processo de eliminação das cianotoxinas (AMADO; MONSERRAT, 2010; GLADE, 2010; HELLOU; ROSS; MOON, 2012; PAMPLONA; COSTANTINI, 2011b).

O processo de biotransformação tem grande importância na atenuação da toxicidade das STXs, já que muitos trabalhos reportam bioacumulação em diferentes órgãos e não somente no cérebro. De fato, camundongos expostos à concentrações sub letais de STXs (300 µg/kg) apresentaram alteração na atividade da SOD e GPx no fígado (HONG; LAM; HSIEH, 2003). Um aumento da GPx foi observada em uma cultura primária neuronal de *H. malabaricus* após exposição a 3,0 µg/L STXs, lembrando que essa concentração é a máxima permitida na legislação brasileira.

Em uma situação pró-oxidante, a indução de genes associados ao metabolismo de GSH (GCL, GPx e GST) ocorre através da rota de ativação celular Keap1-Nrf2-ARE, como pode ser observado na **figura 4**. (ZHANG et al., 2010). A proteína Nrf2 ("nuclear factor erythroid2-related factor 2") é um fator de transcrição que interage com o elemento de resposta antioxidante (ARE), presente na região promotora de genes de importância antioxidante (MUKAIGASA et al., 2012; PI et al., 2010; TAN et al., 2013). Em condições basais, a proteína repressora Keap1, rica em grupos sulfidrilas e ancorada à actina do citoesqueleto, se liga à Nrf2 no citoplasma e promove a sua degradação (KORIYAMA et al., 2013).

Embora os mecanismos de dissociação Keap1-Nrf-2 ainda não estejam completamente elucidados, acredita-se que na presença de EAO, Keap1 é inativado e libera Nrf2, quando os grupos sulfidrila da Keap1 ficam oxidados, formando pontes dissulfetos, resultando em sua translocação nuclear. Mutações dos genes Nrf2 e Keap1 favorecem maior expressão e ação de Nrf2 (KORIYAMA et al., 2013; PI et al., 2010). Sendo assim, as STXs podem ser capazes de potencializar esse processo, aumentando a transcrição de enzimas como a glutamato-cisteína-ligase (GCL), enzima chave da síntese da GSH (**Figura 4**).

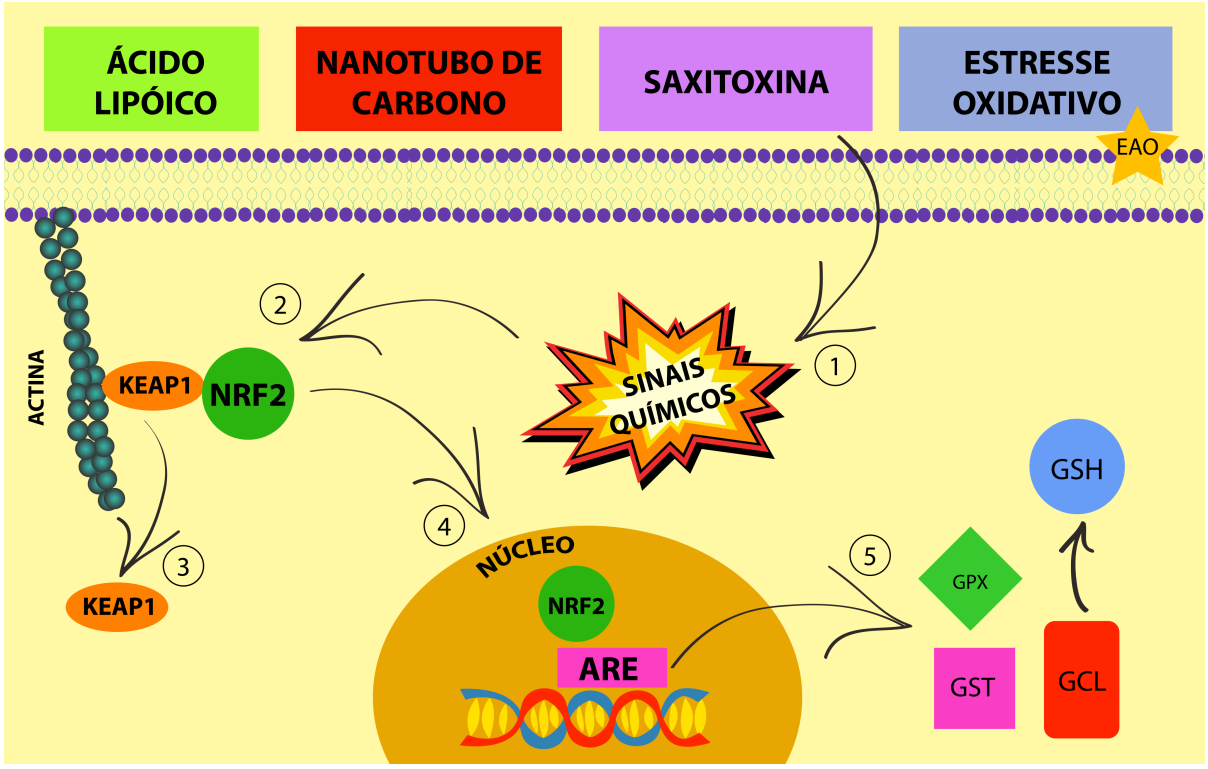

Figura 4: Indução de transcrição de enzimas associadas ao metabolismo de GSH. Legendas: EAO (espécies ativas de oxigênio), Nrf2 (fator transcriptacional ("nuclear factor erythroid2-related factor 2"), Keap 1(proteína repressora), GPx (glutationa peroxidase), GST (glutationa-S -transferase), GCL (glutamato cisteína-ligase), GSH (glutationa reduzida).

A biodisponibilidade de uma grande variedade de compostos, incluindo substâncias endógenas, drogas e xenobióticos, é determinada pelo equilíbrio entre transportadores de absorção e efluxo que facilitam o seu movimento através das membranas (LI; JAIMES; ALLER, 2014; SILVA et al., 2015). Estes transportadores são importantes para manter a homeostase celular e também para desintoxicar substâncias potencialmente tóxicas (DEGORTER et al., 2012; LI; JAIMES; ALLER, 2014). A glicoproteína-P (P-gp ou ABCB 1), produto do gene de resistência a múltiplos fármacos (MDR) em humanos, é um transportador dependente de ATP presente nas membranas celulares (LACHER et al., 2015) e funciona como uma bomba de extrusão de drogas anti-cancerígenas e outros compostos para fora da

célula (AMÉ et al., 2009; HAN; CHIN TAN; LIM, 2008; HUANG et al., 2015). Como inibidores clássicos da P-gp podem ser citados a ciclosporina e verapamil (LACHER et al., 2015).

De fato, a P-gp pode desempenhar um papel crucial na absorção e distribuição de xenobióticos nocivos, diminuindo sua acumulação e potenciais efeitos intracelulares devido à sua ampla especificidade de substrato, à sua expressão em muitos tecidos excretores e de barreira e à sua grande capacidade de efluxo, (HAN; CHIN TAN; LIM, 2008; HUANG et al., 2015; SILVA et al., 2015). AMÉ et al (2009) observaram um aumento da expressão da P-gp no fígado, brânquias e cérebro do peixe *Jenynsia multidentata* após exposição dose-dependente à cianotoxina microcistina. Contudo, ainda não há publicado na literatura trabalhos que evidenciam atividade e/ou expressão da P-gp após a exposição por saxitoxinas.

1.4. Potenciais mecanismos que atenuam a toxicidade das saxitoxinas

1.4.1. Interações com nanotubos de Carbono

Os nanotubos de carbono (NTCs) são nanoestruturas cilíndricas que se assemelham à folhas de grafite enroladas com extremidades fechadas com grande razão comprimento/diâmetro (APUL; KARANFIL, 2015; REDDY et al., 2011; ROLDO; FATOUROS, 2013). Podem ser classificados quanto ao número de folhas de grafeno em nanotubos de parede única (SWCNT, do inglês “single-walled carbon nanotubes”) e nanotubos de parede múltipla (MWCNT, do inglês “multi-walled carbon nanotubes”) (**Figura 5**) (COSTA et al., 2016; FIRME; BANDARU, 2010).

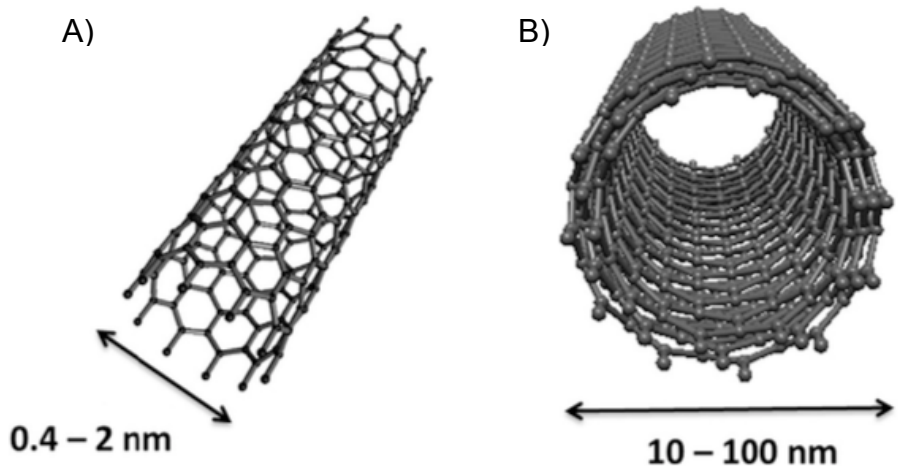

Figura 5: Representação dos nanotubos de: A) parede simples (SWCNT) e dos B) nanotubos de parede múltipla (MWCNT). Obtido de Costa et al. (2016)

Os NTCs podem apresentar diferentes tipos de funcionalização. Os NTCs pristinos são aqueles que não apresentam funcionalização, tendo solubilidade limitada e uma maior tendência à agregação. O tipo e o grau de funcionalização de um NTC pode aumentar sua solubilidade e minimizar a agregação (GALANO, 2009; SAYES et al., 2006; SONG et al., 2013).

Devido às suas importantes propriedades físicas, químicas, térmicas e elétricas, a produção e o uso de NTCs tem crescido rapidamente, trazendo novos paradigmas para diversos campos de estudo (EMA; GAMO; HONDA, 2016; FIRME; BANDARU, 2010; KAFA et al., 2015). Na biomedicina, NTCs podem ser utilizados na detecção e reconhecimento molecular de alta sensibilidade, possuem capacidade de administrar fármacos através da BHE e de interagir com células e membranas celulares, especialmente das mitocôndrias (**Figura 6**) (ZHAO; LIU, 2012; MAKOTO et al., 2015).

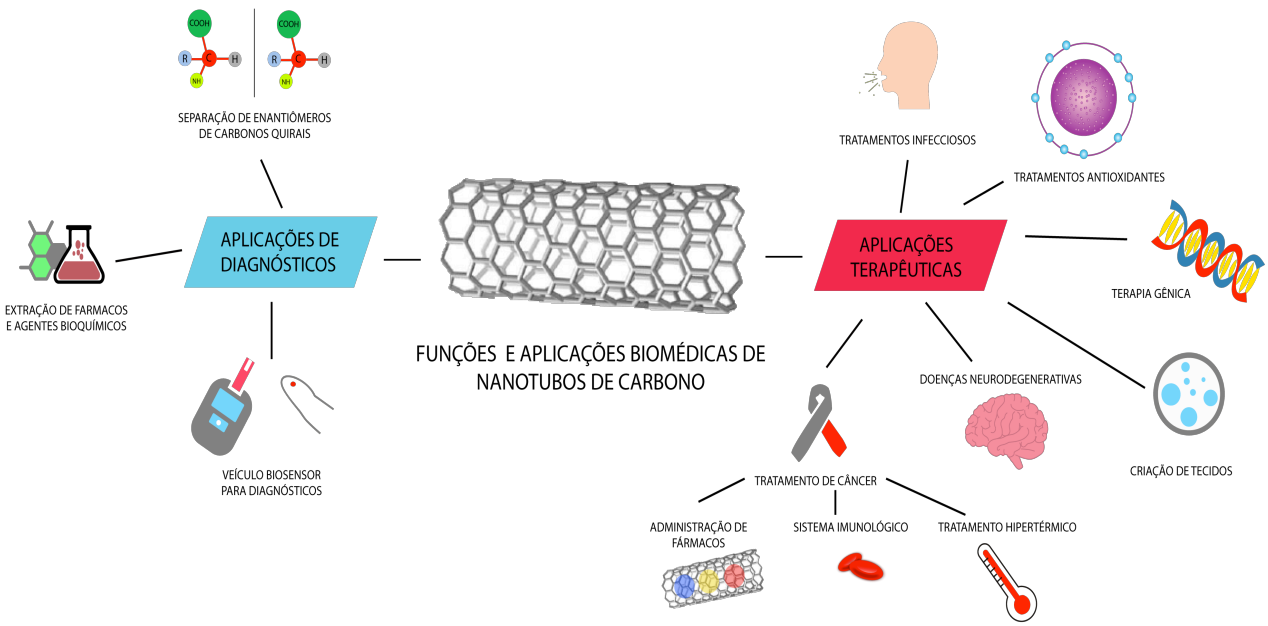

Figura 6: Funções e aplicações biomédicas de Nanotubos de carbono

Apesar de características tão atraentes, questões sobre a potencial toxicidade dos NTCs para os seres humanos e ambientes foram levantadas nos últimos anos (COSTA et al., 2016). A toxicidade dos NTCs tem sido relacionada às suas propriedades físicas como comprimento, tipo de funcionalização, concentração, duração da exposição e até mesmo os dispersantes utilizados para solubilizar os NTCs (APUL; KARANFIL, 2015). Além disso, o modo como os NTCs atravessam a membrana lipídica pode influenciar na toxicidade. Até o momento, os mecanismos principais de entrada dos NTCs nas células amplamente considerados são endocitose, fagocitose e nanopenetração. A nanopenetração consiste no processo passivo (semelhante à difusão passiva) através do qual os NTCs atravessam a membrana celular (FIRME; BANDARU, 2010; KAFA et al., 2015; LAWAL, 2016).

Vários trabalhos *in vitro* tem demonstrado que NTCs são capazes de induzir aumento de EAO, estresse oxidativo, resposta inflamatória, apoptose e necrose, causando efeitos citotóxicos, genotóxicos, e carcinogênicos, entre outros (CHENG et al., 2011; KESHARWANI; MISHRA; JAIN, 2015; PICHARDO et al., 2012; WANG et al., 2011). Por exemplo, SWCNT e MWCNT induziram dano de DNA na linhagem de células mesoteliais (MET-5A) e na linhagem de células bronquiais (BEAS2B) após 72 h de exposição. SWCNT (30 µg/mL) induziu a diminuição de DNA total em uma cultura primária de células gliais após 24 h de exposição (BELYANSKAYA et al., 2009). Diminuição de viabilidade celular e acumulação de autofagossomos foram observadas na linhagem celular HUVECs após 24 horas de exposição à MWCNTs pristino e carboxilado (100 µg/mL). Estes autores sugerem que a estimulação farmacológica do fluxo autofágico pode representar um novo método de citoproteção contra os efeitos tóxicos dos NTCs.

Contudo, os dados de toxicidade são muito variados e as vezes, contraditórios. Alguns autores defendem a ideia que a toxicidade dos NTCs depende de fatores como tipo, concentração e natureza química. De fato, NTCs vêm sendo amplamente utilizado como carreadores de fármacos para doenças neurodegenerativas do SNC e resultados sugerem que NTCs podem aliviar o dano (BATTIGELLI et al., 2013). Em outro trabalho, SWCNT (15 µg/mL e 30 µg/mL) não induziram efeitos citotóxicos na linhagem celular epitelial A549 após 24 horas de exposição (KAISER; BUERKI-THURNHERR; WICK, 2013).

NTCs são considerados adsorventes promissores em virtude da sua alta hidrofobicidade associada à sua elevada área superficial. Além disso, interações eletrostáticas e ligações de hidrogênio influenciam consideravelmente a adsorção dos NTCs (APUL; KARANFIL, 2015). De fato, a capacidade de adsorção dos

nanomateriais com contaminantes, tais como hidrocarbonetos aromáticos policíclicos (PAHs), produtos farmacêuticos, derivados do benzeno, compostos fenólicos, inseticidas, cianotoxinas e íons metálicos tem sido amplamente relatados (APUL et al., 2013; APUL; KARANFIL, 2015; PAVAGADHI et al., 2013). Sendo assim, é de se esperar que NTCs possam interagir com as cianotoxinas como as STXs, e possivelmente ser responsáveis pela modulação de sua toxicidade. O notável aumento na produção e uso de NTCs levanta preocupações ambientais e de saúde, particularmente quando liberado para o meio ambiente, mas também levanta a possibilidade de ser utilizado na remediação de ambientes poluídos.

O efeito “cavalo de tróia” é definido como a associação de nanomateriais, como os NTCs, com moléculas tóxicas, facilitando o ingresso de contaminantes para as células quando adsorvidos aos nanomateriais, induzindo uma ampla gama de respostas, incluindo efeitos aditivos, sinérgicos ou antagonistas (**Figura 7**) (COSTA et al, 2012; CANESI et al., 2015). A análise de superfície e o estudo de adesão celular sugeriram que superfícies como as dos NTCs podem aumentar a adsorção de proteínas e a ligação celular permitindo a diferenciação neuronal de células embrionárias humanas (hESCs) (CHAO et al., 2009). Nesse sentido, SWNTC combinado com cádmio foi capaz de inibir a atividade de enzimas antioxidantes SOD, CAT e GPx, além de induzir uma diminuição notável no nível de GSH e elevação simultânea do conteúdo de malondialdeído, um subproduto de peroxidação lipídica, no peixe *Carassius auratus* (QU et al., 2014).

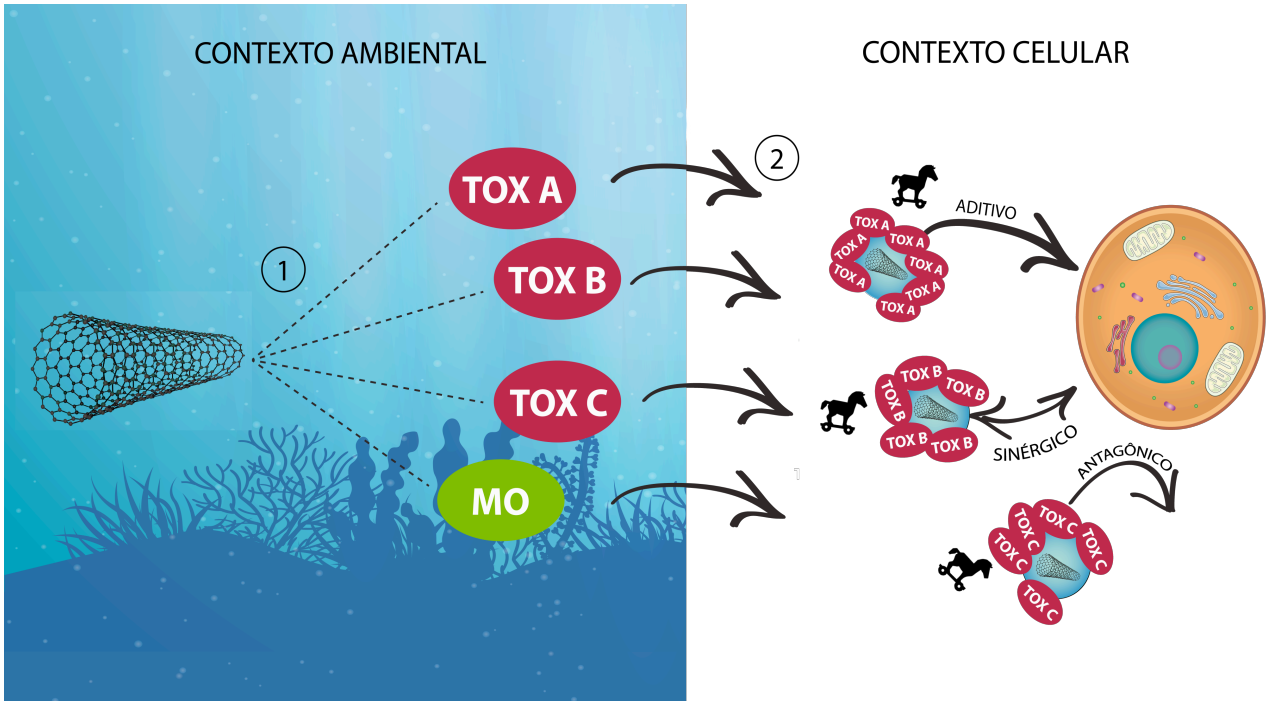

Figura 7: Representação do Efeito "Cavalo de Tróia". 1) Nanomateriais são capazes de interagir com diferentes contaminantes (TOX A, TOX B, TOX C) e matéria orgânica (MO) no ambiente aquático e 2) facilitando o ingresso dos nanomateriais às células, induzindo efeitos aditivos, sinérgicos ou antagônicos.

1.4.2. O papel do ácido lipóico como agente quimioprotetor

Como dito anteriormente, as STXs causam estresse oxidativo por, dentre outros fatores, provocar um aumento da geração de EAO associado a uma diminuição de defesas antioxidantes. Frente a esta situação pró-oxidante, o estudo de estratégias de quimioprevenção contra os efeitos danosos das STXs é indispensável. Quimioprevenção pode ser definida como a utilização de agentes químicos naturais ou sintéticos que atuam na reversão, bloqueio ou prevenção de doenças (AMADO et al., 2011; KÜTTER et al., 2012, 2014). A utilização/administração de compostos exógenos não enzimáticos, como por exemplo, o ácido lipóico, com o objetivo de verificar estratégias de quimioprevenção

para atenuar os efeitos deletérios causados por essas cianotoxinas em animais é de extrema importância (AMADO et al., 2011; GORĄCA et al., 2011; GRUBER et al., 2013) e uma alternativa de baixo custo.

O DL-α- ácido lipóico (AL), um antioxidante ditiól não enzimático de baixo peso molecular (GRUBER et al., 2013), é encontrado naturalmente nas mitocôndrias desempenhando papel essencial como cofator de enzimas desidrogenases do ciclo de Krebs (GORĄCA et al., 2011; GRUBER et al., 2013). Além de seu importante papel no metabolismo energético mitocondrial, também é considerado um potente agente quimio e neuroprotetor capaz de atravessar a BHE (VALDOVINOS-FLORES; GONSEBATT, 2012) e tem sido amplamente utilizado como agente terapêutico no tratamento de doenças crônicas associadas a altos níveis de estresse oxidativo (GLADE, 2010; GRUBER et al., 2013; HILLER et al., 2016), como por exemplo diabetes mellitus, doenças neurodegenerativas como Alzheimer e Parkinson (HILLER et al., 2016; SHAY; MOREAU; SMITH, 2009; WEI et al., 2015) e esteatose (KUO et al., 2012)

O AL e sua forma reduzida, ácido dihidrolipóico (DHLA), facilmente absorvidos por meio de dieta, formam um potente par redox e exibem um conjunto expressivo de funções antioxidantes (DÖRSAM; FAHRER, 2016). São capazes de quelar metais e interceptar radicais livres tanto em ambientes aquosos quanto em ambientes lipídicos (KÜTTER et al., 2014; LONGARAY-GARCIA et al., 2013; MONSERRAT et al., 2008), além de regenerar antioxidantes oxidados como ácido ascórbico e α-tocoferol e de controlar a migração do fator transcripcional Nrf2 do citoplasma para o núcleo, ativando genes associados à defesa antioxidante, conforme demonstrado anteriormente na **Figura 4** (KORIYAMA et al., 2013; PILAR VALDECANTOS et al., 2015; ZHANG et al., 2010). Também já foi demonstrado que

AL tem potencialidade para atenuar respostas inflamatórias (ASTIZ; DE ALANIZ; MARRA, 2012; ZHANG et al., 2010).

Devido seu potencial de redox, o DHLA é capaz de reduzir a GSSG a GSH, regenerando antioxidantes celulares, e induzir a atividade de enzimas de fase II, como a GST (DÖRSAM; FAHRER, 2016). De fato, o trabalho de Amado et al. (2011) evidenciou que o pré tratamento com AL aumentou a atividade da GST no cérebro do peixe *Cyprinus carpio* e foi capaz de reverter a inibição da GST no fígado causada pela cianotoxina microcistina. Deve ser salientado que, de acordo com os trabalhos mencionados acima, é possível esperar que o ácido lipóico tenha a capacidade de atuar como um neuroprotetor em células hipocampais HT-22, minimizando os efeitos causados pelas saxitoxinas.

1.5. Novas abordagens metodológicas

Na busca incessante por uma melhor compreensão da toxicidade de xenobióticos e suas consequências na homeostasia celular, novas abordagens computacionais vêm sendo propostas, dentre as quais podem ser citadas a abordagem *in silico* utilizando simulações *ab initio* e o docking molecular .

A metodologia computacional é uma ferramenta poderosa para a compreensão dos fenômenos químicos, físicos e biológicos. Com o aumento na capacidade de processamento dos computadores, a simulação computacional torna-se uma aliada na investigação teórica das propriedades das substâncias de estudo, como por exemplo, os NTCs (HAO et al., 2015).

As interações potenciais de NTCs com moléculas de interesse biológico podem ser analisadas *in silico.* O método *ab initio* está baseado no estudo da estrutura de moléculas e sólidos, bem como sua descrição microscópica,

fundamentado na mecânica quântica. (JAVADIAN et al., 2012). A Teoria Funcional da Densidade (DFT, do inglês, Density Functional Theory) se apresenta como uma boa escolha para a obtenção das propriedades energéticas, eletrônicas, vibracionais e estruturais (HAO et al., 2015; JAVADIAN et al., 2012). Por exemplo, simulações *ab initio* utilizando a Teoria Funcional da Densidade demonstram que SWCNT puro e carboxilado podem apresentar diferente capacidade de eliminação de EAO (GALANO et al., 2010).

Por sua vez, a docagem (*docking*) molecular é um procedimento computacional utilizado para auxiliar a compreensão da interação entre macromoléculas biológicas que são chamadas de receptores (MENG et al., 2011), como por exemplo a proteína P-gp, e uma pequena molécula chamada de ligante, como poderiam ser os NTCs e as neurotoxinas produzidas por cianobactérias. Ao analisar esses tipos de interações, é possível compreender se os ligantes atuam como inibidores ou antagonistas de um processo fisiológico (VERLI et al., 2014). Por esse motivo, o *docking* molecular vem sendo cada vez mais utilizado nas áreas de saúde e biotecnologia.

2. OBJETIVOS

2.1. Objetivo Geral

Avaliar mecanismos envolvidos na redução dos efeitos tóxicos das saxitoxinas e suas interações físico-químicas e biológicas com nanotubos de carbono e ácido lipóico na linhagem hipocampal HT-22.

2.2. Objetivos específicos

- Determinar o potencial tóxico das saxitoxinas (saxitoxina e neo-saxitoxina) através de ensaios *in vitro* utilizando a linhagem hipocampal HT-22;
- Identificar e relacionar as possíveis interações físico-quimicas das saxitoxinas com nanotubos de carbono e ácido lipóico através de ensaios *in silico* baseadas em técnicas ab *initio*;
- Determinar os efeitos das interações físico-quimicas das saxitoxinas (saxitoxina e neo-saxitoxina) com nanotubos de carbono e ácido lipóico utilizando parâmetros bioquímicos de estresse oxidativo e consumo de oxigênio na linhagem hipocampal HT-22;
- Determinar interações de acoplamento molecular (docagem molecular) relacionadas ao potencial tóxico das saxitoxinas (saxitoxina e neo-saxitoxina) e os fatores que modificam (minimizam) a toxicidade da mesma;
- Propor um mecanismo de atenuação da toxicidade mediada pelas saxitonas através da interação com a glicoproteína-P da linhagem hipocampal HT-22 relacionando os efeitos *in silico* e *in vitro.*

3. RESULTADOS

Os resultados do presente estudo foram divididos em um artigo científico e um manuscrito, os quais compõem a seção de resultados desta tese.

Artigo 1:

INTERACTION OF SINGLE-WALLED CARBON NANOTUBES AND SAXITOXIN: AB INITIO SIMULATIONS AND BIOLOGICAL RESPONSES IN HIPPOCAMPAL CELL LINE HT-22

Artigo publicado na revista **Environmental Toxicology and Chemistry**

(Fator de impacto: 2.763)

SETAC PRESS

Environmental Toxicology and Chemistry, Vol. 9999, No. 9999, pp. 1–10, 2016

SETAC Latin America

INTERACTION OF SINGLE-WALLED CARBON NANOTUBES AND SAXITOXIN: AB INITIO SIMULATIONS AND BIOLOGICAL RESPONSES IN HIPPOCAMPAL CELL LINE HT-22

Patrícia Ramos,*†‡ Marcos Schmitz,† Daza Filgueira,† Ana Paula Votto,†‡ Michael Durruthy,†‡ Marcos Gelesky,§ Caroline Ruas,§ João Yunes,‖ Mariana Tonel,#†† Solange Fagan,#†† and José Monserrat†‡

†Institute of Biological Science, Federal University of Rio Grande (FURG), Rio Grande, Rio Grande do Sul, Brazil
‡Postgraduate Program in Physiological Sciences, Comparative Animal Physiology, Federal University of Rio Grande (FURG), Rio Grande, Rio Grande do Sul, Brazil
§Postgraduate Program in Technological and Environmental Chemistry, Federal University of Rio Grande (FURG), Rio Grande, Rio Grande do Sul, Brazil
‖Cyanobacteria and Ficotoxin Laboratory, Federal University of Rio Grande (FURG), Rio Grande, Rio Grande do Sul, Brazil
#Franciscan University Center (UNIFRA), Santa Maria, Rio Grande do Sul, Brazil
††Postgraduate Program in Nanoscience, Franciscan University Center (UNIFRA), Santa Maria, Rio Grande do Sul, Brazil

(Submitted 29 February 2016; Returned for Revision 15 April 2016; Accepted 30 June 2016)

Abstract: Saxitoxins (STXs) are potent neurotoxins that also induce cytotoxicity through the generation of reactive oxygen species. Carbon nanotubes (CNTs) are nanomaterials that can promote a Trojan horse effect, facilitating the entry of toxic molecules to cells when adsorbed to nanomaterials. The interaction of pristine single-walled (SW)CNTs and carboxylated (SWCNT-COOH) nanotubes with STX was evaluated by ab initio simulation and bioassays using the cell line HT-22. Cells (5×10^4 cells/mL) were exposed to SWCNT and SWCNT-COOH (5 μg mL^{-1}), STX (200 μg L^{-1}), SWCNT+STX, and SWCNT-COOH+STX for 30 min or 24 h. Results of ab initio simulation showed that the interaction between SWCNT and SWCNT-COOH with STX occurs in a physisorption. The interaction of SWCNT+STX induced a decrease in cell viability. Cell proliferation was not affected in any treatment after 30 min or 24 h of exposure ($p > 0.05$). Treatment with SWCNT-COOH induced high reactive oxygen species levels, an effect attenuated in SWCNT-COOH+STX treatment. In terms of cellular oxygen consumption, both CNTs when coexposed with STX antagonize the toxin effect. Based on these results, it can be concluded that the results obtained in vitro corroborate the semiempirical evidence found using density functional theory ab initio simulation. *Environ Toxicol Chem* 2016;9999:1–10. © 2016 SETAC

Keywords: Saxitoxin Carbon nanotubes HT-22 cell Density functional theory Cell viability

INTRODUCTION

Saxitoxins (STXs) are classified as one of the most potent natural neurotoxins associated with the paralytic shellfish poisoning phenomenon [1]. To date, more than 30 STX analogs have been described [2]. Saxitoxins are biosynthesized by marine dinoflagellates and freshwater cyanobacteria such as *Cylindrospermopsis raciborskii* [3]. During bloom events, STXs produced by *C. raciborskii* are frequently observed in public water supply reservoirs in Brazil and thus constitute a serious public health risk [4]. They are capable of crossing the blood–brain barrier [5] and affect the central nervous system by blocking voltage-gated sodium channels and binding to calcium and potassium channels in excitable cells. Thus STXs affect ion permeability, interfering with the speed of ion channel opening and closing [6,7]. This mechanism can damage cellular homeostasis and can induce neuromuscular paralysis, respiratory arrest, and death in organisms from different trophic levels [1,3,7].

Several recent reports have also argued for another toxicity mechanism, involving the generation of reactive oxygen species (ROS). Cyanotoxins not only can cause an overproduction of ROS but also can alter antioxidant levels, which may lead to oxidative stress, defined as a disruption in redox signaling and control of the redox state [8,9]. Thirty-day consumption of STX-contaminated water reduced the activity of antioxidant (or important for antioxidant synthesis) and detoxification enzymes such as glutamate cysteine ligase and glutathione-S-transferases, as well as the levels of the nonenzymatic antioxidant reduced glutathione, in both brain and liver of rats [10]. However, few studies have reported on the specific cytotoxic effects of STX in cell lines. Some reports indicate that STX causes a decrease in cell viability [2] and an increase in the lipid peroxidation byproduct malondialdehyde [7], which was observed in Neuro-2A cells after exposure to STX.

Carbon nanotubes (CNTs) are composed of carbon atoms and are characterized by their cylindrical shape. Carbon nanotubes possess a unique structure and important and valuable chemical, physical, thermal, and electrical properties [11,12]. They can be classified into 2 broad categories on the basis of their structural diameter and length as single-walled carbon nanotubes (SWCNTs) and multiwalled carbon nanotubes (MWCNTs) [12,13]. Because of their wide variety of properties, which offer a large range of potential biomedical applications, CNTs have gained enormous popularity. Of particular interest is the ability of CNTs to deliver drugs across the blood–brain barrier and their ability to interact with cells and cross cell membranes, especially into mitochondria [13].

The role of CNTs as electrochemical nanobiosensors for food and water analysis is another important application [14]. Some studies show that water-dispersed CNTs can interact with algae and influence biochemical alterations in algae [15]. Also,

* Address correspondence to pattybramos@gmail.com
Published online 2 July 2016 in Wiley Online Library (wileyonlinelibrary.com).
DOI: 10.1002/etc.3544

an MWCNT-biocompatible electrochemical immunosensor was designed to detect a highly toxic cyanotoxin (microcystin) with high sensitivity and selectivity [16]. To the best of our knowledge, however, there are no studies demonstrating the ability of CNTs to immobilize STX or examining whether the interaction with CNTs can modulate the toxicity of STX. The toxicity of CNTs has been extensively studied and may be dependent on many factors, including concentration, the metal (particularly iron) content, physical form, surface chemistry, and degree of aggregation [11,17]. Recently, many conflicting reports concerning the biocompatibility and safety of CNTs have been published [11,12,18]. There is growing concern over the potential detrimental impact of manufactured nanoparticles on the natural environment, particularly in aquatic environments, where little is known about their interactions with other contaminants, such as organic xenobiotics and heavy metals, and whether these interactions affect CNTs' bioavailability, bioconcentration, and nanotoxicity [17,18].

The "Trojan horse" effect, whereby toxic molecules interact with nanomaterials [19], inducing a wide range of responses, including additive, synergistic, or antagonistic effects [18], has been widely discussed in the literature. For example, in zebrafish hepatocytes, fullerene C_{60} increased arsenic uptake [20], and coexposure of the organic nanomaterial fullerene C_{60} with benzo[*a*]pyrene decreased cell viability and impaired the phase II detoxification response [21]. Indeed, in vitro studies have confirmed that exposure to different CNTs causes oxidative damage and increases ROS [12,17,19] in a cell type–dependent manner. Moreover, SWCNTs functionalized with polyethylene glycol (SWCNT-PEG) and directly infused into rat hippocampus reduced ROS and induced antioxidant defenses 7 d after injection, suggesting that the biopersistence of nanomaterial in the tissue can induce an antioxidant response [22].

The hippocampus is a vertebrate brain structure responsible for consolidating short-term memories into long-term memories. According to Ramos et al. [10], STX decreases the antioxidant defenses of the hippocampus, and these deleterious effects occur at STX concentrations allowed by Brazil Regulation 2914/2011. Furthermore, several studies have indicated that hippocampal neuronal networks grown on CNT substrates show an increased frequency of spontaneous synaptic events [23]. Hence, the hippocampal cell line HT-22 (subclone of cell line HT-4) is considered an extremely useful model for studying the mechanisms of STX neurotoxicity [24]. Many studies have demonstrated that oxidative stress is a key mechanism responsible for STX- and CNT-induced cytotoxicity. We hypothesized that the interaction between STX and SWCNTs (pristine and carboxylated) affects the integrity of hippocampal neuronal cells.

Based on this idea, the potential interactions of pristine and carboxylated SWCNTs with molecules of biological interest can be analyzed in silico. In the same way, a density functional simulation was used to investigate the adsorption of the amino acid alanine (ALA) with pristine and functionalized SWCNTs, indicating that the interaction occurred through the amine group [25]. With the pristine SWCNTs, the interaction was observed homogenously with all carbon atoms of the tube to the sp^2 hybridization, and remained a metal system. In contrast, for carboxylated SWCNTs, the system properties (carboxylated SWCNT–ALA complex) were independent of the alanine adsorption position [25]. Studies using density functional theory showed that pristine SWCNTs and carboxylated SWCNTs can have different free radical scavenging capabilities [26]

In this regard, the main objective of the present study was to evaluate the potential interaction between STX and SWCNTs (pristine and carboxylated) by both theoretical calculations and the execution of bioassays using the rat hippocampal HT-22 cell line. Our aim was to understand the interaction of STX with pristine SWCNTs and carboxylated SWCNTs using ab initio calculations that were carried out by using the density functional theory to evaluate the physical and chemical properties involved in the STX–SWCNT interactions.

MATERIALS AND METHODS

Cell culture

Cells of the mouse hippocampal cell line H-22 (kindly provided by the Salk Institute for Biological Studies, La Jolla, CA, USA), were grown on bottles for cell culture in Dulbecco's modified Eagle's medium (DMEM) containing high glucose (Gibco) supplemented with sodium bicarbonate (1.5 g/L; Vetec), 10% fetal bovine serum (Invitrogen Brazil), and 1% antibiotics and antimycotics (penicillin [100 U/mL], streptomycin [100 U/mL], and amphotericin [0.25 μg/mL]; Gibco). Cells were cultured at 37 °C in 5% CO_2. Growth media were changed every day. The cells used in assays were previously transferred to 24-well or 96-well plates for cell culture, followed by a 24-h period grip. The treatments were carried out in quadruplicate. Experiments were performed at 70% to 80% confluence.

Carbon nanotubes

Two kinds of SWCNTs were used. Pristine SWCNTs were purchased from a commercial supplier (SWNTC lot ps-09607; SES Research,) with 10-nm to 30-nm diameter and 99.9% purity. To ensure the removal of metal traces from the SWCNTs, they were mixed in a solution containing sulfuric acid, sonicated for 6 h, and centrifuged (3000 *g* for 20 min). This procedure was repeated 5 times, and then SWCNT samples were further oven dried for 48 h at 50 °C [27]. Carboxylic functionalized SWCNTs (SWCNT-COOH: 2.73 wt%) were provided by Cheaptubes. Both pristine SWCNT and SWCNT-COOH were analyzed by means of Fourier transform infrared (FT-IR) spectroscopy. The FT-IR spectra were performed in the range of 4000 cm^{-1} to 400 cm^{-1} using an IR spectrophotometer (Shimadzu PRESTIGE-21) with FT-IR spectroscopy for the analytical identification of the -COOH functional group. Samples of CNTs were analyzed in the solid state by diffuse reflectance. All spectra were baseline corrected and vector normalized. The scan number was fixed at 45, and spectral resolution was set at 4 cm^{-1}. The morphology and impurities of the CNTs were evaluated through scanning electron microcscopy and electron dispersive spectroscopy (EDS) analysis using JEOL model JSM 6610 with 30 kV and magnification of 40 000×. The same instrument was used for EDS analysis with a Noran detector. Samples were not coated for analysis. A stock suspension of 1 mg mL^{-1} of both kinds of CNTs was prepared in dimethyl sulfoxide (DMSO). The suspension was vortexed 3 times for 10 s each, followed by sonication for 1 h in an ultrasonic bath (ECO-SONICS; 9.3 W, with an energy input of 16.7 kJ at 25 °C). Working concentrations of 5 μg mL^{-1} were prepared after dilution in culture medium.

Source of toxins

Cylindrospermopsis raciborskii cells from the culture collection of the Cyanobacteria and Ficotoxin Laboratory

were grown in ASM-1 [10]. Under fixed laboratory conditions (25 ± 1 °C under continuous cool-white fluorescent light [intensity: 127 $\mu E\,m^{-2}\,s^{-1}$]), the strain produces variants of gonyautoxin (GTX), neoSTX, and STX detected by high-performance liquid chromatography with fluorescence detection (HPLC–FLD), which were analyzed and compared with commercial standards of STX, neoSTX, and decarbamoyl (dc) STX (National Research Counsil Canada). For toxin extraction, cells of *C. raciborskii* were sonicated (3 cycles of 1 min each) to promote cellular wall breakage and the release of toxins. The aqueous extract was then centrifuged at 10 000 *g* at 4 °C for 10 min, and the supernatant was saved for toxin quantification by HPLC. All experiments used working concentration of 15 mM prepared by dilutions in culture medium.

Ab initio calculation of SWCNT–STX interaction

Properties of STX interaction with SWCNTs were evaluated through a double zeta plus polarization (DZP) basis set to describe the pseudo-orbitals. For the exchange and correlation potential, a local density approximation was used with Perdew and Zunger parameterization [28]. To represent the electronic charge in real space 200 Ry of the cutoff grid was used. The atomic structures were relaxed until the residual forces were less than 0.05eV/Å for all the atoms. The binding energy was calculated using the basis set superposition error (BSSE) correction, according to the following equation

$$E_b^{BSSE} = -\left(E[A+B] - E\left[A + B_{ghost}\right] - E\left[A_{ghost} + B\right]\right)$$

The system *A* corresponds to pristine SWCNT or SWCNT-COOH, and system *B* is the STX molecule. They are all calculated with their corresponding atomic basis and with the *A* {*B*} atomic basis centered at the *B* {*A*} atomic positions. The subscript *ghost* refers to the atomic basis placed on the molecule or nanotube positions but without atomic potentials representing real atoms at these positions. The system with positive binding energies implies attractive interaction.

Exposure conditions

Cells were seeded in 24-well or 96-well plates at a density of 5×10^4 cells/mL in DMEM medium. After 24 h of cell attachment, plates were washed with phosphate-buffered saline (PBS). Cells were then exposed for 30 min or 24 h. After 30 min, it is possible to observe responses at the subcellular level, such as the mitochondrial level. After 24 h, in contrast, many responses occur at the cellular level as detoxification mechanisms of xenobiotics (such as STX) and interaction (adsorption) of CNTs. Cells were exposed to the following treatments: suspensions of the test materials (SWCNT and SWCNT-COOH; 5 $\mu g\,mL^{-1}$), STX (200 μg/L), and interaction between CNT and toxin (SWCNT+STX, SWCNT-COOH+STX). Two control groups were run in parallel, 1 containing DMEM medium and the other containing DMEM+DMSO (1%). Based on many reports, this concentration of DMSO is not deleterious for other types of cell line [21]. In addition, the DMSO control group showed no effect on the variables analyzed. Each experiment was repeated independently 3 times. In each experiment all treatments were repeated 6 times per plate. The SWCNT, SWCNT-COOH, and STX concentrations were sublethal, according to the results of previous range-finding tests (data not shown).

Cell viability assays

MTT assay. The HT-22 cells (5×10^4 cells/mL) were seeded into 96-well culture plates. After 30 min or 24 h of incubation with the different treatments, cell viability was measured by the 3(-4,5-dimethylthiazol-2-yl)-2,5-difenyltetrazolium (MTT) method (Sigma-Aldrich). After addition of 20 μL of MTT (5 $mg\,mL^{-1}$) and 3 h of incubation at 37 °C, the resultant formazan crystals were solubilized in 200 μL of DMSO, and the absorbance at 540 nm was determined on a multiwall plate reader (ELX 800 Universal Microplate Reader; Bio-TEK).

Trypan blue assay. The number of viable cells and cell viability were assessed by trypan blue (Gibco) exclusion assay. The HT-22 cells (5×10^4 cells/mL) were seeded into 96-well culture plates. After exposure at 30 min or 24 h with the treatments mentioned above, wells were washed twice with PBS; and after trypsinization, an aliquot of 50 μL cell suspension was mixed with 50 μL of trypan blue and cells were counted immediately on a Neubauer chamber. The protocol considered a cell viable when it had a clear cytoplasm and nonviable if it had blue cytoplasm.

Measurement of intracellular ROS concentration. For measurement of intracellular ROS levels, HT-22 cells (5×10^4 cells/mL) were seeded onto 24-well culture plates. After 30 min and 24 h of incubation with the treatments detailed in the *Exposure conditions* section, cells were incubated for 30 min at 37 °C with 40 μM of the fluorogenic compound 2′,7′-dichlorofluorescin diacetate (H_2DCF-DA; Sigma, Germany). Cellular fluorescence was quantified over 90 min at 37 °C by a fluorometer (Victor 2; PerkinElmer) equipped with a microplate reader, at an excitation wavelength of 485 nm and an emission wavelength of 520 nm [10]. According to a previous study [29], the fluorescence emission of isolated SWCNTs appears in the 900-nm to 1400-nm range, greater than the emission wavelength used in the present study. In addition, no interference from pegylated SWCNTs was observed in H_2DCF-DA fluorescence generation [22]. The ROS area was standardized by the number of viable cells, and ROS levels were expressed in terms of fluorescence area, where the area was obtained by integrating the fluorescence units (FU) over the measurement time (90 min) and expressed as FU/min.

Cellular oxygen consumption. For measurement of oxygen consumption in HT-22 cells, 5×10^4 cells/mL were seeded onto 24-well culture plates. After 30 min and 24 h of incubation with the treatments detailed in the *Exposure conditions* section, the oxygen consumption of cells was measured by a Clark-type electrode (Oxygraph System Hansatech Instruments) in a 2-mL glass chamber equipped with a magnetic stirrer. The electrode was calibrated using the oxygen content of air saturated medium, containing 425 ng atoms mL^{-1} at 20 °C.

Statistical analysis

The variables were analyzed by one-way analysis of variance (ANOVA) [30], followed by comparison of means by the Newman–Keuls method. A p value of 0.05 was considered statistically significant. Previously, assumptions of normality and variance homogeneity were tested. Mathematical transformations were applied in any case in which at least one of them was not verified (i.e., normality and/or variance homogeneity).

RESULTS

Characterization of SWCNT-COOH by FT-IR spectroscopy

As shown in Figure 1A, in the FT-IR spectrum of the pristine SWCNT sample, the water OH-linkages peak like a broad band between 3570 cm^{-1} and 3211 cm^{-1} and the C=C stretch is defined by the peak at 1625 cm^{-1}. Figure 1B and C shows the

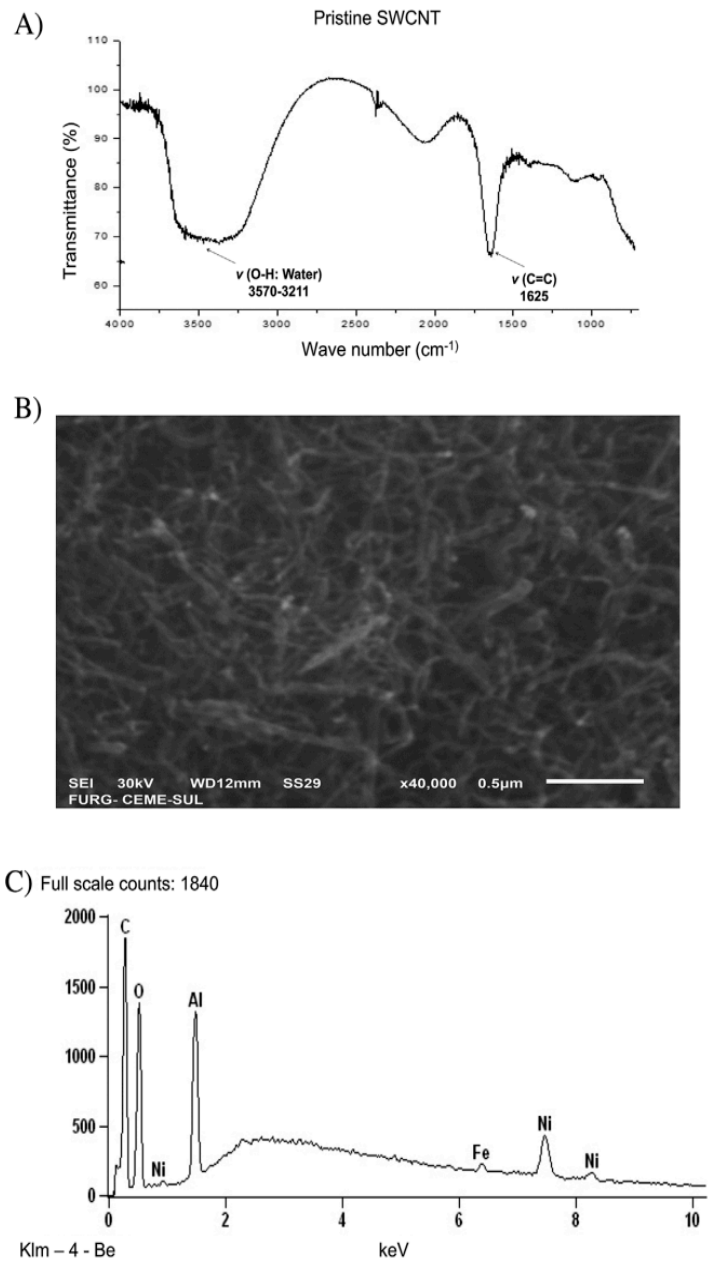

Figure 1. Caracterization of pristine single-walled carbon nanotube (SWCNT) sample. (**A**) Fourier transform infrared (FT-IR) spectrum of SWCNT sample. Peaks marked ν and δ refer to stretching and bending modes, respectively. (**B**) Scanning electron microscopy. (**C**) Impurities detected after electron dispersive spectroscopy analysis in pristine SWCNT sample.

results for scanning electron microscopy and EDS, respectively. The major impurity found was aluminum (Al), representing 8.64% (wt%) of pristine SWCNT. As shown in Figure 2A, the SWCNT-COOH spectrum is characterized by a broad band at 3420 cm^{-1} because of the stretching mode of the OH groups of carboxyl acid, the carbonyl groups of carboxyl acid C=O stretch at 1635 cm^{-1}, the C=C stretch at 1620 cm^{-1}, and the C-OH stretch at 1390 cm^{-1}. Figure 2B and C shows the results for scanning electron microscopy and EDS, respectively. The major impurity found was chromium (Cr), representing 5.10% (wt%) of SWCNT-COOH.

Prediction of CNTs and STX interaction

Four configurations were evaluated for SWCNT and SWCNT-COOH interactions with STX (Figure 3). The binding energy, shortest distance between atoms, and charge transfer values are shown in Table 1. The most stable configuration was SWCNT-STX-4 (Figure 3A), and the binding energy was estimated as 0.60 eV, being the shortest distance between STX and CNT atoms of 2.30 Å and charge transfer of $0.05e^-$ of the SWCNT for STX. The most stable configuration for the carboxylated nanotube is the SWCNT-COOH-STX-3 (Figure 3B); the binding energy is 0.83 eV, the shortest distance between STX and CNT atoms is 1.50 Å, and the charge transfer value is $-0.24e^-$ STX for SWCNT-COOH.

Figure 4A and B presents the electronic band structure for the pristine and carboxylated SWCNT interacting with STX, respectively. The pristine SWCNT, when isolated, has an energy gap of 0.61 eV (Figure 4A). It was observed that in all configurations evaluated for the pristine tube interacting with

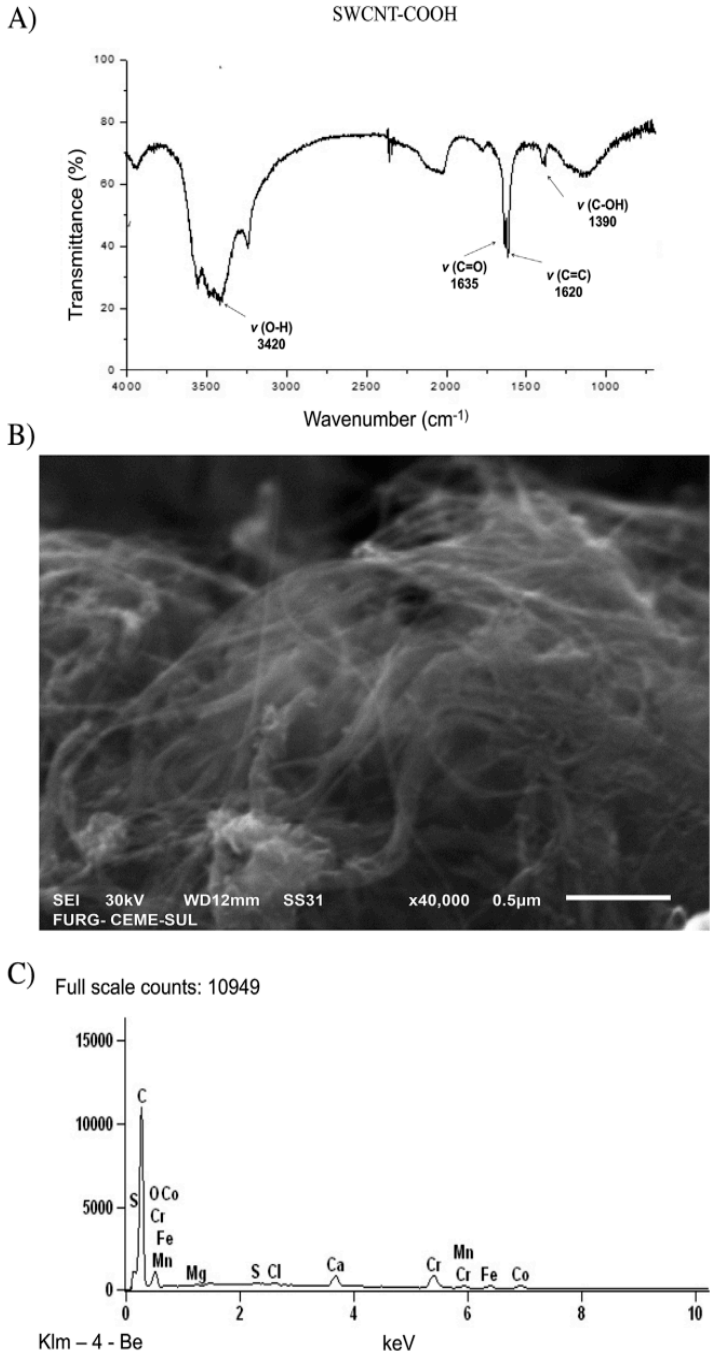

Figure 2. Characterization of carboxylated single-walled carbon nanotube (SWCNT-COOH) sample. (**A**) Fourier transform infrared (FT-IR) spectrum of SWCNT-COOH sample. Peaks marked *v* and *δ* refer to stretching and bending modes, respectively. (**B**) Scanning electron microscopy. (**C**) Impurities detected after electron dispersive spectroscopy analysis in SWCNT-COOH sample.

the STX a slight decrease in the energy gap occurred. However, no significant changes were observed around the Fermi level. Figure 4B shows the energy bands for the SWCNT-COOH and STX configurations investigated. The isolated SWCNT-COOH has a half-filled level in the Fermi region, which was also observed for all configurations studied when the STX is adsorbed. In both systems studied, SWCNT-STX and SWCNT-COOH-STX, no significant changes were noted in the region of the Fermi level, indicating a weak interaction, which is enhanced because of carboxylation, according to the binding energy and charge transfer values, as can be seen in Table 1. The charge plot in the valence and conduction bands (Figure 4C and D) was evaluated, and the electronic charge in the valence band was seen to be concentrated in SWCNT, SWCNT-COOH, and STX. Thus it can be seen that, at these levels, a small quantity of electronic charge is shared between the systems, corroborating the results in Table 1.

Effect of SWCNT, SWCNT-COOH, and STX on cell viability

The MTT assay was used to detect the viability of cells by measuring the formation of formazan, a product that results from cellular mitochondrial dehydrogenase activity. The results are shown in Figure 5, where it can be observed that MTT reduction was not affected ($p > 0.05$) during the 30 min of

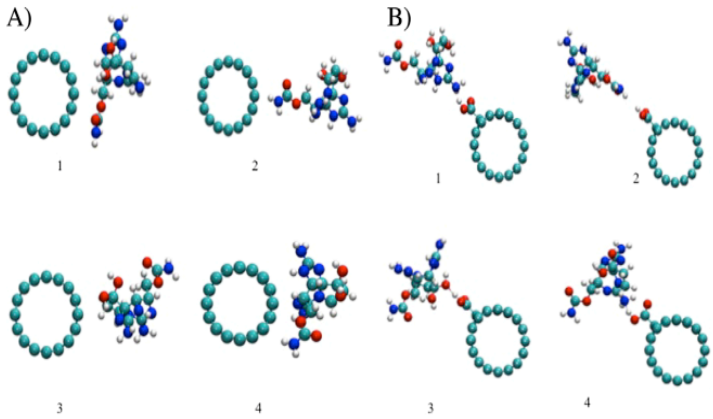

Figure 3. Structural configurations for the optimized positions of (**A**) pristine single-walled carbon nanotubes with saxitoxins (SWCNT-STX) and (**B**) carboxylated single-walled carbon nanotubes with saxitoxins (SWCNT-COOH-STX).

exposure to the different treatments. However, after 24 h, coexposure of SWCNT+STX in HT-22 cells caused a significant ($p < 0.05$) decrease in MTT-reducing ability compared with the SWCNT group.

Trypan blue exclusion was used to determine the number of viable cells and the cell viability present in a cell suspension after exposure to different treatments. It is based on the principle that live cells possess intact cell membranes that avoid penetration of trypan blue. Proliferation of HT-22 cells was not affected by any treatment after either 30 min or 24 h ($p > 0.05$; Figure 6A and B).

Determination of ROS concentration and oxygen consumption

The results of ROS intracellular concentration are given in Figure 7. Exposure of HT-22 cells to SWCNT-COOH for 30 min increased ROS concentrations ($p < 0.05$). This effect was also observed in the SWCNT-COOH+STX treatment, but not as markedly ($p < 0.05$). After 24 h, an increase in intracellular ROS concentration ($p < 0.05$) in HT-22 cells exposed to SWCNT-COOH was observed, an increase that was reversed in the SWCNT-COOH+STX group. In contrast, in cells exposed to SWCNT no differences from the control group were observed ($p > 0.05$) and the opposite was observed in the SWCNT+STX group ($p < 0.05$) after 24 h of exposure. The results of oxygen consumption by HT-22 cells are shown in Figure 8. At both exposure times (30 min and 24 h), an increase in oxygen consumption was observed in HT-22 cells exposed to STX ($p < 0.05$). At 30 min and 24 h, however, this increase was reversed in the SWCNT+STX and SWCNT-COOH+STX treatments.

Table 1. Binding energy, shortest distance, and charge transfer between STX and SWCNT or SWCNT-COOH for all the studied systems

Configuration	Binding energy (eV)	Shortest distance (Å)	Charge transfer (e^-)[a]
SWCNT-STX-1	0.49	2.21	+0.78
SWCNT-STX-2	0.30	2.00	+0.12
SWCNT-STX-3	0.34	2.41	0.00
SWCNT-STX-4	0.60	2.30	+0.05
SWCNT-COOH+STX-1	0.30	1.58	−0.21
SWCNT-COOH+STX-2	−0.53	2.22	0.00
SWCNT-COOH+STX-3	0.83	1.50	−0.24
SWCNT-COOH+STX-4	0.55	1.52	−0.22

[a]Negative values for charge transfer indicate that the STX molecule lost electronic charge.
SWCNT = single-walled carbon nanotube; SWCNT-COOH = SWCNT functionalized with carboxylic acid; STX = saxitoxin.

DISCUSSION

Several lines of evidence indicate that STXs are a serious threat to human health and environmental safety around the world [3,4]. However, CNTs have many useful features and are used in a number of industrial and biomedical applications, including bioengineering and disease treatment. The toxicity of CNTs has been extensively studied, but the results are controversial and uncertain [12,13,17]. Although CNT impurities can contribute to their toxic effects, the maximum Al (the most important impurity observed in pristine SWCNTs; Figure 1C) concentration in pristine SWCNT assays should be 0.43 $\mu g\ mL^{-1}$, a value below the Al concentration known to be cytotoxic in rat hippocampal neurons (0.68 $\mu g\ mL^{-1}$) [31]. Similarly, the maximum Cr (the most important impurity observed in SWCNT-COOH; Figure 2C) concentration in SWCNT-COOH assays should be 0.26 $\mu g\ mL^{-1}$, a value below the Cr concentration known to be cytotoxic to cultured cerebellar neurons (0.52 $\mu g\ mL^{-1}$) [32].

The Trojan horse effect implies that the entrance of toxic molecules to cells is facilitated by adsorption to nanomaterials [19]. Hence, it is important to consider possible interactions between environmental contaminants, such as STX, and nanomaterials, such as CNTs. The interaction of pristine SWCNT and SWCNT-COOH with STX was evaluated both by the density functional theory, using ab initio simulation, and by bioassays using the hippocampal cell line HT-22. The results indicated a weak interaction between STXs and SWCNTs (Figure 3). The presence of the carboxyl group on SWCNTs changes the direction of the charge transfer, and this effect can significantly alter the biological environment of the nanostructures (Figure 4). Through the charge plot in the valence and conduction of the electronic bands, a small quantity of electronic charge shared between these systems was observed, also corroborating the binding energy and charge transfer results that indicated a physisorption method of interaction for the SWCNT–STX complexes.

Many questions about the toxicity of STX and CNTs in vitro remain unanswered (e.g., safe concentrations and the sensitivity of particular cell lines). In the present study, the rat hippocampal HT-22 cell line was used. This cell line represents an interesting model to test the effects of interaction between CNTs and STX

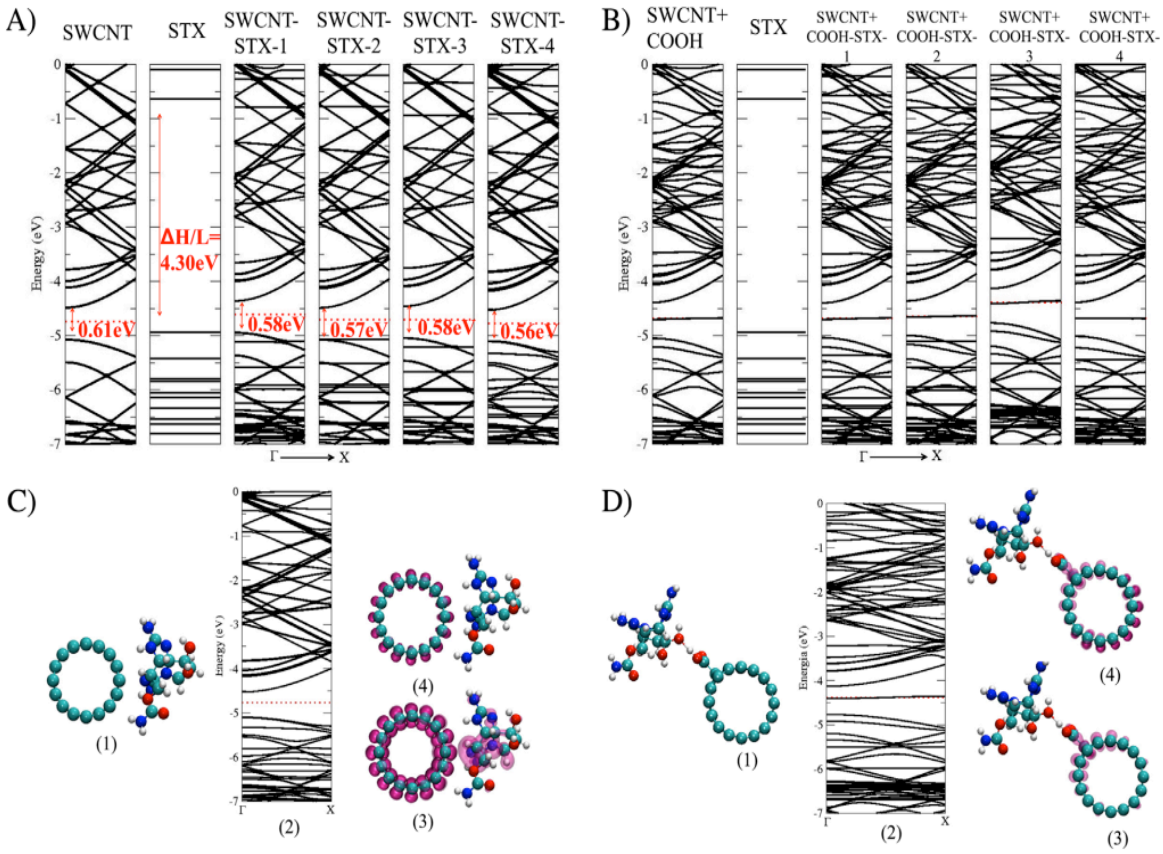

Figure 4. Electronic band structures for the ab initio simulations of (**A**) pristine single-walled carbon nanotubes (SWCNTs) isolated and with the saxitoxin (STX) molecule and (**B**) carboxylated SWCNTs (SWCNT+COOH) isolated and interacting with the STX molecule. Plot of the electronic charge for the most stable configuration SWCNT-STX-4 (**C**) and SWCNT-STX-3 (**D**). Energy ranges used in the valence band (C-3) −5.11 eV to −5.00 eV and (D-3) −4.45 eV to −4.40 eV; conduction band (C-4) −4.60 eV to −4.50 eV and (D-4) −4.20 eV to −4.00 eV. Charge isosurface value is 0.0005 eV/Bohr^3.

on neuronal cytotoxicity. Cell viability and cytotoxicity of CNTs is quite controversial, and further studies are necessary to explain the inconsistent results shown in the literature [11,12]. The effects of pristine SWCNT, SWCNT-COOH, and STX on cellular viability were evaluated using the MTT and Trypan blue assays. The MTT assay demonstrated that after 24 h, a significant decrease in viability of HT-22 cells coexposed to SWCNT+STX occurred compared with the SWCNT group (Figure 5). Studies have demonstrated that low concentrations of SWCNTs do not induce toxic effects. For example, in lung MSTO-211H cells and skin keratinocyte HaCaT cells, pristine SWCNTs did not demonstrate any cytotoxicity at concentrations of 2 μg mL^{-1} and 5 μg mL^{-1} [33].

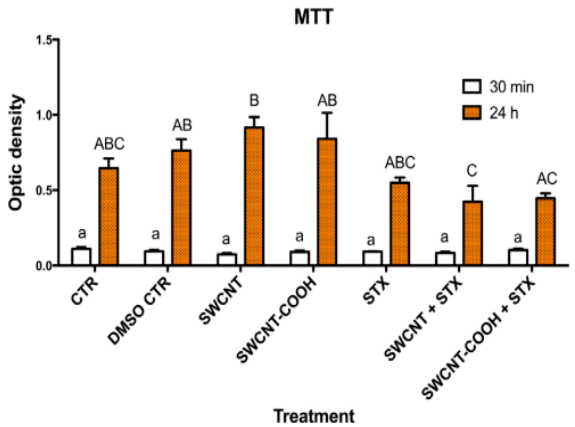

Figure 5. HT-22 cell proliferation measured by the 3(-4,5-dimethylthiazol-2-yl)-2,5-difenyltetrazolium (MTT) assay. Analyses were performed after exposures of 30 min (white bars) and 24 h (orange bars). Data are expressed as mean ± standard error of 3 independent experiments ($n = 6$). Similar letters indicate absence of significant difference ($p > 0.05$) at each time. CTR = control group; DMSO CTR = dimethyl sulfoxide control group; SWCNT = single-walled carbon nanotubes (5 μg mL^{-1}); SWCNT-COOH = SWCNTs functionalized with carboxylic acid (5 μg mL^{-1}); STX = saxitoxin (200 μg/L); SWCNT+STX = SWCNTs with saxitoxin; SWCNT-COOH+STX = SWCNTs functionalized with carboxylic acid with saxitoxin.

However, 2 major mechanisms of cytotoxicity have been widely considered to be induced by CNTs: endocytosis/phagocytosis and nanopenetration [12,13]. Indeed, in human macrophage cells, the cytotoxicity of SWCNTs was reported to be mediated via physical penetration into the cellular cytoplasm and localization within the nucleus [34]. Furthermore, SWCNTs have been reported to interact with various dyes commonly used to assess cytotoxicity, such as MTT [33], a factor that prompted us to use different measures of cell viability, even though other reports indicate that the binding of MTT–formazan to CNTs is negligible and does not influence the results [12,34]. A trypan blue assay of epithelial cells (A549) cultivated for 3 d and 5 d in the presence of 15 μg mL^{-1} SWCNTs indicated that cell viability was not affected [35]. In the present study, the results of the trypan blue assay demonstrated that HT-22 cell viability and proliferation were not affected by any of the treatments (Figure 6). Similarly, no differences in cell viability were observed (as measured by the MTT assay) in the neuroblastoma Neuro-2A cell line when exposed to 400 μg L^{-1} of STX [36]. Saxitoxins have an affinity for the voltage-gated sodium channel

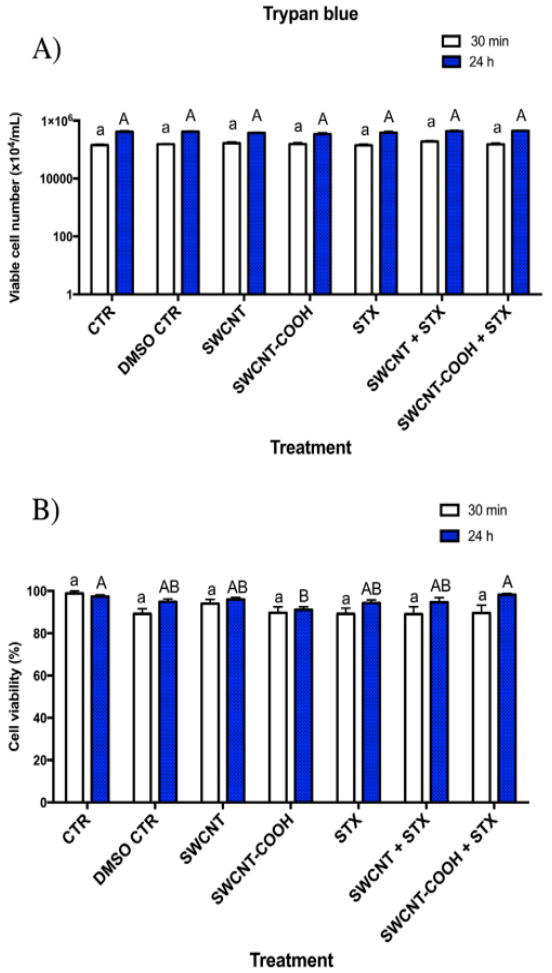

Figure 6. Viable cell number and cell viability (%) of HT-22 cells assessed by trypan blue exclusion assay. Analysis were performed after exposures of 30 min (white bars) and 24 h (blue bars). (**A**) Viable cell number and (**B**) cell viability (%). Data are expressed as mean ± standard error of 3 independent experiments ($n = 6$). Similar letters indicate absence of significant difference ($p > 0.05$) at each time. CTR = control group; DMSO CTR = dimethyl sulfoxide control group; SWCNT = single-walled carbon nanotubes (5 μg mL^{-1}); SWCNT-COOH = SWCNTs functionalized with carboxylic acid (5 μg mL^{-1}); STX = saxitoxin (200 μg/L), SWCNT+STX = SWCNTs with saxitoxin; SWCNT-COOH+STX = SWCNTs functionalized with carboxylic acid with saxitoxin.

present in excitable cells, such as neurons. [3,7]. However, the number of high- and low-affinity sites depends on the cellular system studied. Therefore, cells that contain a large number of voltage-dependent sodium channels can be expected to be highly sensitive to the effects of STX. Indeed, Neuro-2A cells have been shown to be a very sensitive model for the evaluation of STX–induced cytotoxicity [3,7,36]. According to our results, it is probable that the HT-22 cell line has a lower number of voltage-dependent sodium channels, as it showed a lower sensitivity to STX. However, cotreatment with STX and SWCNT induced a significant reduction in viability, highlighting the importance of evaluating the interaction of nanomaterials with environmental pollutants.

Accordingly, several studies have reported on the interaction between CNTs and contaminants [20,21]. For example, coexposure to fullerene (C_{60}) and microcystin induced oxidative stress in the gills of the fish *Cyprinus carpio* under ultraviolet radiation [37]. In another study, C_{60} provoked a loss in cellular viability when coadministered with benzo[*a*]pyrene at different

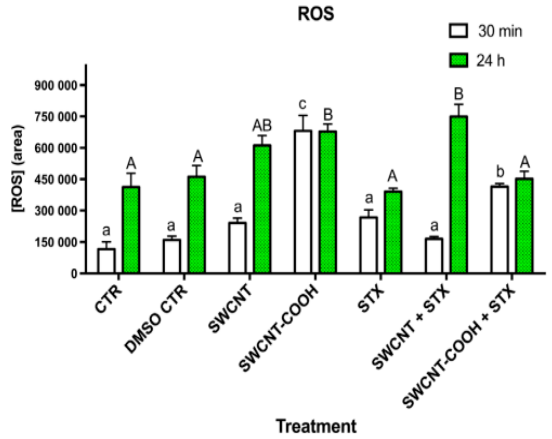

Figure 7. Intracellular reactive oxygen species (ROS) concentrations in HT-22 cells after exposures of 30 min (white bars) and 24 h (green bars). Data are expressed as mean ± standard error. Similar letters indicate absence of significant difference ($p > 0.05$) at each time ($n = 8$). CTR = control group; DMSO CTR = dimethyl sulfoxide control group; SWCNT = single-walled carbon nanotubes (5 μg mL^{-1}); SWCNT-COOH = SWCNTs functionalized with carboxylic acid (5 μg mL^{-1}); STX = saxitoxin (200 μg/L); SWCNT+STX = SWCNTs with saxitoxin; SWCNT-COOH+STX = SWCNTs functionalized with carboxylic acid with saxitoxin.

concentrations in a *Danio rerio* (zebrafish) hepatocyte cell line [21]. In the present study, results of ab initio simulation showed that a slight decrease in the Fermi gap energy occurred in all SWCNT configurations when interacting with STX. This decrease can, in turn, change the biological environment of the cell. Indeed, we observed that coexposure of SWCNT+STX induced a decrease in cell viability, as measured by the MTT assay. This result suggests that SWCNTs can change the bioavailability of STX, as evidenced by the differences in the

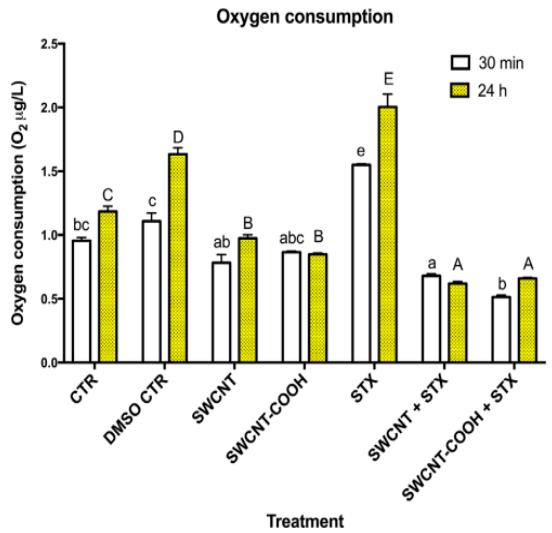

Figure 8. Oxygen consumption in HT-22 cells after exposures of 30 min (white bars) and 24 h (yellow bars). Data are expressed as mean ± standard error of 3 independent experiments ($n = 4$). Similar letters indicate absence of significant difference ($p > 0.05$). CTR = control group; DMSO CTR = dimethyl sulfoxide control group; SWCNT = single-walled carbon nanotubes (5 μg mL^{-1}); SWCNT-COOH = SWCNTs functionalized with carboxylic acid (5 μg mL^{-1}); STX = saxitoxin (200 μg/L); SWCNT+STX = SWCNTs with saxitoxin; SWCNT-COOH+STX = SWCNTs functionalized with carboxylic acid with saxitoxin.

effects of these molecules on cell viability when the cells were treated individually versus in combination.

Both in vitro and in vivo studies have reported that exposure to STX or CNTs causes oxidative damage and ROS generation [10,37]. In the present study, at both exposure times, SWCNT-COOH induced a significant increase in ROS generation in HT-22 cells (Figure 7). Similarly, SWCNTs did not influence mitochondrial activity and ROS production in breast cancer cell line MCF7 cells at concentrations between 5 $\mu g\,mL^{-1}$ and 80 $\mu g\,mL^{-1}$ [38]. However, coexposure with SWCNT-COOH and STX was able to attenuate the effects because of SWCNT-COOH alone, suggesting an antagonistic effect of the interaction between SWCNT-COOH and STX. In contrast, cotreatment with SWCNT and STX showed a synergistic effect in terms of ROS generation. In this regard, the results obtained in vitro corroborate the semiempirical evidence demonstrated using the density functional theory ab initio simulation. Carboxylation of SWCNTs was able to change the direction of the charge transfer, a change that can profoundly affect the biological environment. The variation in the direction of the charge transfer allowed an interaction between SWCNT-COOH and STX, with a concomitant decrease in ROS production compared with SWCNT-COOH alone.

Mitochondrial function requires the balanced interaction among many critical mitochondrial proteins, including cytochrome c, which is a key component of the mitochondrial respiration and plays an important role in mitochondrial electron transport and cell metabolism [39]. It also plays an important role in ROS clearance. Indeed, mitochondrial oxygen uptake was greatly decreased in human epithelial KB cells treated with SWCNT [39]. This result is consistent with our findings in HT-22 cells treated with SWCNT or SWCNT-COOH. The effects of CNTs on mitochondrial function and cellular respiration should be considered when using SWCNTs for different applications such as electrochemical biosensors for toxins, water analysis, or pharmaceutical carriers. Overall, our results demonstrated that oxygen consumption of HT-22 cells was increased by STX exposure for 30 min and 24 h (Figure 8). However, after 30 min and 24 h, the interaction between SWCNT or SWCNT-COOH and STX was able to antagonize the STX-induced increase in oxygen consumption. It is also important to note that, although an increase in ROS concentration was observed in cells treated with SWCNT, SWCNT-COOH, and SWCNT+STX, this increase was not correlated with mitochondrial respiration. The modulation of mitochondrial complexes I and III could be associated with decreased mitochondrial membrane potential, favoring ROS production, as observed for the SWCNT, SWCNT-COOH, and SWCNT-COOH+STX groups, compared with the control group (Figure 8). On the other hand, cellular responses to ROS injury usually occur in the first 24 h [7–9]. In addition, such mechanisms could be involved in CNT detoxification, as enzymatic degradation processes by enzyme peroxidases [39,40] or concomitant interaction phenomena of adsorption between the pristine SWCNT and SWCNT-COOH+STX that decrease the reactivity/toxicity of the CNTs, modulating or inducing the antioxidant defense in HT-22 cells.

CONCLUSIONS

The present study has demonstrated by ab initio theoretical analysis that the interaction between pristine and carboxylated SWNCTs with the STX molecule occurs through physisorption, and this effect could alter the environment of HT-22 cells after exposure to CNTs. In terms of the interaction of SWCNTs with STX, a decrease in cell viability was observed by using the MTT assay, whereas the SWCNT-COOH+STX treatment did not induce a decrease in cell viability. The ROS data showed a clearly different pattern of the interaction of CNTs with STX: SWCNT+STX had a synergistic effect, whereas SWCNT-COOH+STX induced an antagonistic effect. Finally, in terms of cellular oxygen consumption, both CNTs when coexposed with STX antagonized the toxic effect. Based on these results, it can be concluded that the in vitro results corroborate the semiempirical evidences found using the density functional theory ab initio simulation.

Acknowledgment—The authors thank the Brazilian agency CAPES, the laboratory technicians working at the Instituto de Ciências Biológicas (ICB), the Cyanobacteria and Ficotoxin Laboratory (LCF) at FURG, and the Centro Universitário Franciscano (UNIFRA). J.M. Monserrat and S.B. Fagan are productivity fellows from CNPq (process numbers PQ 307880/2013-3 and PQ 304583/2011-1, respectively). The present study was partly supported by funds from CNPq (552131/2011-3 and 452088/2015-1) given to J.M. Monserrat.

Conflict of Interest—The authors declare they have no conflicts of interest.

Data availability—Data, associated metadata, and calculation tools are available from the corresponding author (pattybramos@gmail.com).

REFERENCES

1. Wiese M, D'Agostino PM, Mihali TK, Moffitt MC, Neilan BA. 2010. Neurotoxic alkaloids: Saxitoxin and its analogs. *Mar Drugs* 8:2185–2211.
2. Zhang D, Hu C, Wang G, Li D, Li G, Liu Y. 2011. Zebrafish neurotoxicity from aphantoxins—Cyanobacterial paralytic shellfish poisons (PSPs) from *Aphanizomenon flos-aquae* DC-1. *Environ Toxicol* 28:239–254.
3. Perreault F, Matias MS, Melegari SP, Creppy EE, Popovic R, Matias WG. 2011. Investigation of animal and algal bioassays for reliable saxitoxin ecotoxicity and cytotoxicity risk evaluation. *Ecotoxicol Environ Saf* 74:1021–1026.
4. Yunes J, Cunha N, Barros L, Proença L, Monserrat JM. 2003. Cyanobacterial neurotoxins from Southern Brazilian freshwaters. *Comments Toxicol* 9:103–115.
5. Cervantes Cianca R, Pallares M, Barbosa R, Adan L, Martins J, Martinez A. 2007. Application of precolumn oxidation HPLC method with fluorescence detection to evaluate saxitoxin levels in discrete brain regions of rats. *Toxicon* 49:89–99.
6. Corbel S, Mougin C, Bouaicha N. 2014. Cyanobacterial toxins: Modes of actions, fate in aquatic and soil ecosystems, phytotoxicity and bioaccumulation in agricultural crops. *Chemosphere* 96:1–15.
7. Melegari SP, Perreault F, Moukha S, Popovic R, Creppy EE, Matias W. 2012. Induction to oxidative stress by saxitoxin investigated through lipid peroxidation in Neuro 2A cells and *Chlamydomonas reinhardtii* alga. *Chemosphere* 89:38–43.
8. Amado L, Monserrat J. 2010. Oxidative stress generation by microcystins in aquatic animals: Why and how? *Environ Int* 36:226–235.
9. Jones D. 2006. Disruption of mitochondrial redox circuitry in oxidative stress. *Chem Biol Interact* 163:38–53.
10. Ramos PB, Diehl F, Dos Santos JM, Monserrat JM, Yunes JS. 2014. Oxidative stress in rats induced by consumption of saxitoxin contaminated drink water. *Harmful Algae* 37:68–74.
11. Zhao X, Liu R. 2012. Recent progress and perspectives on the toxicity of carbon nanotubes at organism, organ, cell and biomacromolecule levels. *Environ Int* 40:244–256.
12. Fime CP III, Bandaru PR. 2010. Toxicity issues in the application of carbon nanotubes to biological systems. *Nanomed Nanotech Biol Med* 6:245–256.
13. Makoto E, Masashi G, Kazumasa H. 2015. A review of toxicity studies of single-walled carbon nanotubes in laboratory animals. *Regul Toxicol Pharm* 74:42–63.
14. Sharma R, Ragavan KV, Thakur MS, Raghavarao KSMS. 2015. Recent advances in nanoparticle based aptasensors for food contaminants. *Biosensors Bioelectron* 74:612–627.
15. Rhiem S, Riding MJ, Baumgartner W, Martin FL, Semple KT, Jones KC, Schaffer A, Maes HM. 2015. Interactions of multiwalled carbon nanotubes with algal cells: Quantification of association, visualization

of uptake, and measurement of alterations in the composition of cells. *Environ Pollut* 196:431–439.
16. Gan C, Ling L, He Z, Lei H, Liu Y. 2016. In-situ assembly of biocompatible core–shell hierarchical nanostructures sensitized immunosensor for microcystin-LR. *Biosensors Bioelectron* 78: 381–389.
17. Shvedova AA, Pietroiusti A, Fadeel B, Kagan VE. 2012. Mechanisms of carbon nanotube-induced toxicity: Focus on oxidative stress. *Toxicol Appl Pharm* 261:121–133.
18. Canesi L, Ciacci C, Balbi T. 2015. Interactive effects of nanoparticles with other contaminants in aquatic organisms: Friend or foe? *Mar Environ Res* 111:128–134.
19. Limbach LK, Wick P, Manser P, Grass RN, Bruinink A, Stark WJ. 2007. Exposure of engineered nanoparticles to human lung epithelial cells: Influence of chemical composition and catalytic activity on oxidative stress. *Environ Sci Technol* 41:4158–4163.
20. Costa CLA, Chaves IS, Ventura-Lima J, Ferreira JLR, Ferraz L, Carvalho LMD, Monserrat JM. 2012. In vitro evaluation of co-exposure of arsenium and an organic nanomaterial (fullerene, C_{60}) in zebrafish hepatocytes. *Comp Biochem Physiol C* 155:206–212.
21. Ferreira JLR, Lonné MN, França TA, Maximilla NR, Lugokenski TH, Costa PG, Filmmann G, Soares FAA, De la Torre FR, Monserrat JM. 2014. Co-exposure of the organic nanomaterial fullerene C_{60} with benzo[a]pyrene in *Danio rerio* (zebrafish) hepatocytes: Evidence of toxicological interactions. *Aquat Toxicol* 147:76–83.
22. Dal Bosco L, Weber GE, Parfitt GM, Cordeiro AP, Sahoo SK, Fantini C, Klosterhoff MC, Romano LA, Furtado CA, Santos AP, Monserrat JM, Barros DM. 2015. Biopersistence of PEGylated carbon nanotubes promotes a delayed antioxidant response after infusion into the rat hippocampus. *PLoS One* 10:30129156.
23. Bosi S, Fabbro L, Cantarutti C, Mihajlovic M, Ballerini L, Prato M. 2016. Carbon based substrates for interfacing neurons: Comparing pristine with functionalized carbon nanotubes effects on cultured neuronal networks. *Carbon* 97:87–91.
24. El-Orabi NF, Rogers CB, Edwards RH, Schwartz DD. 2011. Heat-induced inhibition of superoxide dismutase and accumulation of reactive oxygen species leads to HT-22 neuronal cell death. *J Therm Biol* 36:49–56.
25. Carneiro MA, Venezuela P, Fagan SB. 2008. First principles calculations of alanine radicals adsorbed on pristine and functionalized carbon nanotubes. *J Phys Chem C* 112:14812–14815.
26. Galano A, Francisco-Marquez M, Martinez A. 2010. Influence of point defects on the free radical scavenging capability of single-walled carbon nanotubes. *J Phys Chem C* 114:8302–8308.
27. Chen CM, Chen M, Leu F, Hsu SY, Wang SC, Shi SC. 2004. Purification of multi-walled carbon nanotubes by microwave digestion method. *Diam Relat Mater* 13:1182–1186.
28. Perdew JP, Zunger A. 1981. Self-interaction correction to density-functional approximations for many-electron systems. *Phys Rev B* 23: 5048–5079.
29. Wang F, Dukovic G, Brus L, Heinz T. 2004. Time-resolved fluorescence of carbon nanotubes and its implication for radiative lifetimes. *Phys Rev Lett* 92:1–4.
30. Zar JH. 1984. *Biostatistical Analysis*, 2nd ed. Prentice Hall, Upper Saddle River, NJ, USA.
31. Kawahara M, Kato-Nigishi M, Hosoda R, Imamura L, Tsuda M, Kuroda Y. 2003. Brain-derived neurotrophic factor protects cultured rat hippocampal neurons from aluminum maltolate neurotoxicity. *J Inorg Biochem* 97:124–131.
32. Dashti A, Soodi M, Amani N. 2016. Cr (VI) induced oxidative stress and toxicity in cultured cerebellar granule neurons at different stages of development and protective effect of rosmarinic acid. *Environ Toxicol* 31:269–277.
33. Hu X, Cook S, Wang P, Wang HM, Liu X, Williams QL. 2010. *In vitro* evaluation of cytotoxicity of engineered carbon nanotubes in selected human cell lines. *Sci Total Environ* 408:1812–1817.
34. Lanone S, Andujar P, Kermanizadeh A, Boczkowski J. 2013. Determinants of carbon nanotube toxicity. *Adv Drug Deliver Rev* 65:2063–2069.
35. Kaiser P, Buerki-Thurnherr T, Wick P. 2013. Influence of single walled carbon nanotubes at subtoxical concentrations on cell adhesion and other cell parameters of human epithelial cells. *J King Saud Univ Sci* 25:15–27.
36. Nicolas J, Bovee TFH, Kamelia L, Rietjens IMCM, Hendriksen PJM. 2015. Exploration of new functional endpoints in neuro-2a cells for the detection of the marine biotoxins saxitoxin, palytoxin and tetrodotoxin. *Toxicol In Vitro* 30:341–347.
37. Britto R, Flores JA, Mello DL, Porto CC, Monserrat JM. 2015. Interaction of carbon nanomaterial fullerene (C_{60}) and microcystin-LR in gills of fish *Cyprinus carpio* (Teleostei: Cyprinidae) under the incidence of ultraviolet radiation. *Water Air Soil Pollut* 226:2215.
38. Song M, Zeng L, Yuan S, Yin J, Wang H, Jiang G. 2013. Study of cytotoxic effects of single-walled carbon nanotubes functionalized with different chemical groups on human MCF7 cells. *Chemosphere* 92: 576–582.
39. Ma X, Zhang LH, Wang LR, Xue X, Sun JH, Wu Y, Zou G, Wu X, Wang PC, Wamer WG, Yin JJ, Zheng K, Lianh JG. 2013. Single-walled carbon nanotubes alter cytochrome c electron transfer and modulate mitochondrial function. *ACS Nano* 6:10486–10496.
40. Kagan VG, Konduru NV, Feng W, Allen BL, Conroy J, Volkov Y, Vlasova II, Belikova NA, Yanamala N, Kapralov A, Tyurina YY, Shi J, Kisin ER, Murray AR, Franks J, Stolz D, Gou P, Seetharaman JK, Fadeel B, Star A, Shvedova AA. 2010. Carbon nanotubes degraded by neutrophil myeloperoxidase induce less pulmonary inflammation. *Nat Nanotechnol* 5:354–359.

Manuscrito 1:

CYTOPROTECTION OF LIPOIC ACID AGAINST TOXICITY INDUCED BY SAXITOXIN IN HIPPOCAMPAL CELL LINE HT-22 THROUGH *IN SILICO* MODELING AND *IN VITRO* ASSAYS

Será submetido à revista **Environmental International**

(Fator de impacto: 5.929)

Graphical Abstract

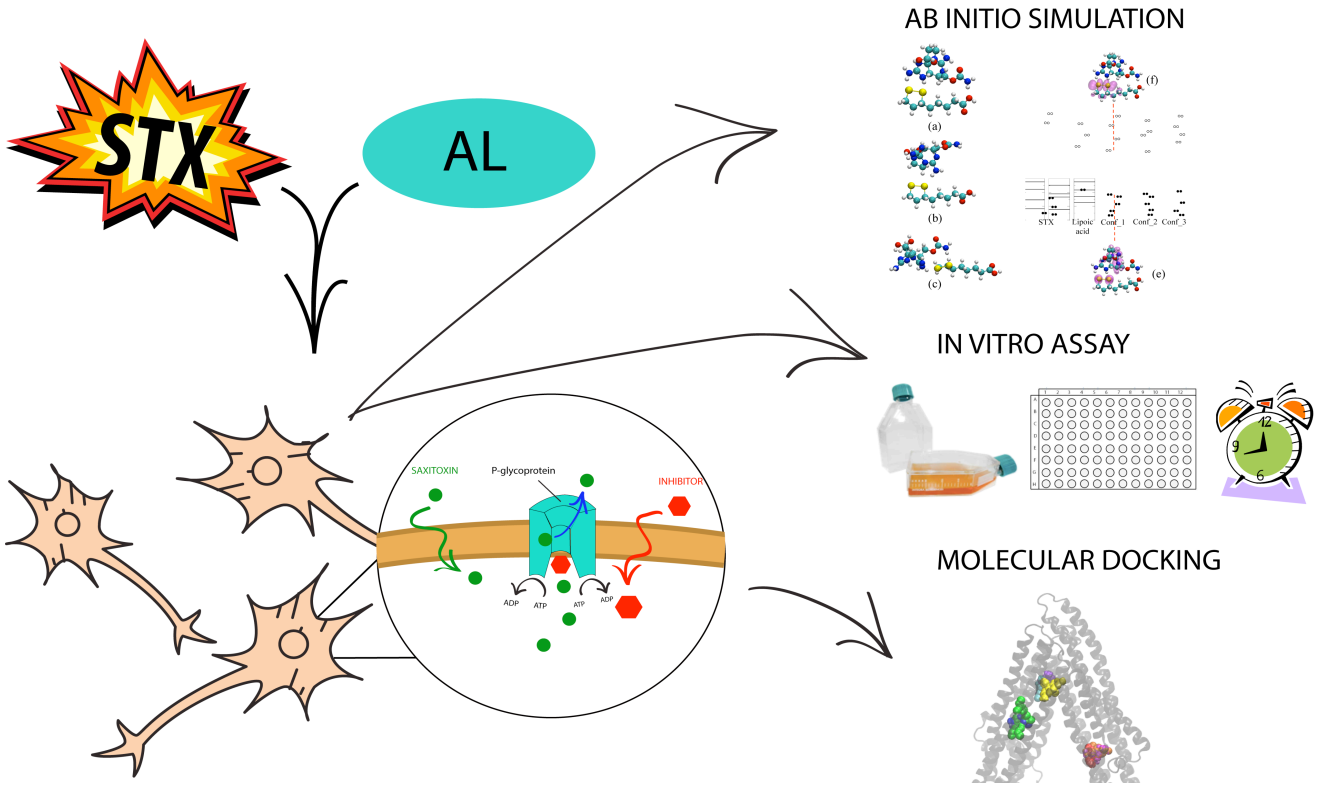

CYTOPROTECTION OF LIPOIC ACID AGAINST TOXICITY INDUCED BY SAXITOXIN IN HIPPOCAMPAL CELL LINE HT-22 THROUGH *IN SILICO* MODELING AND *IN VITRO* ASSAYS

Patrícia Ramos[a,b*], Marcos Schmitz[c], Sibele Gama[a], Aline Portantiolo[a,b], Michael Gonzalez Durruthy[a,b], Ana Paula de Souza Votto[a,b], Luisa Rodrigues Cornetet[d], Karina dos Santos Machado[d], Adriano Wehrli[d], Mariana Zancan Tonel[e,f], Solange Binotto Fagan[e,f], João Sarkis Yunes[c], José Maria Monserrat[a,b]

[a]Institute of Biological Science, Federal University of Rio Grande - FURG, Rio Grande, RS, Brazil

[b]Post-Graduate Program in Physiological Sciences - Rio Grande, RS, Brazil

[c]Cyanobacteria and Ficotoxin Laboratory, FURG, Rio Grande, RS, Brazil

[d]Center of Computational Science (C3), FURG, Rio Grande, RS, Brazil

[e]Franciscan University Center, UNIFRA, Santa Maria, RS, Brazil

[f]Post-Graduate Program in Nanoscience, UNIFRA, Santa Maria, RS, Brazil

*Address correspondence to pattybramos@gmail.com

Abstract

Saxitoxins (STXs) are potent neurotoxins that block voltage-gated channels in neurons and induce cytotoxicity through the generation of reactive oxygen species. The non-enzymatic antioxidant Lipoic acid (LA) represents an alternative to mitigate the deleterious effects induced by neurotoxins as STX. P-glycoprotein (P-gp) is a well-known ATP-binding cassette (ABC) transporter and represents a crucial role in the uptake and distribution of toxic substances, decreasing the accumulation and potential intracellular effects in virtue of its broad substrate specificity, its expression in many excretory tissues and its large efflux capacity. The interaction of STX with LA was evaluated by *ab initio* simulation, molecular docking and bioassays using the cell line HT-22. Cells were exposed to STX and LA for 30 min and 24 h. The interaction of STX with LA occurs by physisorption. LA treatment minimizes STX cytotoxicity, evaluated by trypan blue and MTT assay. For the first time it has been shown that the HT-22 cell line express glycoprotein-P (P-gp). Both STX and STX-LA treatments

were efficient to induce P-gp extrusion activity by rhodamine 123 (Rho 123) dye extrusion, induced low reactive oxygen species levels and low oxygen consumption. The LA treatment efficiently induced an increase in levels of antioxidant glutathione and high levels of protein sulfhydryl groups were also observed. Molecular docking suggests that STX can be the substrate of P-gp and, estimating the Free Energy of Binding (FEB), LA has lower amino acids residues binding sites, similar to verapamil, while STX and STX+LA_1 have similar amino acids residues and binding sites with similar FEB between this ligands. Based on these results, it can be concluded that LA was able to induce cytoprotection and the STX+LA interaction minimizes effects of toxicity induced by STX. The results obtained in vitro corroborate the semi-empirical evidence found using density functional theory *ab initio* simulation and molecular docking.

Keywords: neurotoxin, antioxidant, molecular docking, P-glycoprotein

1. Introduction

The increasing frequency of blooms of cyanobacteria producing cyanotoxins in fresh, brackish and marine water has become a growing problem worldwide, especially in Brazil (Zabaglo et al., 2016). Studies concerning the toxicity of Saxitoxin (STX), a neurotoxin produced by freshwater cyanobacteria such as *Cylindrospermopsis raciborskii*, have demonstrated high toxicity in mammal cells, especially in brain cells (Ramos et al., 2016; Takser et al., 2016), since they can cross the blood-brain barrier (BBB) (Cervantes et al., 2009). STX analogues presented a diverse toxicity: the most potent toxins are saxitoxins (STX), neosaxitoxin (Neo-STX) and gonyautoxins (GTX) (Ramos et al., 2014; Silva et al., 2014).

STX is toxic because it can block voltage-gated sodium channels and can also bind to calcium (Ca^{+2}) and potassium (K^{+}) channels in neurons, altering the membrane's selective permeability and the flow of ions, disrupting cellular homeostasis (Corbel et al., 2014; Zheng et al., 2015). STX can be harmful to cells components through the formation of reactive oxygen species (ROS), promoting

significant changes in the antioxidant defense system (Ramos et al., 2016, 2014; Zheng et al., 2015) and leading to a situation of oxidative stress, common to several cyanotoxins (Amado et al., 2009; Amado and Monserrat, 2010; da Silva et al., 2011; O'Neill et al., 2016; Ramos et al., 2016, 2014), which may oxidize unsaturated lipids in cell membranes, proteins and DNA, contributing to their toxicity (Contardo-Jara et al., 2008).

In this kind of pro-oxidative situation, the use of non-enzymatic antioxidants such as lipoic acid (LA) represents an alternative to mitigate the deleterious effects induced by neurotoxins as STX. LA is well known as a cofactor of mitochondrial dehydrogenases, being a hydro and liposoluble molecule with chemo and neuroprotective capacity, due to its ability to cross the BBB, considered as an "universal antioxidant" (Gorąca et al., 2011; Packer et al., 1995). LA and its reduced form, dihydrolipoic acid (DHLA), have several properties including their capacity to chelate metals, to scavenge ROS, to express important genes in antioxidants defense system and to interact with other antioxidants (Hiller et al., 2016; Longaray-Garcia et al., 2013; Monserrat et al., 2008).

Many studies in the last years have reported the neuroprotective potential of LA after oxidative stress induction in several *in vitro* and *in vivo* models. For example, it was observed an increase in antioxidants defense in brain and liver of fish *Corydora paleatus* fed with a diet supplemented with LA, as well as the reduction of ROS production in the brain, and low levels of oxidized proteins in muscle and liver (Monserrat et al., 2008). The results of other studies showed that the oxidative damage and inflammation caused by pesticides like dimethoate, glyphosate and zineb were reverted by LA in rat brain (Astiz et al., 2012), suggesting that LA administration is a promising therapeutic strategy. In addition, LA induces an increase in the activity of enzyme glutathione-S-transferase (GST) in brain, reverting the inhibitory effect triggered by microcytins on these enzymes in the liver of common carp (Amado et al., 2011). Indeed, GST is involved in the metabolism of glutathione

(GSH) and takes part in phase II xenobiotic metabolizing reactions, responsible for eliminating EAO (Pamplona and Costantini, 2011; Zhang et al., 2010).

The mouse hippocampal line HT-22 is frequently studied to investigate chemoprevention approaches through neurotoxicity associated with oxidative stress. Indeed, LA prevents ethanol induced protein oxidation in mouse hippocampal HT-22 cells (Pirlich et al., 2002). Kling et al. (2014) showed cytoprotection mediated by different types of flavonoids in the hippocampal HT-22 line after induction of oxidative stress with tert-butyl hydroperoxide. However, to date, still there is no bibliography showing the modulation of the antioxidant system LA in cell line HT-22 exposed to STX, which certainly indicates the need for information about it, considering the neurotoxicity elicited by this toxin.

At the cellular level, the balance between absorption and efflux transporters that facilitate their movement through cell membranes determines the availability of endogenous substances, drugs, and xenobiotics (Silva et al., 2015). These transporters are important for maintaining cellular homeostasis and for detoxifying potentially toxic substances (DeGorter et al., 2012; Silva et al., 2015). P-glycoprotein (P-gp), a well-known ATP-binding cassette (ABC) transporter, is responsible for the multidrug resistance phenotype (Lacher et al., 2015; Muthusamy et al., 2016), acting as an extrusion pump for anti-cancer drugs and other compounds out of the cell (Amé et al., 2009; Han et al., 2008; Muthusamy et al., 2016). P-gp is a 170 kDa membrane protein with 1280 amino acids residues (Kim et al., 2014), it is composed of two homologous halves, where each half part begins with a transmembrane domain (TMD) with six transmembrane (TM) segments followed by a nucleotide-binding domain (NBD) (Loo and Clarke, 2017).

P-gp is expressed in many tissues and cell cultures of mammals, as well as in endothelial cells lining the blood capillaries present in the brain blood barrier (Silva et al., 2015), being one of the major factor in limiting the entry of xenobiotics in the brain, such as neurotoxins. In fact, P-gp represents a crucial role in the uptake and

distribution of toxic substances, decreasing the accumulation and potential intracellular effects in virtue of its broad substrate specificity, its expression in many excretory tissues and its large efflux capacity (Han et al., 2008; Muthusamy et al., 2016; Silva et al., 2015).

P-gp has ecotoxicological importance, being a key component of multixenobiotic resistance (MXR) for organisms in polluted environments, through the increase in P-gp expression that restricts xenobiotic uptake (Kennedy et al., 2014). Indeed, P-gp expression is involved in the excretion of cyanotoxin microcystin in the gills of the mussel *Dreissena polymorpha* (Contardo-Jara et al., 2008) as also in liver, gills, and brain of fish *Jenynsia multidentata* (Amé et al., 2009). The MDR phenotype Lucena cell line when exposed to microcystin demonstrated higher antioxidant competence and also by the higher α-tubulin content (de Souza Votto et al., 2007). However, there is a lack of study regarding P-gp activity and/or expression after exposure to STX, a mechanism that may play an important role in protection of cells against the harmful effects caused by these neurotoxins.

In the last years, *in silico* techniques, as density functional simulation (DFT) and molecular docking have been proposed to predict the potential toxicity of xenobiotics and their consequences in several cellular and subcellular targets. Based on this idea, Ramos et al. (2016) showed that the interaction of single-walled carbon nanotubes with STX occurs by physisorption process and antagonized the toxin effect promoting biological responses in hippocampal cell line HT-22. By the other hand, molecular docking simulation is a computational technique used to evaluate the interaction between a macromolecule (receptor) and a small molecule (ligand) (Trott and Olson, 2009; Zhao and Caflisch, 2015). We hypothesized that STX can act as the substrate to P-gp protein from the blood brain barrier in the nervous system. Therefore, P-gp can pump the STX out of the cell, being able to prevent or minimize the perpetration in the integrity of hippocampal neuronal cells. Besides, LA should lower the deleterious effects caused by STX. Indeed, Monserrat et al. (2014)

observed that co-treatment with LA was able to induce of P-gp expression in the fish *Jenisia multidentate* after exposure to endosulfan. To the best of our knowledge, there are no experimental or *in silico* evidences demonstrating P-gp activity after STX exposure in mouse hippocampal cell line HT-22.

In this context, the main objective of the present study was to investigate the role of lipoic acid in the by cellular assays in hippocampal HT-22 cell line. Appraising the potential interactions between STX and LA by using theoretical approaches, basing density functional theory calculations and molecular docking simulation.

2. Materials and Methods

2.1. Cell culture

An immortalized mouse hippocampal neuronal cell line HT-22 was a generous gift from Salk Institute for Biological Studies (San Diego, CA, USA). Briefly, cells were maintained at 37 °C and 5% CO_2 in Dulbecco's modified Eagle's medium containing high glucose, (DMEM) (Sigma) and supplemented with sodium bicarbonate (1.5 g/L; Vetec), 10% fetal bovine serum (Invitrogen) and 1% antibiotics and antimycotics (100 U/mL penicillin, 100 µg/mL streptomycin; Gibco and 0,25 µg/mL amphotericin; Gibco). Cells passed by trypsinization every two days. The cells were maintained in a way that did not exceed 80% confluence.

2.2 Exposure conditions

To perform the assays, the cells (5×10^4 cells/mL) were previously transferred to 24-well or 96-well plates for cell culture, followed by a 24-h period for cell attachment. The plates were washed with phosphate-buffered saline (PBS) and cells were exposed to 30 min or 24 h to the following treatments: two control groups, one containing DMEM medium and the other containing DMEM+ Dimetilsulfoxide (DMSO) (1%); STX (200 µg/L); LA (50 µM) and the interaction between toxin and antioxidant (STX+LA). In this case, DMSO has been used as a solvent for LA, The

STX and LA concentrations were sub-lethal and were selected after performing range-finding tests. The treatments were carried out in quadruplicate or sextuplicate. Each experiment was repeated independently 3 times, performed at 70% to 80% confluence.

2.3. Source of toxins

Cells of *C. raciborskii* from the Cyanobacteria and Ficotoxin Laboratory (FURG) culture collection were cultured in ASM-1 medium at 25 ± 1 °C and employed as a source of STX (Gorhan et al., 1964), the strain produces variants of neosaxitoxin, dc-saxitoxin and STX detected by liquid chromatography with fluorescence detection (HPLC–FLD, Shimadzu, CBM-20A) which were analyzed and compared with the five commercial standards of STXs (NRC, Canada). All experiments used working concentration of 200 µg/L prepared in culture medium (Ramos et al., 2016).

2.4. Lipoic acid solution

The α-lipoic acid racemic (Sigma-Aldrich) was diluted in DMSO. The working concentration of 50 µM was prepared by dilution in culture medium.

2.5. Ab initio calculations of STX-LA interaction

The properties of the interaction of STX with LA were evaluated through a zeta base plus polarization (DZP) defined to describe the pseudo-orbitals. To represent the electronic load in its real space, 200 Ry of the cutting grid was used. The atomic structures were relaxed until the residual forces were less than 0.05 eV/Å for all atoms. For the exchange and correlation potential, a local density approximation was used with the parameterization of Perdew and Zunger (1981). The binding energy was calculated using the base overlap error correction (BSSE) (Boys and Bernardi, 1970), according to the following equation 1:

$$E_b^{BSSE} = -\left[E(A+B) - E\left(A+B_{ghost}\right) - E\left(A_{ghost}+B\right)\right] \quad (1)$$

The system A corresponds to STX, and system B is LA. They were calculated with their corresponding atomic basis and with the A {B} atomic basis centered at the B {A} atomic positions. The subscript ghost refers to the atomic basis placed on the STX or LA positions but without atomic potentials representing real atoms at these positions. The system with positive binding energies implies attractive interaction. Similar computational procedures were done in a previous study of our group (Ramos et al., 2016). We evaluate the electronic properties through the difference between HOMO (highest occupied molecular orbital) and LUMO (lowest unoccupied molecular orbital).

2.6. Cell viability assays

Trypan Blue assay: The number of viable cells and cell viability were assessed by trypan blue (Gibco) exclusion assay. HT-22 cells ($5x10^4$ cells/mL) were plated into 96-well microtitre plates. After the exposure period (30 min or 24 h) with the treatments detailed in the Exposure conditions section, the wells were washed once with PBS, passed by trypsinization, an aliquot of 50 µL of cell suspension was mixed with 50 µL of trypan blue and cells were counted immediately on a Neubauer chamber.

MTT assay: The cell viability was also analyzed in presence or absence of verapamil (VP), considered a classical P-gp inhibitor. HT-22 cells ($5x10^4$ cells/mL) were plated into 96-well microtitre plates and treated as detailed in the Exposure conditions section, with or without verapamil (VP). Briefly, it was added 10 µL of VP (30 µM) in treatments with VP and 10 µL of sterile water in treatment without VP. After the exposure period (30 min or 24 h), it was added 20 µL of 3(-4,5-dimethylthiazol-2-yl)-2,5-difenyltetrazolium (MTT) (5 mg/ml) and following 3 h of incubation at 37 °C, the resultant formazan crystals were solubilized in 200 µL of DMSO. The absorbance

(540 nm) was determined using a spectrophotometer plate reader (ELX 800 Universal Microplate Reader; Bio-TEK).

2.7. Rhodamine 123 efflux assay

This technique is based on the adapted methodology reported by Carrett-Dias et al. (2016) and Daflon-Yunes et al. (2013). P-gp transport activity was investigated using the fluorescent probes Rhodamine 123 (Rho) in an efflux assay. In brief, after the exposure period (30 min or 24 h) with the treatments detailed in the Exposure conditions section, HT-22 cells ($5x10^4$ cells/mL) were incubated with Rho 123 (300 ng/mL) for 60 min at 37 °C in an atmosphere of 5 % CO_2. This incubation was performed in presence or absence of VP (30 µM, Sigma). After the incubation, the cells were washed and re-incubated with or without VP for more 60 min, in the absence of the dye, to allow its extrusion. After this, cells were washed with PBS and dye accumulation was assessed immediately. Excitation/emission values were determined using a multiwall plate reader (ELX800 Universal Microplate Reader; Bio-TEK) at 485/590nm.

2.8. Measurement of intracellular ROS concentration

Intracellular reactive oxygen species (ROS) were detected using the fluorogenic compound 2'7'-dichloro-fluorescin diacetate (H_2DCF-DA; Sigma) following the methodology described by Ramos et al. (2016). After the exposure period (30 min or 24 h) with the treatments detailed in the Exposure conditions section, HT-22 cells ($5x10^4$ cells/mL) were washed with PBS and then stained with 40 µM H2-DCF- DA for 30 min at 37 °C in the dark. Cellular fluorescence was quantified over 90 min at 37 °C by a fluorometer (Victor 2; PerkinElmer) equipped with a microplate reader, at an excitation wavelength of 485 nm and an emission wavelength of 520 nm.

2.9. Cellular oxygen consumption

For measurement of oxygen consumption, HT-22 cells ($5x10^4$ cells/mL) were seeded into 24-well culture plates. After the exposure period (30 min or 24 h) with the treatments detailed in the Exposure conditions section, the continuous monitoring of HT-22 cell oxygen consumption was measured by a Clark-type electrode (Oxygraph System Hansatech Instruments) in a 2-mL glass chamber equipped with a magnetic stirrer as previously described by González-Durruthy et al. (2016) and Ramos et al. (2016).

2.10. Measurement of intracellular reduced glutathione (GSH) and protein sulfhydryl groups (P-SH) concentration

The method was based in the methodology reported by Chen et al. (2008) and White et al. (2003). After the exposure period (30 min or 24 h) with the treatments detailed in Section 2.2, HT-22 cells' pellets ($5x10^4$ cells/mL) were re-suspended in PBS and their proteins were precipitated with trichloro acetic acid (TCA, 5%). After, the samples were then centrifuged at 20,000 × g during 10 min at 4 °C. The supernatant, containing reduced glutathione (GSH) was kept and the pellet, containing proteins, was re-suspended with 120 µL of PBS. Both GSH and P–SH were detected using 2,3 naphthalene dicarboxialdehyde (NDA, Invitrogen) that forms a fluorescent conjugate. An aliquot of 20 µL of the supernatant or pellet was transferred to specific microplates for fluorescence detection, 180 µL NDA was then added to all wells, and after 30 min of incubation, the fluorescence intensity of the NDA-GSH complex was quantified by a fluorometer (Victor 2; PerkinElmer) (excitation wavelength: 485 nm; emission wavelength: 520 nm). A standard curve of GSH (range: 0.015–20 µM) was prepared and data expressed in terms of µmoles of GSH equivalents/mg of proteins. The total protein content was determined in triplicate using a commercial kit (Doles Brazil) (590 nm), and a microplate reader (BioTek LX 800).

2.11. Molecular docking

There are different software to perform molecular docking simulations, among them, Autodock Vina stands out due to its efficiency and multithreading (Trott and Olson, 2009). Given the tridimensional structures of a receptor, a ligand, and a parametrized simulation box, Autodock Vina is capable of estimating the Free Energy Binding (FEB). A more negative value of FEB (kcal/mol) implies a higher affinity between the receptor (P-gp glycoprotein) and the ligand (Rhodamine 123, verapamil, lipoic acid, saxitoxin, neo-saxitoxin, and STX+LA interaction). The simulation box is used to delimited the search space of the protein by the ligand.

We performed molecular docking experiments with Autodock Vina and Autodock Tools (Morris et al., 2009) to predict the interactions between the P-gp glycoprotein with STX, LA and the interaction STX+LA. To perform molecular docking simulations the *Mus musculus* P-gp protein structure was obtained from the *RCSB Protein Data Bank* (PDB) ID: 4KSB (Ward et al., 2013). According to Subhani et al. (2015), mouse MXR1 (PDB ID: 4KSB) is the best template for modeling with a sequence identity 84% homolog to human MDR1. The ligands structures were obtained from PubChem (Bolton et al., 2008) (Saxitoxin PubChem CID:37165; NeoSaxitoxin PubChem CID:104753; Lipoic acid PubChem CID:864; Rhodamine 123 Pubchem CID:65217; Verapamil PubChem CID:2520). We also considered in the experiments three different STX-LA complexes as pdb model structure, obtained from *ab initio* results. Before executing the docking simulations, we used the Autodock Tools to prepare the P-gp protein structure, converting the PDB input file format to PDBQT format, removing water molecules, and other co-crystallized ligand molecules. Besides, we performed the inclusion of hydrogens atoms and the addition of partial charges to the P-gp protein also using Autodock Tools. To perform the experiments, we used one simulation box that determinates the searching area for the ligands. This theoretical procedure was performed using the P-gp grid-box size

with dimensions of X=65 Å, Y =40 Å, Z =45 Å and a center coordinates of X=55 Å, Y=-10 Å, Z=20 Å to evaluate the STX and LA interactions with P-gp. After the determination of the P-gp grid box, Autodock Vina was run to perform the molecular docking experiments, setting the parameter *exhaustiveness* set to 128. To analyze the receptor-ligands interactions (Rhodamine 123, verapamil, lipoic acid, saxitoxin, neo-saxitoxin, and STX+LA interaction) the software LigPlot (Laskowski and Swindells, 2011) was employed. To prepare all the files, and generate the PDB-input files for LigPlot, we used a Framework for Virtual Screening (Seus et al., 2015). This framework allows to configure the experiments on a web interface and download a python script, which runs the entire experiment including all the modules for performing Autodock Tools, AutoDock Vina and Ligplot.

2.12 Statistical analysis

Data from each treatment (CTR, CTR DMSO, STX, AI and STX+AL) were expressed as mean ± 1 standard error and analyzed with one-way ANOVA, for each exposure time (30 min or 24 h). Assumptions of variance homogeneity and normality were checked and mathematical transformations were applied if at least one of them was violated. Mean comparisons of treatments were performed using Newman–Keuls test. A *p* value lower than 0.05 was considered statistically significant.

3.Results

3.1 Prediction of STX and LA interaction

Three different configurations were analyzed to study the interaction between STX and LA **(Figure S1a-c; supplementary material)**. The binding energy, charge transfer, shortest distance between atoms and the HOMO/LUMO difference values are shown in material supplementary **(Table S.1; supplementary material)**.

The most stable configuration is STX+LA_1, with a binding energy of 0.69 eV, charge transference from LA to the STX of -0.12e^{-}, and the shortest distance of 1.85

Å. **Figure S.1 (d)** shows the energy levels of the systems studied, as well as the load plot in HOMO **(Figure S.1 (e))** and LUMO **(Figure S.1 (f))**. The isolated STX molecule presents a HOMO/LUMO 4.30 eV difference, and LA presents 2.47 eV. In the interaction between two systems we observed that there is a slight increase in the HOMO/LUMO difference in relation to the isolated LA. The most stable configuration (STX+LA_1) has a HOMO/LUMO difference of 2.56 eV. We observed in the plot of the HOMO charge **(Figure S.1 (e))** that the charge is on the sulfur atoms of LA and on the STX, and LUMO **(Figure S.1 (f))** mainly on the sulfur atoms of LA.

3.2 Effects of STX and LA on cell viability and P-gp activity

Trypan blue exclusion was used to determine the number of viable cells and the cell viability present in a cell suspension, based on the principle that live cells possess intact cell membranes that avoid penetration of trypan blue. Proliferation of HT-22 cells was not affected by any treatment after either 30 min or 24 h ($p > 0.05$; **Figure 1A**). In addition, a decrease ($p < 0.05$) of HT-22 cell viability by trypan blue was observed in STX treatment after 30 min exposure **(Figure 1B)**.

Cell viability was determined by MTT assay in presence or absence of verapamil (VP) to evaluate if the saxitoxin acts as a substrate for the P-gp pump. The results of cell viability by verapamil are given in **Figure 2**. HT-22 cells viability was not affected by any treatment after 30 min exposure ($p > 0.05$). However, exposure of HT-22 cells to STX with VP for 24 h decreased ($p < 0.05$) cell viability, suggesting that STX is behaving as substrate for the P-gp pump. In contrast, an increase ($p<0.05$) in HT-22 cell viability was observed in co-exposure STX+LA with VP when compared to STX_VP treatment, indicating that LA treatment minimizes STX toxicity against HT-22 cells. Indeed, exposure of HT-22 cells to LA for 24 h increased ($p < 0.05$) cell viability, but it was observed a decrease ($p < 0.05$) in HT-22 cells viability

after exposure of LA with VP, probably indicating that the solvent used for LA (DMSO) can promote toxic effect when the P-gp pump is not functional or is inhibited by VP, for example. Note that the same effects were observed when cells were exposed to DMSO+VP (**Figure 2**).

The results of P-gp activity by rhodamine 123 (Rho) dye extrusion are presented in **Figure 3**. After 30 min of HT-22 cells exposure, it was observed a higher ($p < 0.05$) Rho accumulation in LA, STX, STX+LA and DMSO ctr_VP treatments when compared to the control group, suggesting possible P-gp activity inhibition. In contrast, after 24 h of exposure of HT-22 cells, STX treatment induced P-gp extrusion activity and a decrement ($p < 0.05$) of accumulated Rho was observed. Nevertheless, LA treatment was the most efficient to promote P-gp extrusion activity with a markedly decrease ($p < 0.05$) of accumulated Rho after 24 h of exposure. This effect was also observed in the STX+LA treatment ($p < 0.05$).

3.3 Determination of ROS and oxygen consumption

The results of intracellular concentration of ROS and oxygen consumption by HT-22 cells are given in **Figure 4**. ROS intracellular concentration of HT-22 cells was not affected by treatments after 30 min ($p > 0.05$) (**Figure 4A**). After 24 h of exposure it was observed a decrease ($p < 0.05$) on ROS concentration in cells from LA and LA+STX treatments. **Figure 4B** shows a significant increase ($p < 0.05$) of oxygen consumption by STX treatment after 30 min of exposure. In contrast, LA treatment induced a decrease in the oxygen consumption of cells ($p < 0.05$) when compared with DMSO Ctr. This effect was also observed in the STX+LA treatment, but even more pronounced ($p < 0.05$). After 24 h exposure, the LA treatment induced an increase ($p < 0.05$) in the oxygen consumption of HT-22 cells.

3.4 Concentrations of reduced glutathione (GSH) and levels of protein sulfhydryl groups (P-SH)

Results of reduced glutathione (GSH) levels and levels of P-SH in HT-22 cells are shown in **Figure 5**. GSH concentration of HT-22 cells was not affected by any treatment after 30 min ($p > 0.05$). However, after 24 h of exposure, LA treatment induced an increased ($p < 0.05$) GSH concentration (**Figure 5A**). Levels of P-SH were not affected by any treatment after 30 min exposure ($p > 0.05$). In contrast, LA treatment induced ($p < 0.05$) higher levels of P-SH in HT-22 cells (**Figure 5B**).

3.6 Results of molecular docking

The interaction of STX, LA and STX+LA ligands (for the three complexes obtained from *ab initio* experiments that were transformed to pdb-format) with P-gp (PDB ID: 4KSB) was evaluated by molecular docking simulations. The ligands names and binding characteristics are depicted in **Table S.2** (**supplementary material**) and the final positions of these ligands after docking simulations on the structure of P-gp protein are shown on **Figure 6**. In Table S.2 and figure 7 we describe the amino acid residues of P-gp protein that stablish non bonded and/or H-H bonded interactions with each ligand. A variety of chemicals have been reported as P-gp substrates, such as verapamil (VP) and Rhodamine 123 (Rho 123). VP is a potent blocker of P-gp and Rho 123 is a nontoxic lipophilic cationic fluorescent that allocates in mitochondria and is efficiently effluxed by P-gp. In this study, VP and Rho 123 were used as control and both ligands presented a higher estimated free energy of binding and do not have amino acid residues interacting with P-pg like the other molecules (**Table S.2**). A lower FEB was observed for LA (-5.0 Kcal/mol) when compared with the remaining ligands, but LA has amino acids residues binding sites like verapamil (**Figure 7**). It was observed higher FEB value for STX+LA_1 complex when compared to complexes 2 and 3, LA, STX and Neo-STX ligands alone **(Table S.2).** STX+LA_1 has amino acids residues binding sites similar to STX (**Figure 8**). The Neo-STX, STX+LA_2 and STX+LA_3 showed intermediate values of FEB and have amino

acids residues binding sites similar to each other (**Figure S.2; supplementary material**).

4. Discussion

The brain is an organ with high metabolic demand and STXs are neurotoxins that have been reported by the ability to block voltage-gated ions channels (Corbel et al., 2014; Zheng et al., 2015). Indeed, STX has the pharmacokinetics widespread distribution as neuronal organs, which allows its great ability to cross the BBB (O'Neill et al., 2016), causing changes in the antioxidant mechanisms, what makes this organ vulnerable to oxidative stress and affect neurodevelopment in several organisms (Perreault et al., 2011; Ramos et al., 2016). Multi xenobiotic resistance (MXR) proteins have been identified in different cell types providing an effective mechanism in cell defense against accumulation of various xenobiotics (Szewczyk et al., 2015). In this context, P-gp is an ATP-dependent efflux pump with broad substrate specificity able to affect the bioavailability, pharmacokinetics and efficacy of cytotoxic chemicals as cyanotoxins (Contardo-Jara et al., 2008; Subhani et al., 2015).

Following this idea, defense strategies against oxidative stress play an important role in neuronal damage. The use of the natural metabolic antioxidant LA can induce potential protective effects by preventing or slowing down the oxidation caused by other molecules and increasing the expression of antioxidant enzymes (Dwivedi et al., 2014; Kling et al., 2014). In this present study, we investigated the possible cytoprotective effects induced by LA during concomitant exposure to saxitoxin. The interaction of LA with STXs was evaluated by the density functional theory, using *ab initio* simulation. Posteriorly, we have performed modeling of P-gp, investigated its docking to STX, LA and STX+LA, and relied upon the question that STX and LA could be P-gp substrates.

Now-a-days, computational models provide fast, inexpensive, and non-

laborious promising and valuable results (Zhao and Caflisch, 2015). The role of lipoic acid in the chemoprevention against saxitoxin induced cytotoxicity was evaluated by bioassays using the hippocampal cell line HT-22. *Ab initio* results (**Figure S.1, supplementary material**) indicated the interaction between LA and STX and the complex 1 is the more stable configuration, possessing a higher binding energy and a smaller binding distance among the atoms. The results indicated a weak interaction between STXs and LA. From the HOMO and LUMO it is observed a small amount of shared electronic charge between these systems, also corroborating the binding energy and charge transfer indicating a physisorption interaction method for the STX-LA complexes.

Studies using *in vitro* cellular models are important components towards the understanding of relevant molecular and cellular processes (Alboni et al., 2014; Liu et al., 2009; Nicolas et al., 2015). In this context, HT-22 murine hippocampal neuronal cell line possesses important characteristics to investigate neurotoxicity as sensibility to a variety of metabolites and cholinergic properties (Alboni et al., 2014). Because this, HT-22 cells are used as a hippocampal cell model to investigate molecular mechanisms, neurotoxicity induced by xenobiotics, or neuroprotective effects induced by natural products with potential neuroprotective agents, as lipoic acid (Nguyen et al., 2014). The results of the Trypan blue assay (**Figure 1**) demonstrated that HT-22 proliferation was not affected by any treatment. However, after 30 min, a significant decrease in the viability of HT-22 exposed to STX treatment was noticed, a result not observed for STX+LA.

Therefore, there is the possibility that LA may play a role in cytoprotection against the effects of saxitoxins. Besides that, as the cellular defense mechanism, the activity of the P-gp pump may be involved in this cytoprotection process. Although the biological effects of LA have been intensively studied, it is not yet clear whether the neuroprotective effect of LA against STX in HT-22 cell is mediated by the P-gp pump activity, or the modulation of the antioxidant defense system. Indeed, the

results of the cell viability by MTT assay after 24 h of exposure showed a decrease in HT-22 viability after exposure to STX treatment and in presence of verapamil (**Figure 2**), indicating that STX is a P-gp substrate. The LA treatment was able to increase the cell viability and the co-exposure STX+LA minimized the STX toxicity. Different studies indicate that cyanotoxins, as microcystin and okadaic acid, possess the ability of inducing P-gp activity (Amé et al., 2009; Contardo-Jara et al., 2008; Ehlers et al., 2014), supporting the hypothesis that P-gp is involved in the excretion of cyanotoxins.

Recent studies have demonstrated that the cellular Rho 123 accumulation in the presence or absence of P-gp modulators as verapamil, supply the valuable information on P-gp presence and activity in different cell lines. In this study, we demonstrated the P-gp activity by Rho dye extrusion in the HT-22 cells (**Figure 3**). After 30 min of exposure it was observed that STX, LA and STX+LA treatments inhibited P-gp activity. This result fitted with the decrease in cell viability by Trypan blue assay after STX exposure. On the other hand, after 24 h of the exposure the LA and STX+LA treatments were the most efficient to promote the extrusion of Rho. This effect was also observed in the STX treatment, but not as pronounced.

Hence, the presence of P-gp on HT-22 cell line suggests that this protein protects the hippocampus from environmental neurotoxins. According to Silva et al. (2014), some physicochemical characteristic features, such as lipophilicity and hydrogen-bonding ability may contribute to the drug binding ability of the substrate to P-gp. Indeed, LA has such characteristics and study published by Monserrat et al. (2014) show modulation of P-gp expression by LA after endosulfan exposure. Antioxidants as flavonoids and astaxanthin possess protective effects in HT-22 neuronal cells through the direct induction of antioxidant defense system (Cho et al., 2012; Wen et al., 2015).

Saxitoxins are known to enhance the production of reactive oxygen species (ROS) and the tight control of ROS levels by antioxidant molecules and detoxifying

enzymes are important to restore the levels of the antioxidants in cells challenged with neurotoxins (Corbel et al., 2014; Ramos et al., 2014; Zheng et al., 2015). Several studies have reported the cytoprotection mediated by LA (Amado et al., 2011; Astiz et al., 2012; Hiller et al., 2016). For example, LA attenuated homocystein-induced oxidative stress then reduced human aortic endothelial cells apoptosis and inflammation (Hu et al., 2016). In this study we observed that, in fact, LA treatment was efficient to decrease ROS levels (**Figure 4A**) and that the interaction STX+LA was able to minimize the STX cytotoxic effects in 24 hr. Regarding this, the *in vitro* results corroborate with the semi-empirical evidence demonstrated using the density functional theory with *ab initio* simulation.

A study of Ramos et al. (2016) showed that STX increased oxygen consumption in HT-22 cell line after 30 min and 24 h of exposure, an effect that could be associated to moderate mitochondrial uncoupling effects. However, the STX+LA co-exposure decreased oxygen consumption promoted by STX and LA when incorporated separately as HT-22 cell treatments after 30 min of exposure (**Figure 4B**). The increase in O_2 consumption, which was observed in the LA treatment, can be related to the ATP required during the synthesis of the antioxidant glutathione.

Glutathione (GSH) is the principal low molecular weight thiol antioxidant and the co-substrate for a variety of antioxidant and detoxifying enzymes (phase II reactions) particularly abundant in animal tissues (Pamplona and Costantini, 2011). Low GSH levels adversely affects cellular thiol redox balance and increasing GSH confers enhanced protection against oxidative stress (Kütter et al., 2014). The Nrf-2 protein (nuclear factor erythroid 2-related factor 2) is a transcription factor of the “leucine zipper” family and interacts with the Response Element Antioxidant (ARE), present in the promoter region of genes encoding antioxidant enzymes, including the limiting enzyme for GSH synthesis, glutamate cysteine ligase (Dörsam and Fahrer, 2016; Kütter et al., 2014; Gorąca et al., 2011; Pamplona and Costantini, 2011).

In fact, we observed an increase of GSH levels after 24 h by LA treatment

(**Figure 5A**). It is also important to note that for a synthesis of GSH it is necessary spend two ATP molecules per GSH molecule produced and an increase of oxygen consumption is expected for ATP synthesis, as after in HT 22 cells after 24 h exposure to lipoic acid. In addition, after 24 h of exposure, LA seems to contribute to the maintenance of a reduced redox state, as shown for the higher levels of protein sulfhydryl groups observed in HT-22 cell exposed with LA (**Figure 5B**). Indeed, some authors propose that the sulfhydryl-rich inhibitory protein (Keap1) could act as a sensor to change the redox state of the cell, releasing the transcription factor Nrf-2 when the sulfhydryl groups become oxidized, forming disulfide bonds (Hellou et al., 2012; Pamplona and Costantini, 2011; Pilar Valdecantos et al., 2015). Overall, the obtained results agree with the expected molecular relationship between the presence of antioxidants such as LA and regulation of several endogenous antioxidant components through the Keap1–Nrf2 pathway, that in turn contribute as an important mechanism of defense against free radicals (Enamorado et al., 2015; Kütter et al., 2014).

Recently, researches have been directed to the understanding of the environmental relevance of P-gp in different organism exposed to a variety of natural and anthropogenic chemicals, many of which are potent neurotoxins with take action in the central nervous system (CNS) (Kennedy et al., 2014). P-gp presents wide poly-specificity, able to identify a number of hydrophobic compounds of different sizes (300-4000 Da) (Aller et al., 2009). P-gp consists of two pseudo symmetric halves, each containing a nucleotide-binding domain (NBD) and a transmembrane domain (TMD) (Ward et al., 2013). Hydrolysis of ATP induces P-gp to undergo a large conformation, able to alter the TMD from opening to the cytoplasm to opening to the extracellular space conformations (McCormick et al., 2015; Ward et al., 2013).

In virtue of these facts, molecular docking experiments were performed to identify potential binding sites for P-gp and widely known transports of unspecific modulators as VP and Rho 123 were used. Most of ligands were located in TMD

where there is an overlap of amino acid residues between the ligands (**Figure 6**). Indeed, TMDs are arranged together to form a large highly hydrophobic cavity that could accommodate multiple substrates while the NBDs are highly conserved regions, and are sites of ATP binding/hydrolysis (Prajapati and Sangamwar, 2014). When more than one substrate binds to P-gp, conformational changes can occur in the transmembrane helices that may induce a dynamic way in the flexibility and plasticity of substrates binding to P-gp, possibly altering the affinity of the ligands with the P-gp protein (McCormick et al., 2015; Ward et al., 2013; Wise, 2012).

Furthermore, the same ligand with P-gp binds on up to several different sites of its surface, hence P-gp has to adapt the specific size and binding properties of the certain ligand (Mukhametov and Raevsky, 2017). Indeed, our molecular docking results demonstrated that modulators such as Rho and VP were identified at far P-gp binding sites **(Figure 6)**. Although the amino acids residues interaction is not the same found described in previous reports, they are in places very close to those already described (see **Table S.2, Figure S1**). For example, McCormick et al. (2015) observed that the residues W232, F303, Q725, Q990, and F770 interacted with the VP and that the residues I302, F728,Y307, F343, and V982 interected with the Rho123 in the X-ray structures of mouse P-gp and generally VP and Rho 123 ligands interacted with non-polar and aromatic residues. In our molecular docking results the residues W228, F299, Q721, Q986, and F766 interacted with the VP and the residues I302, F728, Y306, and V978 interacted with the ligand Rho123. Besides, the hightest estimated the FEB to Rho123 (-9.1 Kcal/mol^{-1}) and at its site of interaction with P-gp no other ligand of interest was observed, possibly because the Rho123 binding site is not competitive. It has been proposed that P-gp has multiple drug binding sites with different specificity (Li et al., 2014; McCormick et al., 2015). Indeed, different reports show P-gp contains 2 different sites for site binding (site H) and transport (site R) of drugs. For example, rhodamine binds to site R, whereas Hoechst 33342 and the antioxidant quercetin binds to site H (Chufan et al., 2013). It was

observed that the FEB for VP (-7.6 Kcal/mol) was different from that to LA (-5.0 Kcal/mol), although both interacted with some equals residues of P-gp, sharing a similar binding site (**Figure 7**).

The verapamil is a pharmacologically active substance and have the ability to P-gp inhibit, acting as P-gp modulator (Amin, 2013). In contrast, LA is considered as an "universal antioxidant" with chemo and neuroprotective capacity (Kling et al., 2014; Kütter et al., 2014; Monserrat et al., 2008). Our results suggest that VP and LA interact with similar residues occurring at the same point of attachment but present distinct functional effects: verapamil acts by blocking the P-gp pump whereas LA induces P-gp activity. This result is in accordance with the results observed in the *in vitro* experiments, in which the lipoic acid efficiently promoted rhodamine extrusion. In brief, the results of our research permit to propose different sites binding (site H) and transport (site R) to Rho, VP and LP. Indeed, possible Rho binds to site R whereas VP and LA binds to site H. Therefore, LA possible can be act as P-gp substrate establishing two types of response: (1) short-term: LA induces the activation of P-gp and facilities the extrusion of Rho; (2) long-term: LA induces the gene expression of genes associated with the antioxidant defense system, increasing GSH concentration. Both kind of responses should minimize STX toxicity.

In our molecular docking study, we use STX and NeoSTX. These STX analogues present a varied toxicity due to side chain residues such as hydroxyl, sulfate and carbamoyl (Ramos et al., 2014). These molecules are not sulfated and while that STX have hydrogen atom on radical 1, NeoSTX have a hydroxyl radical on radical 2. The presence of hydrogen or the hydroxyl radical modifies the affinity of the toxin and consequently the toxicity (O'Neill et al., 2016). Two different binding sites to STX and NeoSTX can be indicate that STX and NeoSTX are P-gp substrate (**Table S.2; Figure 1c, g, h**). The binding site for STX and STX+LA_1 are located in TMD2 region of P-gp, FEB values to STX (-6.1 Kcal/mol) were close to STX+LA_1 (-6.5 Kcal/mol) and both interacted with some equals residues of P-gp (N838, L839, L858,

G842, and V861), sharing a similar binding site (**Figure 9**). In addition, STX interacted with residue A976, implicated in the binding of the non-competitive substrates as colchicine (Subramanian et al., 2016). The STX+LA_1 was the most stable complex according to the *ab initio* simulation. Indeed, some of the effects commented in the *in vitro* assays showed that the STX+LA interaction treatment reduced the deleterious effects caused only by STX. Probably, the presence of hydroxyl radical or hydrogen proton was determinant to the position-binding site in P-gp. In contrast, the opposite position-binding site was observed for NeoSTX (FEB: -6.4 Kcal/mol) which was near to STX+LA_2 and STX+LA_3 (FEB: -6.2 Kcal/mol) (**Table S.2; Figure S.2**) and both interacted with some equals residues of P-gp (W132, K930, D882, A879, N179) sharing a similar binding site. The binding site to NeoSTX and STX+LA_2, STX+LA_3 are located in TMD1 in P-gp. In addition, NeoSTX interacted with residue Q132, it described as previous reports as amino acid residues of substrate transport (Subramanian et al., 2016).

5. Conclusions

This present study evidentiates, by means of ab initio simulations, that the LA-STX interaction occurs by physisorption processes which are capable of mitigate the toxic effects caused by exposition to STXs. LA and STX + LA reduced the cytotoxic effects of STX. Besides that, it was observed the presence of p-glyprotein in hippocampal cell line HT-22, since both STX and STX-LA treatments were efficiently to induce P-gp extrusion activity by Rho 123 dye extrusion, as for low levels of ROS and oxygen consumption. By the other hand, the LA treatment induced an increase in oxygen consumption which is linked to the increase of the antioxidant glutathione and the levels of protein sulfhydryl groups. Molecular docking suggests that P-glycoprotein is present in hippocampal cell line HT-22 and is involved in the defense system against xenobiotics. In fact, we were able to demonstrate that STX acts as a

substrate of P-gp. In addition, LA may play a role as a modulator for P-gp. The results obtained in vitro corroborate the semi-empirical evidence found using density functional theory ab initio simulation and molecular docking.

6. References

Alboni, S., Montanari, C., Benatti, C., Sanchez-Alavez, M., Rigillo, G., Blom, J.M.C., Brunello, N., Conti, B., Pariante, M.C., Tascedda, F., 2014. Interleukin 18 activates MAPKs and STAT3 but not NF-κB in hippocampal HT-22 cells. Brain. Behav. Immun. 40, 85–94. doi:10.1016/j.bbi.2014.02.015

Aller, S.G., Yu, J., Ward, A., Weng, Y., Chittaboina, S., Zhuo, R., Harrell, P.M., Trinh, Y.T., Zhang, Q., Urbatsch, I.L., Chang, G., 2009. Structure of P-Glycoprotein Reveals a Molecular Basis for Poly-Specific Drug Binding. Science (80-.). 323, 1718–1722. doi:10.1126/science.1168750

Amado, L.L., Garcia, M.L., Pereira, T.C.B., Yunes, J.S., Bogo, M.R., Monserrat, J.M., 2011. Chemoprotection of lipoic acid against microcystin-induced toxicosis in common carp (Cyprinus carpio, Cyprinidae). Comp. Biochem. Physiol. Part C Toxicol. Pharmacol. 154, 146–153. doi:10.1016/j.cbpc.2011.04.007

Amado, L.L., Garcia, M.L., Ramos, P.B., Freitas, R.F., Zafalon, B., Ferreira, J.L.R., Yunes, J.S., Monserrat, J.M., 2009. A method to measure total antioxidant capacity against peroxyl radicals in aquatic organisms: Application to evaluate microcystins toxicity. Sci. Total Environ. 407, 2115–2123. doi:10.1016/j.scitotenv.2008.11.038

Amado, L.L., Monserrat, J.M., 2010. Oxidative stress generation by microcystins in aquatic animals: Why and how. Environ. Int. 36, 226–235. doi:10.1016/j.envint.2009.10.010

Amado, L.L., Rosa, C.E., Castro, M.R., Votto, A.P., Santos, L.C., Marins, L.F.F., Trindade, G.S., Fraga, D.S., Damé, R.C.F., Barros, D.M., Geracitano, L.A., Bianchini, A., de la Torre, F.R., Monserrat, J.M., 2011. Integrated biological responses of zebrafish (Danio rerio) to analyze water quality in regions under anthropogenic influence. Chemosphere 82, 1563–1570. doi:10.1016/j.chemosphere.2010.11.060

Amé, M.V., Baroni, M.V., Galanti, L.N., Bocco, J.L., Wunderlin, D.A., 2009. Effects of microcystin–LR on the expression of P-glycoprotein in Jenynsia multidentata. Chemosphere 74, 1179–1186. doi:10.1016/j.chemosphere.2008.11.068

Amin, M.L., 2013. P-glycoprotein inhibition for optimal drug delivery. Drug Target Insights 2013, 27–34. doi:10.4137/DTI.S12519

Astiz, M., de Alaniz, M.J.T., Marra, C.A., 2012. The oxidative damage and inflammation caused by pesticides are reverted by lipoic acid in rat brain. Neurochem. Int. 61, 1231–1241. doi:10.1016/j.neuint.2012.09.003

Bolton, E.E., Wang, Y., Thiessen, P.A., Bryant, S.H., 2008. PubChem: Integrated

Platform of Small Molecules and Biological Activities. pp. 217–241. doi:10.1016/S1574-1400(08)00012-1

Boys, S.F., Bernardi, F., 1970. The calculation of small molecular interactions by the differences of separate total energies. Some procedures with reduced errors. Mol. Phys. 19, 553–566. doi:10.1080/00268977000101561

Carrett-Dias, M., Almeida, L.K., Pereira, J.L., Almeida, D.V., Filgueira, D.M.V.B., Marins, L.F., Votto, A.P. de S., Trindade, G.S., 2016. Cell differentiation and the multiple drug resistance phenotype in human erythroleukemic cells. Leuk. Res. 42, 13–20. doi:10.1016/j.leukres.2016.01.008

Cervantes, C.R.C., Durán, R., Faro, L.F., Alfonso, P.M., 2009. Effects of Systemic Administration of Saxitoxin on Serotonin Levels in Some Discrete Rat Brain Regions. Med. Chem. (Los. Angeles). 336–342.

Chen, W., Zhao, Y., Seefeldt, T., Guan, X., 2008. Determination of thiols and disulfides via HPLC quantification of 5-thio-2-nitrobenzoic acid. J. Pharm. Biomed. Anal. 48, 1375–1380. doi:10.1016/j.jpba.2008.08.033

Cho, N., Choi, J.H., Yang, H., Jeong, E.J., Lee, K.Y., Kim, Y.C., Sung, S.H., 2012. Neuroprotective and anti-inflammatory effects of flavonoids isolated from Rhus verniciflua in neuronal HT22 and microglial BV2 cell lines. Food Chem. Toxicol. 50, 1940–1945. doi:10.1016/j.fct.2012.03.052

Chufan, E.E., Kapoor, K., Sim, H.M., Singh, S., Talele, T.T., Durell, S.R., Ambudkar, S.A., 2013. Multiple transport-active binding sites are available for a single substrate on human P-glycoprotein (ABCB1). PLoS One 8, 1–16. doi:10.1371/journal.pone.0082463

Contardo-Jara, V., Pflugmacher, S., Wiegand, C., 2008. Multi-xenobiotic-resistance a possible explanation for the insensitivity of bivalves towards cyanobacterial toxins. Toxicon 52, 936–943. doi:10.1016/j.toxicon.2008.09.005

Corbel, S., Mougin, C., Bouaïcha, N., 2014. Cyanobacterial toxins: Modes of actions, fate in aquatic and soil ecosystems, phytotoxicity and bioaccumulation in agricultural crops. Chemosphere 96, 1–15. doi:10.1016/j.chemosphere.2013.07.056

da Silva, C. a, Oba, E.T., Ramsdorf, W. a, Magalhães, V.F., Cestari, M.M., Oliveira Ribeiro, C.A., Silva de Assis, H.C., 2011. First report about saxitoxins in freshwater fish Hoplias malabaricus through trophic exposure. Toxicon 57, 141–147. doi:10.1016/j.toxicon.2010.10.015

Daflon-Yunes, N., Pinto-Silva, F.E., Vidal, R.S., Novis, B.F., Berguetti, T., Lopes, R.R.S., Polycarpo, C., Rumjanek, V.M., 2013. Characterization of a multidrug-resistant chronic myeloid leukemia cell line presenting multiple resistance mechanisms. Mol. Cell. Biochem. 383, 123–135. doi:10.1007/s11010-013-1761-0

de Souza Votto, A.P., Renon, V.P., Yunes, J.S., Rumjanek, V.M., Marques Capella, M.A., Neto, V.M., Sampaio de Freitas, M., Alicia Geracitano, L., Monserrat, J.M., Trindade, G.S., 2007. Sensitivity to microcystins: A comparative study in human cell lines with and without multidrug resistance phenotype. Cell Biol. Int. 31, 1359–1366. doi:10.1016/j.cellbi.2007.05.010

DeGorter, M.K., Xia, C.Q., Yang, J.J., Kim, R.B., 2012. Drug transporters in drug efficacy and toxicity. Annu. Rev. Pharmacol. Toxicoloy 52, 249–273. doi:10.1146/annurev-pharmtox-010611-134529

Dörsam, B., Fahrer, J., 2016. The disulfide compound α-lipoic acid and its derivatives: A novel class of anticancer agents targeting mitochondria. Cancer Lett. 371, 12–19. doi:10.1016/j.canlet.2015.11.019

Dwivedi, N., Flora, G., Kushwaha, P., Flora, S.J.S., 2014. Alpha-lipoic acid protects oxidative stress, changes in cholinergic system and tissue histopathology during co-exposure to arsenic-dichlorvos in rats. Environ. Toxicol. Pharmacol. 37, 7–23. doi:10.1016/j.etap.2013.10.010

Ehlers, A., These, A., Hessel, S., Preiss-Weigert, A., Lampen, A., 2014. Active elimination of the marine biotoxin okadaic acid by P-glycoprotein through an in vitro gastrointestinal barrier. Toxicol. Lett. 225, 311–317. doi:10.1016/j.toxlet.2013.12.019

Enamorado, A.D., Martins, A.C., Flores, J.A., Tesser, M.B., Caldas, S.S., Primel, E.G., Monserrat, J.M., 2015. Biochemical responses over time in common carp Cyprinus carpio (Teleostei, Cyprinidae) during fed supplementation with α-lipoic acid. Comp. Biochem. Physiol. Part A Mol. Integr. Physiol. 188, 9–16. doi:10.1016/j.cbpa.2015.05.023

González-Durruthy, M., Werhli, A. V., Cornetet, L., Machado, K.S., González-Díaz, H., Wasiliesky, W., Ruas, C.P., Gelesky, M.A., Monserrat, J.M., 2016. Predicting the binding properties of single walled carbon nanotubes (SWCNT) with an ADP/ATP mitochondrial carrier using molecular docking, chemoinformatics, and nano-QSBR perturbation theory. RSC Adv. 6, 58680–58693. doi:10.1039/C6RA08883J

Gorąca, A., Huk-Kolega, H., Piechota, A., Kleniewska, P., Ciejka, E., Skibska, B., 2011. Lipoic acid – biological activity and therapeutic potential. Pharmacol. Reports 63, 849–858. doi:10.1016/S1734-1140(11)70600-4

Han, Y., Chin Tan, T.M., Lim, L.-Y., 2008. In vitro and in vivo evaluation of the effects of piperine on P-gp function and expression. Toxicol. Appl. Pharmacol. 230, 283–289. doi:10.1016/j.taap.2008.02.026

Hellou, J., Ross, N.W., Moon, T.W., 2012. Glutathione, glutathione S-transferase, and glutathione conjugates, complementary markers of oxidative stress in aquatic biota. Environ. Sci. Pollut. Res. 19, 2007–2023. doi:10.1007/s11356-012-0909-x

Hiller, S., DeKroon, R., Hamlett, E.D., Xu, L., Osorio, C., Robinette, J., Winnik, W., Simington, S., Maeda, N., Alzate, O., Yi, X., 2016. Alpha-lipoic acid supplementation protects enzymes from damage by nitrosative and oxidative stress. Biochim. Biophys. Acta - Gen. Subj. 1860, 36–45. doi:10.1016/j.bbagen.2015.09.001

Hu, H., Wang, C., Jin, Y., Meng, Q., Liu, Q., Liu, K., Sun, H., 2016. Alpha-lipoic acid defends homocysteine-induced endoplasmic reticulum and oxidative stress in HAECs. Biomed. Pharmacother. 80, 63–72. doi:10.1016/j.biopha.2016.02.022

Kennedy, C.J., Tierney, K.B., Mittelstadt, M., 2014. Inhibition of P-glycoprotein in the

blood-brain barrier alters avermectin neurotoxicity and swimming performance in rainbow trout. Aquat. Toxicol. 146, 176–185. doi:10.1016/j.aquatox.2013.10.035

Kim, N., Shin, J., No, K.T., 2014. In silico Study on the Interaction between P-glycoprotein and Its Inhibitors at the Drug Binding Pocket. Bull. Korean Chem. Soc. 35, 2317–2325. doi:10.5012/bkcs.2014.35.8.2317

Kling, B., Bücherl, D., Palatzky, P., Matysik, F.M., Decker, M., Wegener, J., Heilmann, J., 2014. Flavonoids, flavonoid metabolites, and phenolic acids inhibit oxidative stress in the neuronal cell line HT-22 monitored by ECIS and MTT assay: A comparative study. J. Nat. Prod. 77, 446–454. doi:10.1021/np400518k

Kütter, M.T., Romano, L.A., Ventura-Lima, J., Tesser, M.B., Monserrat, J.M., 2014. Antioxidant and toxicological effects elicited by alpha-lipoic acid in aquatic organisms. Comp. Biochem. Physiol. Part C Toxicol. Pharmacol. 162, 70–76. doi:10.1016/j.cbpc.2014.03.008

Lacher, S.E., Skagen, K., Veit, J., Dalton, R., Woodahl, E.L., 2015. P-Glycoprotein Transport of Neurotoxic Pesticides. J. Pharmacol. Exp. Ther. 355, 99–107. doi:10.1124/jpet.115.226373

Laskowski, R.A., Swindells, M.B., 2011. LigPlot+: Multiple Ligand–Protein Interaction Diagrams for Drug Discovery. J. Chem. Inf. Model. 51, 2778–2786. doi:10.1021/ci200227u

Li, J., Jaimes, K.F., Aller, S.G., 2014. Refined structures of mouse P-glycoprotein. Protein Sci. 23, 34–46. doi:10.1002/pro.2387

Liu, J., Li, L., Suo, W.Z., 2009. HT22 hippocampal neuronal cell line possesses functional cholinergic properties. Life Sci. 84, 267–271. doi:10.1016/j.lfs.2008.12.008

Longaray-Garcia, M., Flores, J.A., Külkamp-Guerreiro, I.C., Guterres, S.S., Pereira, T.C.B., Bogo, M.R., Monserrat, J.M., 2013. Modulation of antioxidant and detoxifying capacity in fish Cyprinus carpio (Cyprinidae) after treatment with nanocapsules containing lipoic acid. Comp. Biochem. Physiol. Part A Mol. Integr. Physiol. 165, 468–475. doi:10.1016/j.cbpa.2013.02.004

Loo, T.W., Clarke, D.M., 2017. Attachment of a “molecular spring” restores drug-stimulated ATPase activity to P-glycoprotein lacking both Q loop glutamines. Biochem. Biophys. Res. Commun. 483, 366–370. doi:10.1016/j.bbrc.2016.12.137

McCormick, J.W., Vogel, P.D., Wise, J.G., 2015. Multiple Drug Transport Pathways through Human P-Glycoprotein. Biochemistry 54, 4374–4390. doi:10.1021/acs.biochem.5b00018

Monserrat, J.M., Garcia, M.L., Ventura-Lima, J., González, M., Ballesteros, M.L., Miglioranza, K.S.B., Amé, M.V., Wunderlin, D.A., 2014. Antioxidant, phase II and III responses induced by lipoic acid in the fish Jenynsia multidentata (Anablapidae) and its influence on endolsulfan accumulation and toxicity. Pestic. Biochem. Physiol. 108, 8–15. doi:10.1016/j.pestbp.2013.10.009

Monserrat, J.M., Lima, J.V., Ferreira, J.L.R., Acosta, D., Garcia, M.L., Ramos, P.B.,

Moraes, T.B., dos Santos, L.C., Amado, L.L., 2008. Modulation of antioxidant and detoxification responses mediated by lipoic acid in the fish Corydoras paleatus (Callychthyidae). Comp. Biochem. Physiol. Part C Toxicol. Pharmacol. 148, 287–292. doi:10.1016/j.cbpc.2008.06.011

Morris, G.M., Huey, R., Lindstrom, W., Sanner, M.F., Belew, R.K., Goodsell, D.S., Olson, A.J., 2009. AutoDock4 and AutoDockTools4: Automated docking with selective receptor flexibility. J. Comput. Chem. 30, 2785–2791. doi:10.1002/jcc.21256

Mukhametov, A., Raevsky, O.A., 2017. On the mechanism of substrate/non-substrate recognition by P-glycoprotein. J. Mol. Graph. Model. 71, 227–232. doi:10.1016/j.jmgm.2016.12.008

Muthusamy, G., Balupillai, A., Ramasamy, K., Shanmugam, M., Gunaseelan, S., Mary, B., Prasad, N.R., 2016. Ferulic acid reverses ABCB1-mediated paclitaxel resistance in MDR cell lines. Eur. J. Pharmacol. 786, 194–203. doi:10.1016/j.ejphar.2016.05.023

Nguyen, T., Yang, T., Go, M.-L., 2014. Functionalized acridin-9-yl phenylamines protected neuronal HT22 cells from glutamate-induced cell death by reducing intracellular levels of free radical species. Bioorg. Med. Chem. Lett. 24, 1830–1838. doi:10.1016/j.bmcl.2014.02.006

Nicolas, J., Bovee, T.F.H., Kamelia, L., Rietjens, I.M.C.M., Hendriksen, P.J.M., 2015. Exploration of new functional endpoints in neuro-2a cells for the detection of the marine biotoxins saxitoxin, palytoxin and tetrodotoxin. Toxicol. Vitr. 30, 341–347. doi:10.1016/j.tiv.2015.10.001

O'Neill, K., Musgrave, I.F., Humpage, A., 2016. Low dose extended exposure to saxitoxin and its potential neurodevelopmental effects: A review. Environ. Toxicol. Pharmacol. 48, 7–16. doi:10.1016/j.etap.2016.09.020

Packer, L., Witt, E.H., Tritschler, H.J., 1995. Alpha-lipoic acid as a biological antioxidant. Free Radic. Biol. Med. 19, 227–250. doi:10.1016/0891-5849(95)00017-R

Pamplona, R., Costantini, D., 2011. Molecular and structural antioxidant defenses against oxidative stress in animals. AJP Regul. Integr. Comp. Physiol. 301, R843–R863. doi:10.1152/ajpregu.00034.2011

Perdew, J.P., Zunger, A., 1981. Self-interaction correction to density-functional approximations for many-electron systems. Phys. Rev. B 23, 5048–5079. doi:10.1103/PhysRevB.23.5048

Perreault, F., Matias, M.S., Melegari, S.P., Pinto, C.R.S.D.C., Creppy, E.E., Popovic, R., Matias, W.G., 2011. Investigation of animal and algal bioassays for reliable saxitoxin ecotoxicity and cytotoxicity risk evaluation. Ecotoxicol. Environ. Saf. 74, 1021–6. doi:10.1016/j.ecoenv.2011.01.016

Pilar Valdecantos, M., Prieto-Hontoria, P.L., Pardo, V., Módol, T., Santamaría, B., Weber, M., Herrero, L., Serra, D., Muntané, J., Cuadrado, A., Moreno-Aliaga, M.J., Alfredo Martínez, J., Valverde, Á.M., 2015. Essential role of Nrf2 in the protective effect of lipoic acid against lipoapoptosis in hepatocytes. Free Radic. Biol. Med. 84, 263–278. doi:10.1016/j.freeradbiomed.2015.03.019

Pirlich, M., Kiok, K., Sandig, G., Lochs, H., Grune, T., 2002. Alpha-lipoic acid prevents ethanol-induced protein oxidation in mouse hippocampal HT22 cells. Neurosci. Lett. 328, 93–96. doi:10.1016/S0304-3940(02)00415-9

Prajapati, R., Sangamwar, A.T., 2014. Translocation mechanism of P-glycoprotein and conformational changes occurring at drug-binding site: Insights from multi-targeted molecular dynamics. Biochim. Biophys. Acta - Biomembr. 1838, 2882–2898. doi:10.1016/j.bbamem.2014.07.018

Ramos, P., Schmitz, M., Filgueira, D., Votto, A.P., Durruthy, M., Gelesky, M., Ruas, C., Yunes, J., Tonel, M., Fagan, S., Monserrat, J., 2016. Interaction of single-walled carbon nanotubes and saxitoxin: Ab initio simulations and biological responses in hippocampal cell line HT-22. Environ. Toxicol. Chem. 9999, 1–10. doi:10.1002/etc.3544

Ramos, P.B., Diehl, F., dos Santos, J.M., Monserrat, J.M., Yunes, J.S., 2014. Oxidative stress in rats induced by consumption of saxitoxin contaminated drink water. Harmful Algae 37, 68–74. doi:10.1016/j.hal.2014.04.002

Seus, V.R., Gomes, J., Machado, K.S., 2015. SciForum: Applying a Novel Web-Tool for Performing Virtual Screening Experiments 1, 1–5.

Silva, R., Vilas-Boas, V., Carmo, H., Dinis-Oliveira, R.J., Carvalho, F., de Lourdes Bastos, M., Remião, F., 2015. Modulation of P-glycoprotein efflux pump: induction and activation as a therapeutic strategy. Pharmacol. Ther. 149, 1–123. doi:10.1016/j.pharmthera.2014.11.013

Silva, C.A. Da, Morais, E.C.P. De, Costa, M.D.M., Ribas, J.L.C., Guiloski, I.C., Ramsdorf, W.A., Zanata, S.M., Cestari, M.M., Oliveira Ribeiro, C.A., Magalhães, V.F., Trudeau, V.L., Silva de Assis, H.C., 2014. Saxitoxins induce cytotoxicity, genotoxicity and oxidative stress in teleost neurons in vitro. Toxicon 86, 8–15. doi:10.1016/j.toxicon.2014.04.016

Subhani, S., Jayaraman, A., Jamil, K., 2015. Homology modelling and molecular docking of MDR1 with chemotherapeutic agents in non-small cell lung cancer. Biomed. Pharmacother. = Biomédecine pharmacothérapie 71, 37–45. doi:10.1016/j.biopha.2015.02.009

Subramanian, N., Condic-Jurkic, K., O'Mara, M.L., 2016. Structural and dynamic perspectives on the promiscuous transport activity of P-glycoprotein. Neurochem. Int. 98, 146–152. doi:10.1016/j.neuint.2016.05.005

Szewczyk, P., Tao, H., McGrath, A.P., Villaluz, M., Rees, S.D., Lee, S.C., Doshi, R., Urbatsch, I.L., Zhang, Q., Chang, G., 2015. Snapshots of ligand entry, malleable binding and induced helical movement in P-glycoprotein. Acta Crystallogr. Sect. D Biol. Crystallogr. 71, 732–741. doi:10.1107/S1399004715000978

Takser, L., Benachour, N., Husk, B., Cabana, H., Gris, D., 2016. Cyanotoxins at low doses induce apoptosis and inflammatory effects in murine brain cells: Potential implications for neurodegenerative diseases. Toxicol. Reports 3, 180–189. doi:10.1016/j.toxrep.2015.12.008

Trott, O., Olson, A.J., 2009. AutoDock Vina: Improving the speed and accuracy of docking with a new scoring function, efficient optimization, and multithreading. J. Comput. Chem. 31, NA-NA. doi:10.1002/jcc.21334

Ward, A.B., Szewczyk, P., Grimard, V., Lee, C., Martinez, L., Doshi, R., Caya, A., Villaluz, M., Pardon, E., Cregger, C., Swartz, D.J., Falson, P.G., Urbatsch, I.L., Govaerts, C., Steyaert, J., Chang, G., 2013. Structures of P-glycoprotein reveal its conformational flexibility and an epitope on the nucleotide-binding domain. Proc. Natl. Acad. Sci. 110, 13386–91. doi:10.1073/pnas.1309275110

Wen, X., Huang, A., Hu, J., Zhong, Z., Liu, Y., Li, Z., Pan, X., Liu, Z., 2015. Neuroprotective effect of astaxanthin against glutamate-induced cytotoxicity in HT22 cells: Involvement of the Akt/GSK-3?? pathway. Neuroscience 303, 558–568. doi:10.1016/j.neuroscience.2015.07.034

White, C.C., Viernes, H., Krejsa, C.M., Botta, D., Kavanagh, T.J., 2003. Fluorescence-based microtiter plate assay for glutamate–cysteine ligase activity. Anal. Biochem. 318, 175–180. doi:10.1016/S0003-2697(03)00143-X

Wise, J.G., 2012. Catalytic transitions in the human mdr1 P-glycoprotein drug binding sites. Biochemistry 51, 5125–5141. doi:10.1021/bi300299z

Zabaglo, K., Chrapusta, E., Bober, B., Kaminski, A., Adamski, M., Bialczyk, J., 2016. Environmental roles and biological activity of domoic acid: A review. Algal Res. 13, 94–101. doi:10.1016/j.algal.2015.11.020

Zhang, Q., Pi, J., Woods, C.G., Andersen, M.E., 2010. A systems biology perspective on Nrf2-mediated antioxidant response. Toxicol. Appl. Pharmacol. 244, 84–97. doi:10.1016/j.taap.2009.08.018

Zhao, H., Caflisch, A., 2015. Molecular dynamics in drug design. Eur. J. Med. Chem. 91, 4–14. doi:10.1016/j.ejmech.2014.08.004

Zheng, X., Hu, B., Gao, S.X., Liu, D.J., Sun, M.J., Jiao, B.H., Wang, L.H., 2015. A saxitoxin-binding aptamer with higher affinity and inhibitory activity optimized by rational site-directed mutagenesis and truncation. Toxicon 101, 41–47. doi:10.1016/j.toxicon.2015.04.017

Figure captions

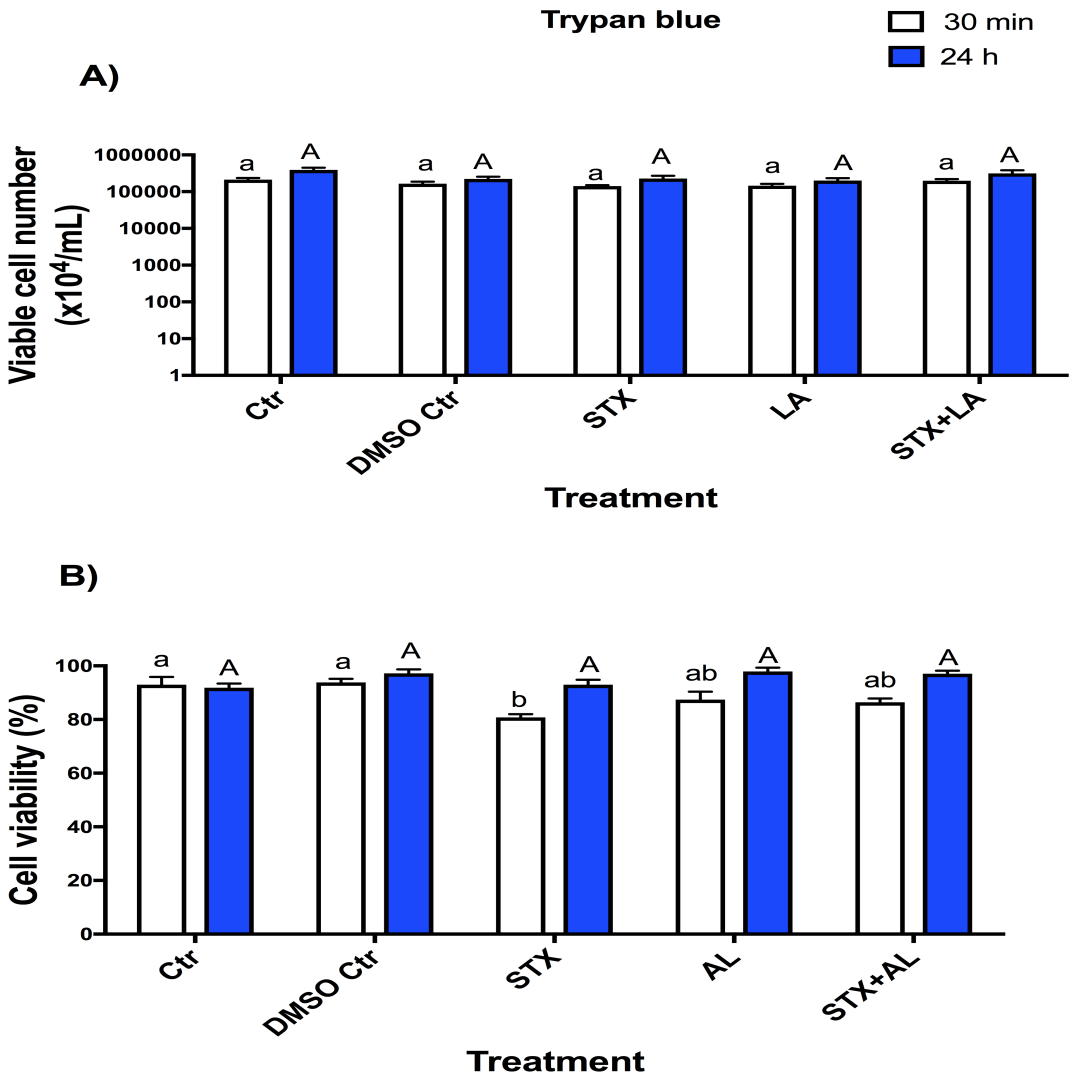

Figure 1: Viable cell number and cell viability (%) of HT-22 cells assessed by Trypan blue exclusion assay. Analyses were performed after exposures of 30 min (white bars) and 24 h (blue bars). (A) Viable cell number and (B) Cell viability (%). CTR: control group, DMSO CTR: DMSO control group, STX: Saxitoxin (200 µg/L), LA: Lipoic acid (50 µM), STX+LA: saxitoxin with lipoic acid. Data are expressed as mean ± standard error of 3 independent experiments (n=6 for each experiment). Equal letters indicate absence of significant difference (p>0.05) at each time.

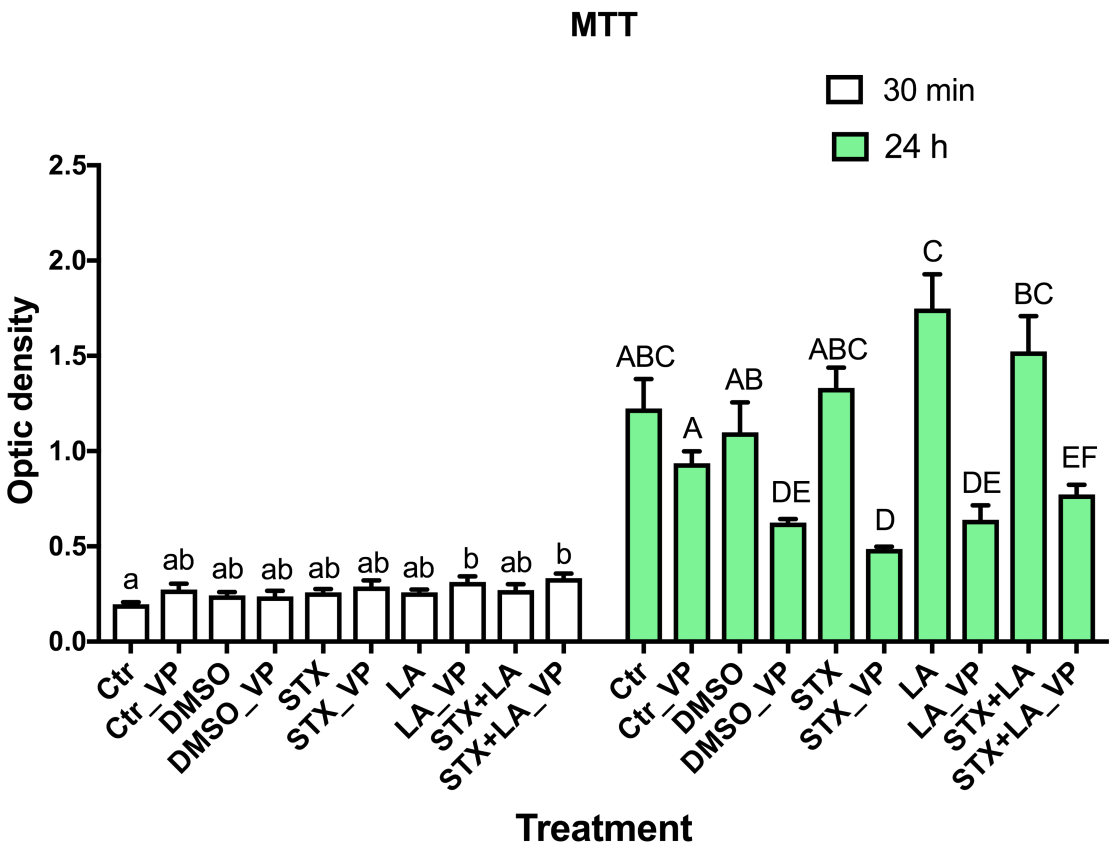

Figure 2: HT-22 cells proliferation measured by the 3(-4,5-dimethylthiazol-2-yl)-2,5-difenyltetrazolium (MTT) assay in presence or absence of verapamil. Analyses were performed after 30 min (white bars) and 24 h (green bars). CTR: control group, DMSO CTR: DMSO control group, STX: Saxitoxin (200 µg/L), LA: Lipoic acid (50 µM), STX+LA: saxitoxin with lipoic acid. Data are expressed as mean ± standard error of 3 independent experiments (n=7 for each experiment). Equal letters indicate absence of significant difference (p>0.05) at each time.

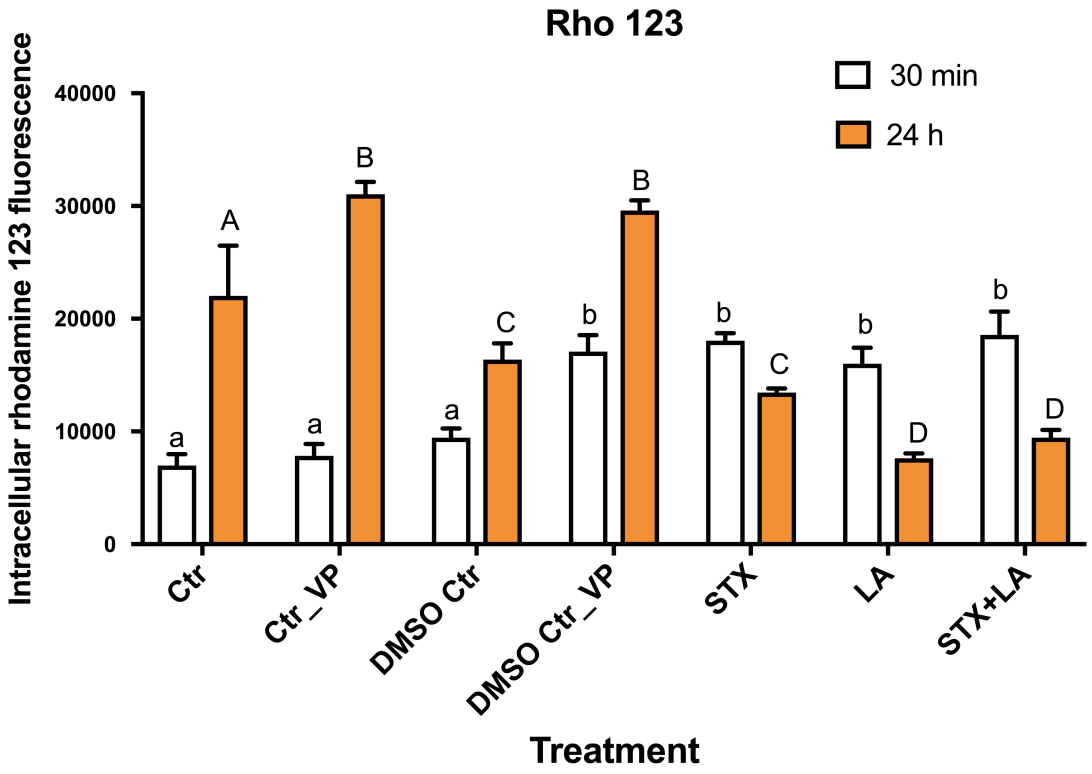

Figure 3: Evaluation of P-gp activity by Rhodamine 123 (Rho) dye extrusion in the HT-22 cell line after exposure of 30 min (white bars) and 24 h (orange bars). CTR: control group, DMSO CTR: DMSO control group, STX: Saxitoxin (200 µg/L), LA:Lipoic acid (50 µM), STX+LA: saxitoxin with lipoic acid. Data are expressed as mean ± standard error of 3 independent experiments (n=4 for each experiment). Equal letters indicate absence of significant difference (p>0.05) at each time.

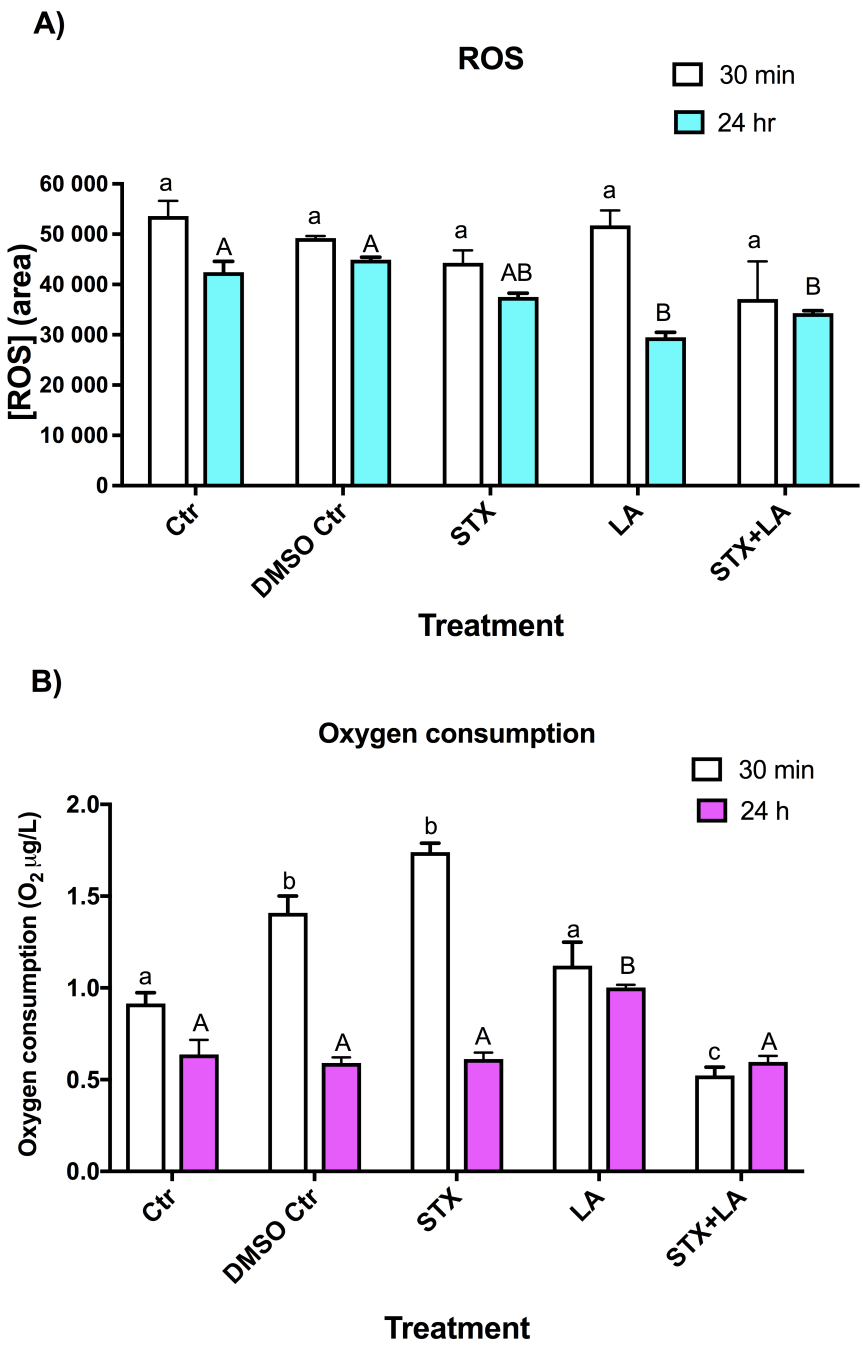

Figure 4: Intracellular reactive oxygen species (ROS) and Oxygen consumption in HT-22 cells. A) ROS concentrations in HT-22 cells after exposures of 30 min (white bars) and 24 h (ice bars). CTR: control group, DMSO CTR: DMSO control group, STX: Saxitoxin (200 µg/L), LA: Lipoic acid (50 µM), STX+LA: saxitoxin with lipoic acid. B) Oxygen consumption in HT-22 cells after 30 min (white bars) and 24 h (magenta bars) exposure. CTR: control group, DMSO CTR: DMSO control group, STX: Saxitoxin (200 µg/L), LA: Lipoic acid (50 µM), STX+LA: saxitoxin with lipoic acid.

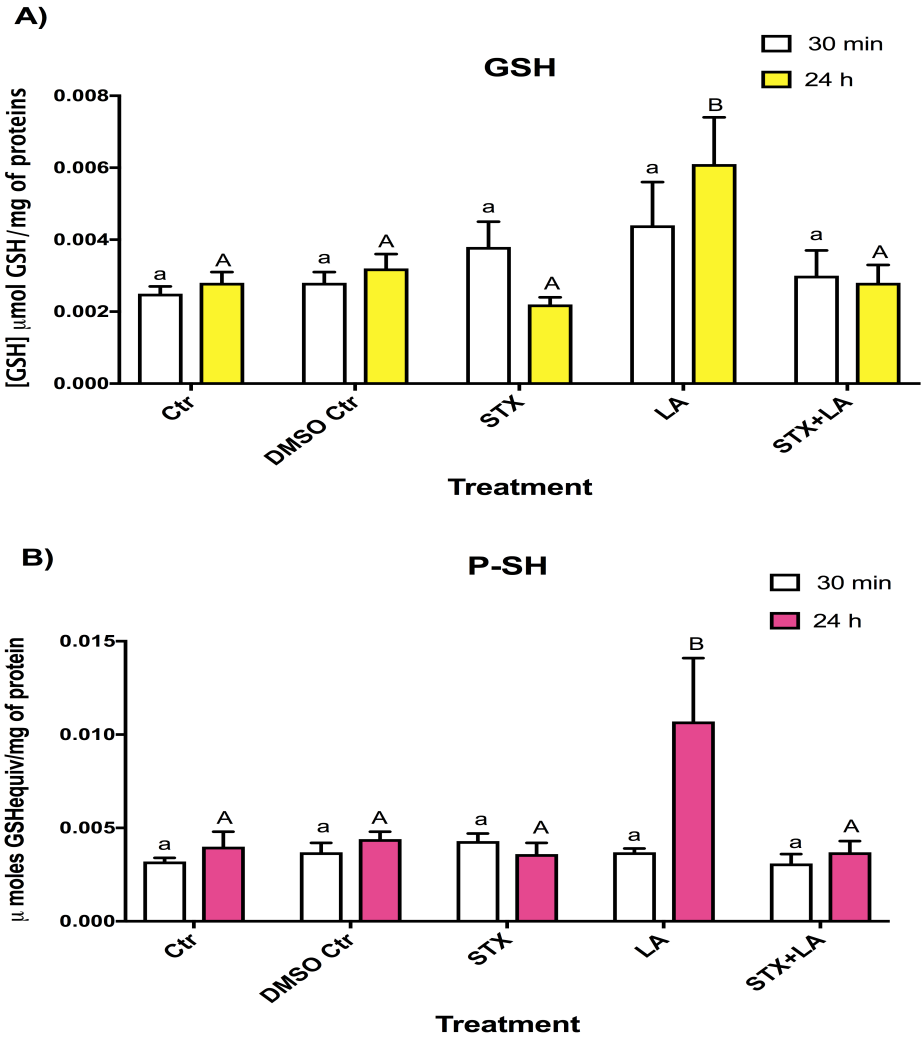

Figure 5: Concentrations of reduced glutathione (GSH) and levels of protein sulfhydryl (P-SH) in HT-22 cells. A) GSH concentration (µM of GSH/mg protein) in HT-22 cells after 30 min (white bars) and 24 h (yellow bars) exposure. B) Levels of P-SH in HT-22 cells after 30 min (white bars) and 24 h (purple bars) exposure. CTR: control group, DMSO CTR: DMSO control group, STX: Saxitoxin (200 µg/L), LA: Lipoic acid (50 µM), STX+LA: saxitoxin with lipoic acid. Data are expressed as mean ± standard error of 3 independent experiments (n=7 for each experiment). Equal letters indicate absence of significant difference (p>0.05) at each time.

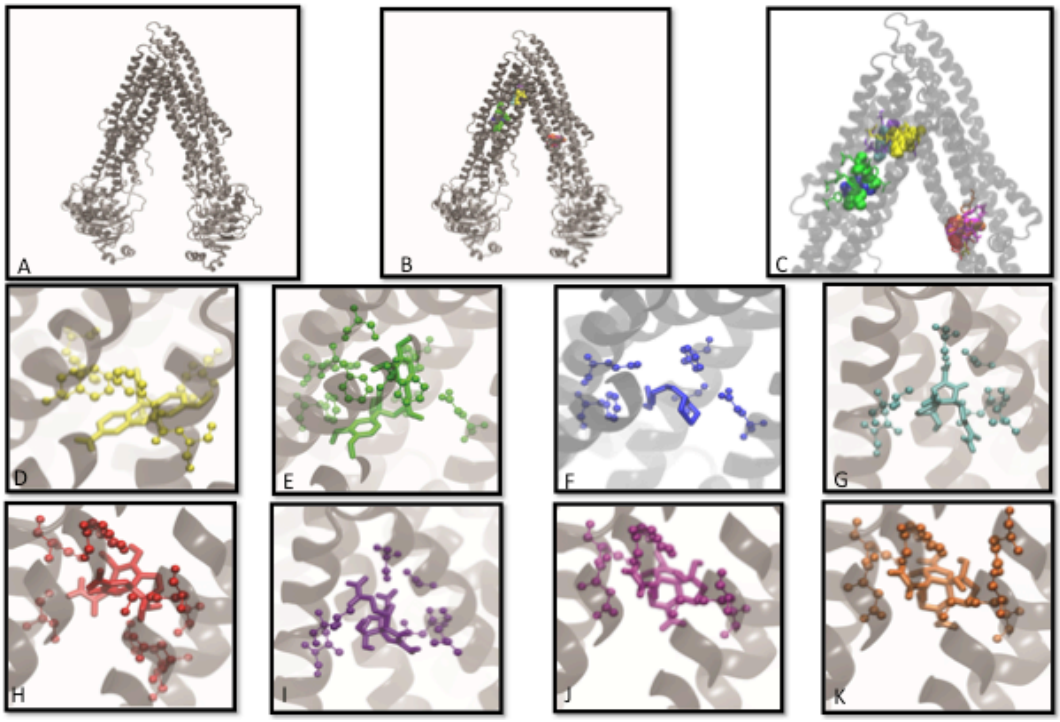

Figure 6. Cartoon representation of general docking results designed using Open-Sourse Pymol 1.7.x show in **A)** X-ray pdb crystallographic structure of glycoprotein P. **B)** and **C)** general superimposed docking poses of the evaluated ligands in the active binding site of glycoprotein P. Individual docking images of the glycoprotein P active binding site for **D)** rhodamine 123 (yellow), **E)** verapamil (green), **F)** Lipoic acid (blue), **G)** STX (light blue), **H)** Neo-STX (red). Active binding site for Complexes of STX_AL like **I)** STX_AL 1 (violet), **J)** STX_AL 2 (purple), and **K)** STX_AL 3 (orange).

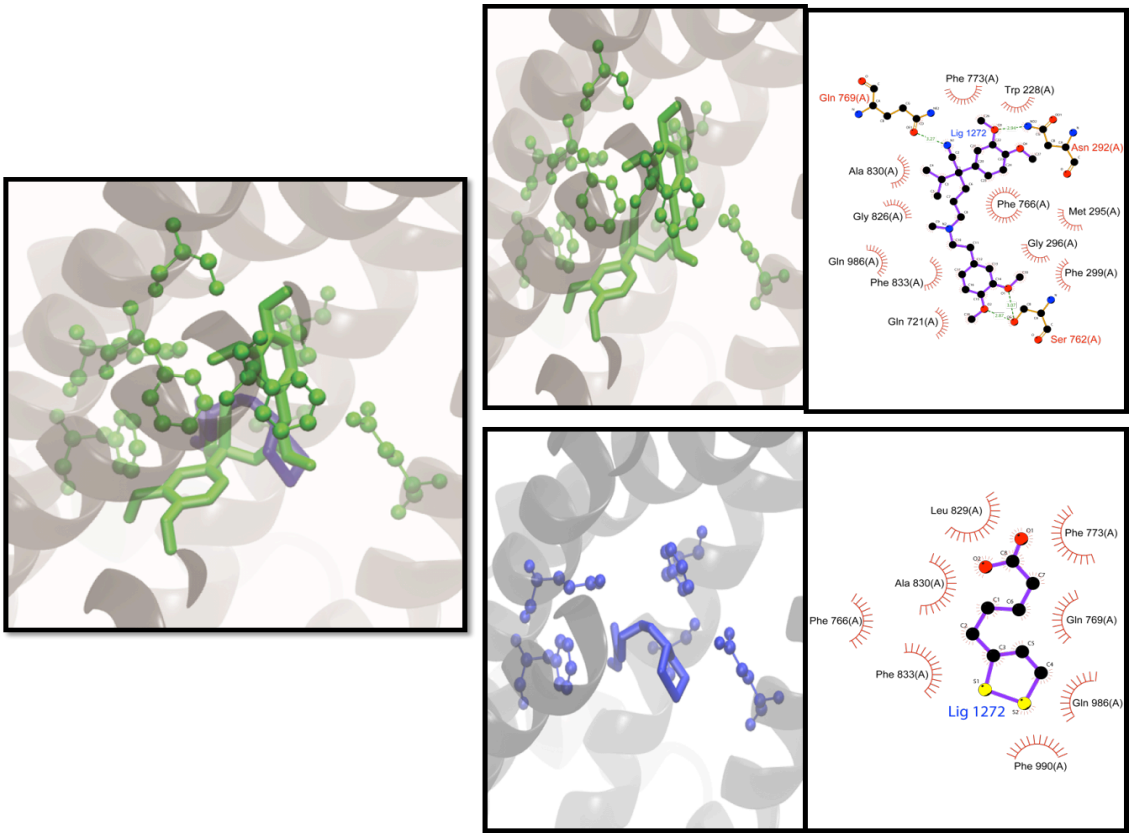

Figure 7. Interaction between lipoic acid and verapamil. **A)** Cartoon representation of superimposed docking poses of verapamil (green) and lipoic acid (blue) at the same biophysical environment from the glycoprotein P active binding site. **B)** and **C)** show details of individual docking images linked to Lig-Plot analyze from the relevant residues in glycoprotein P active binding site for hydrogen bond, hydrophobic interactions of verapamil (green) and lipoic acid (blue).

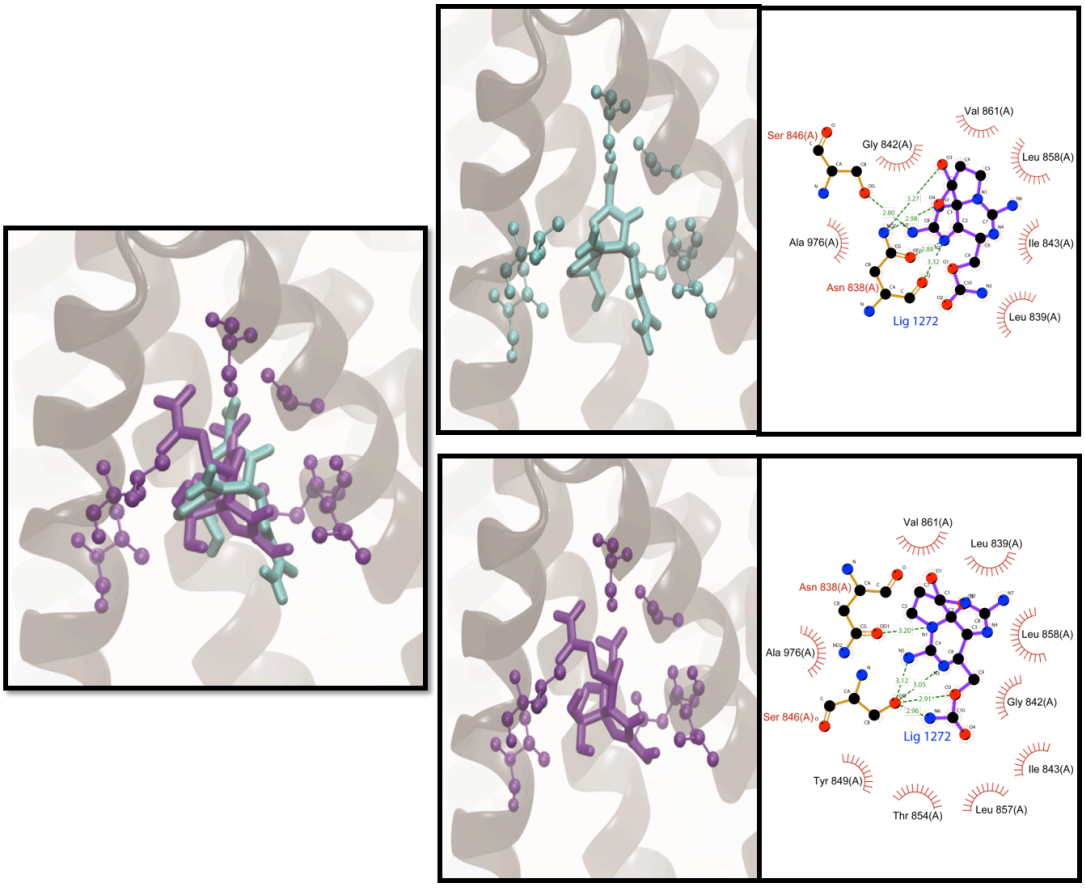

Figure 8. Interaction between lipoic acid and verapamil.**A)** Cartoon representation of superimposed docking poses of STX (light blue) and STX_AI 1 (violet) at the same biophysical environment from the glycoprotein P active binding site. **B)** and **C)** show details of individual docking images linked to Lig-Plot analyze from the relevant residues in glycoprotein P active binding site for hydrogen bond, hydrophobic interactions of STX (light blue) and STX_AI 1 (violet).

Supplementary material:

Table S.1: Binding energy, shortest distance, and charge transfer between STX and LA for all the studied systems

Configuration	Binding energy (eV)	Charge transfer (e^-)*	Shortest distance (Å)	HOMO / LUMO difference (eV)
LA	-	-	-	2.47
STX	-	-	-	4.30
STX+LA_1	0.69	-0.12	1.85	2.56
STX+LA_2	0.25	-0.14	2.39	2.46
STX+LA_3	0.55	-0.04	2.24	2.79

*Negative charge transfer indicates lipoic acid to STX

STX = saxitoxin; LA = Lipoic acid; STX_LA = interaction between saxitoxin and lipoic acid

Table S.2: Complexes of ligands with the structure of P-gp

LIGANDS	FEB (KCAL/MOL)	BINDING SITE RESIDUES (NON BONDED)	BINDING SITE RESIDUES (H-H BONDED)
Rhodamine 123	-9.3	F974, F724, F332, Y306	S333, T329
Verapamil	-7.6	W228, A830, F299, F773, F833, F766, Q721, Q986, Q769	S762
Lipoic Acid	-5.0	I302, F728, Y306, V978, A830, F773, F833, Q986, Q769	----------
Saxitoxin	-6.1	N838, L839, L858, G842, V861	N838, S846
STX+AL 1	-6.5	N838, L838, L839, L858, G842, V861	N838, S846
Neo-Saxitoxin	-6.4	W132, K930, D882, A879	E180, K883, S176
STX+AL 2	-6.2	W132, K930, A879, F934, N179	E180, N179, W132
STX+AL 3	-6.2	W132, K930, A879, N179	E180, N179, W132

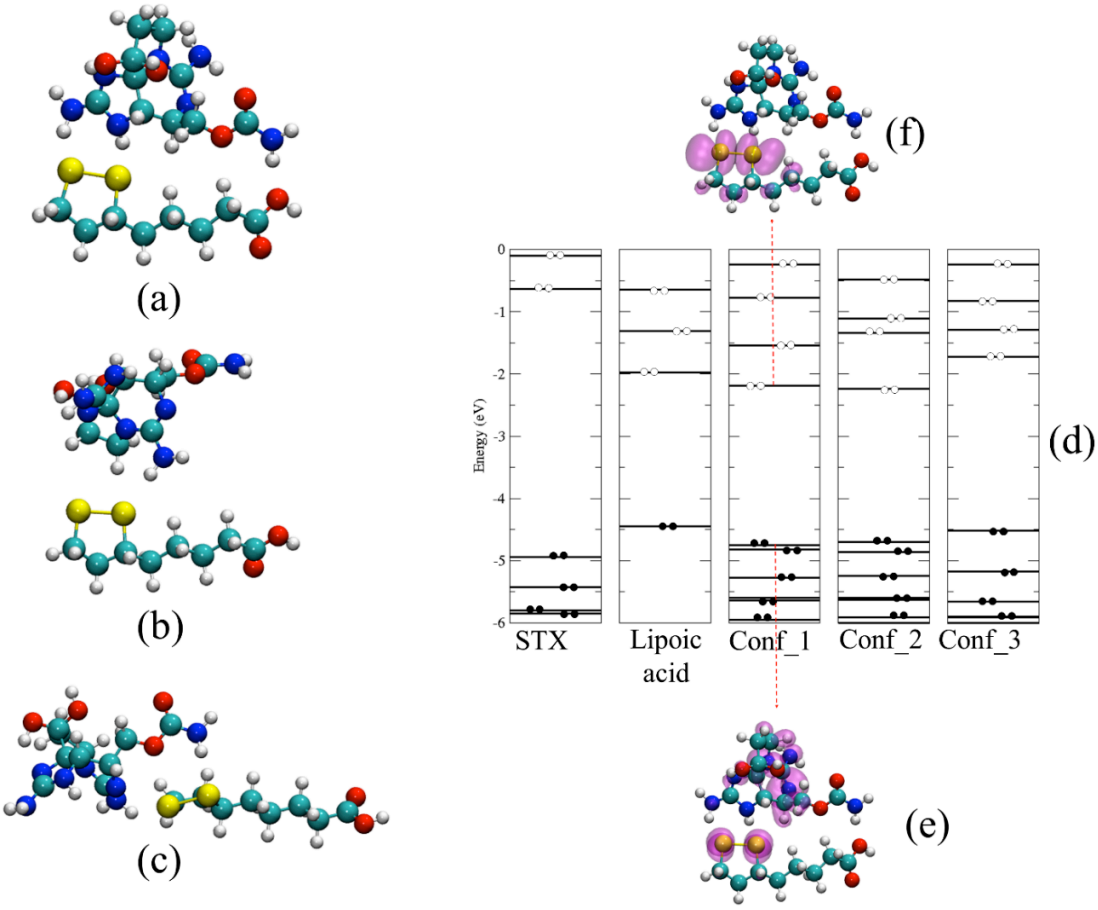

Figure S.1: Structural configurations for the optimized positions of (a) STX+LA_1, (b) STX+LA_2, (c) STX+LA_3, (d) energy levels, (e) HOMO and (f) LUMO more stable configuration.

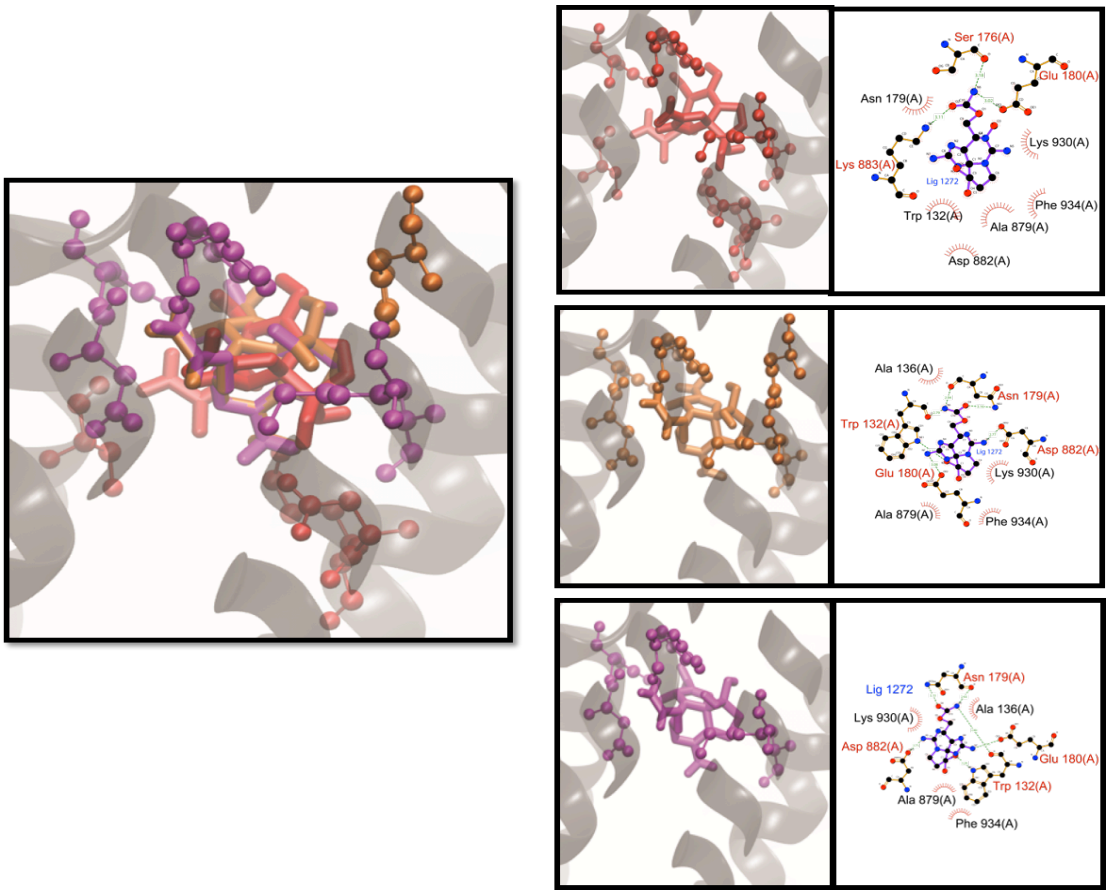

Figure S.2: **a)** Cartoon representation of superimposed docking poses of Neo-STX (red), complexes of STX_AL 2 (orange) and STX_AL 3 (violet) at the same biophysical environment from the glycoprotein P active binding site. **S.2b), S.2c)** and **S.2d)** show details of individual docking images linked to Lig-Plot analyze from the relevant residues in glycoprotein P active binding site for hydrogen bond, hydrophobic interactions of Neo-STX (red), complexes of STX_AL 2 (orange) and STX_AL 3 (violet).

4. DISCUSSÃO GERAL

A qualidade da água ambiental é um dos principais problemas de saúde pública a nível mundial. As saxitoxinas são potentes neurotoxinas que bloqueiam os canais dependentes de voltagem, inibindo a propagação do impulso nervoso (CORBEL; MOUGIN; BOUAÏCHA, 2014; D‘MELLO et al., 2017). Associado a este fato, STXs induzem citotoxicidade por meio da geração de espécies ativas de oxigênio, sendo altamente tóxicas para células de mamíferos, incluindo células cerebrais como as do hipocampo (O’NEILL; MUSGRAVE; HUMPAGE, 2016; ONDRUS et al., 2012a; SILVA et al., 2014).

Frente a uma situação pró-oxidante, o estudo de estratégias de quimioprevenção contra os efeitos tóxicos das STXs é indispensável. O AL e sua forma reduzida ácido dihidrolipóico (DHLA), formam um potente par redox com funções antioxidantes, como interceptar EAO tanto em ambientes aquosos quanto em ambientes lipídicos (DÖRSAM; FAHRER, 2016) outra consideração importante é quanto aos nanomateriais.

Apesar de características atraentes dos nanotubos de carbono (NTCs) que lhe confere grande potencial para aplicações biomédicas, questões sobre a potencial toxicidade dos NTCs para os seres humanos e ambientes foram questionadas em muitos trabalhos (APUL; KARANFIL, 2015; KESHARWANI; MISHRA; JAIN, 2015). Os NTCs são considerados adsorventes promissores em virtude da sua alta hidrofobicidade associada à sua elevada área superficial, podendo causar o efeito “Cavalo de tróia”, facilitando a entrada de moléculas tóxicas quando adsorvidas por nanomateriais (AZEVEDO COSTA et al., 2012; BRITTO et al., 2015; CANESI; CIACCI; BALBI, 2015; CHAO et al.,

2009), mas ao mesmo tempo esta característica pode ser uma vantagem se utilizado em processos de remediação.

Diante do que foi exposto acima, a presente Tese teve como objetivo verificar estratégias que minimizam os efeitos gerados pelas saxitoxinas. O primeiro artigo teve como objetivo avaliar a possível interação das saxitoxinas com SWCNTs (pristino e carboxilado) por meio de ensaios *in silico,* envolvendo simulação *ab initio,* e ensaios *in vitro* utilizando a linhagem hipocampal HT-22. Enquanto que o segundo manuscrito teve como o objetivo verificar estratégias de quimioprevenção mediada ácido lipóico frente à toxicidade induzida pelas STXs, utilizando ensaios *in silico*, incluindo simulação *ab initio* e docagem molecular, e ensaios *in vitro* utilizando a linhagem hipocampal HT-22

Os resultados do primeiro artigo demonstraram que a STX interage com SWCNTs (pristino e carboxilado) por fisisorção. A presença do grupo carboxila em SWCNTs altera a direção da transferência de carga, e este efeito pode alterar significativamente o ambiente biológico das nanoestruturas. De fato, trabalhos demonstram que o grau de funcionalização de um nanomaterial pode interferir na sua toxicidade (CANESI; CIACCI; BALBI, 2015) e os resultados obtidos nos ensaios *in vitro* vão ao encontro deste resultado. A citotoxicidade exercida pelos NTCs é ainda um assunto controverso. Alguns autores sugerem que NTCs podem interferir na interpretação de viabilidade do ensaio, já que são capazes de reagir com vários corantes comumente usados para avaliar citotoxicidade (HU et al., 2010) como o MTT por exemplo, mas outros relatórios indicam que a ligação do NTC com formazam é desprezível e não influencia nos resultados (FIRME; BANDARU, 2010; LANONE et al., 2013). Nesse sentido, diferentes medidas de viabilidade celular foram utilizadas. Os ensaios

in vitro que mediram a viabilidade celular por meio do ensaio MTT demonstraram que a interação SWCNT+STX diminuiu a viabilidade celular de HT-22, mas em contrapartida, não foram observadas diferenças significativas entre os tratamentos na viabilidade celular pelo método de exclusão por azul de tripan.

SWCNT pristino e carboxilado demonstraram um padrão claramente diferente de interação com a STX em relação à produção de espécies ativas de oxigênio. Enquanto que a interação SWCNT+STX induziu um efeito sinérgico, a interação SWCNT-COOH+STX induziu um efeito antagonista. Esses resultados estão relacionados com o possível efeito “Cavalo de Tróia” dos nanomateriais, que quando adsorvidos por xenobióticos para dentro da célula, podem induzir efeitos aditivos, sinérgicos ou antagônicos (AZEVEDO COSTA et al., 2012; BRITTO et al., 2015; CANESI; CIACCI; BALBI, 2015; FERREIRA et al., 2014).

A atividade mitocondrial requer a interação equilibrada entre muitas proteínas mitocondriais críticas no metabolismo aeróbico, incluindo a citocromo C, que é um componente chave da respiração mitocondrial no transporte de elétrons e no metabolismo celular. Além disso, desempenha um importante papel liberação de EAO (HANSEN; GO; JONES, 2006; LI et al., 2013). Os resultados de consumo de oxigênio demonstram que células HT-22 tratadas com STX consumiram oxigênio de maneira significativamente superior em ambos os tempos de exposição, e a interação de SWCNT (pristino e carboxilado) com STX foram eficientes em minimizar o efeito induzido pela toxina em forma isolada. De fato, a exposição por STXs pode alterar o metabolismo celular e o aumento do consumo de oxigênio pode estar envolvido

com a síntese de ATP, molécula requerida para induzir o sistema de defesa antioxidante, como por exemplo, síntese do antioxidante GSH e para o funcionamento da P-gp como visto posteriormente.

O segundo manuscrito, teve como objetivo verificar estratégias de quimioprevenção mediada pelo ácido lipóico frente à toxicidade induzida pelas STXs, demonstraram que nos resultados da simulação *ab initio* que a STX é capaz de interagir com o ácido lipóico por meio de fisisorção. Resultados semelhantes foram encontrados na interação entre STX e SWCNT pristino e carboxilado. A STX é caracterizada como uma molécula altamente polar e estável em solução, facilitando assim, sua interação físico-química com SWCNT pristino e carboxilado, que apresentam grande capacidade de adsorção, como também com o antioxidante ácido lipóico.

Os resultados de viabilidade celular e de concentração de EAO de maneira geral demonstram que uma concentração de 200 µg/L de STXs não é capaz por si só de induzir um efeito citotóxico na célula. Este resultado sugere que a linhagem hipocampal HT-22 pode apresentar uma quantidade inferior de canais iônicos dependentes de voltagem descritas em outros tipos de linhagem celulares (NICOLAS et al., 2015a, 2015b), e sendo assim, a toxina não consegue exercer seu mecanismo de ação. No entanto, não pode ser descartada a hipótese de que algum mecanismo poderia estar protegendo as células ou fazendo a extrusão da toxina, impedindo que a mesma exerça os efeitos tóxicos na linhagem hipocampal HT-22.

O antioxidante glutationa desempenha um papel crítico na defesa contra a geração de estresse oxidativo por xenobiótiocos, como as cianotoxinas (AMADO; MONSERRAT, 2010) mais notavelmente no sistema

nervoso central (VALDOVINOS-FLORES; GONSEBATT, 2012) e o par GSH (glutationa reduzida)/GSSG (glutationa oxidada) atua na manutenção do ambiente redox da célula (HELLOU; ROSS; MOON, 2012). Uma importante característica do AL é a capacidade de controlar a migração do fator transcripcional Nrf2 do citoplasma para o núcleo, ativando genes associados à defesa antioxidante. Devido seu potencial de redox, o DHLA é capaz de reduzir a GSSG a GSH, regenerando antioxidantes celulares (KORIYAMA et al., 2013; PILAR VALDECANTOS et al., 2015; ZHANG et al., 2010). Neste trabalho, os resultados mostram claramente que o AL induziu um aumento dos níveis de GSH após 24 horas de exposição. A síntese de GSH envolve o consumo de ATP, e consequentemente para a síntese de ATP é necessário maior consumo de oxigênio. De fato, foi observado nas células tratadas com AL, após 24 horas de exposição, um aumento do consumo de oxigênio. Este aumento parece estar claramente associado ao aumento dos níveis de GSH observados para AL. Sendo assim, O AL parece contribuir para a manutenção de um estado redox reduzido, já que níveis mais elevados de grupos sulfidrila de proteína observados em células HT-22 expostas com AL. De fato, alguns autores propõem que a proteína inibitória rica em grupos sulfidrila (Keap1) possa atuar como um sensor para alterar o estado redox da célula, libertando o fator de transcrição Nrf-2 quando os grupos sulfidrila se oxidam, formando ligações dissulfeto (HELLOU; ROSS; MOON, 2012; PAMPLONA; COSTANTINI, 2011b; PILAR VALDECANTOS et al., 2015) e que o AL é capaz de induzir a transcrição gênica de genes associados à atividade antioxidante (KORIYAMA et al., 2013; PILAR VALDECANTOS et al., 2015). Em geral, os resultados obtidos vão ao encontro da relação molecular esperada entre a

presença de antioxidantes como AL e a regulação de vários componentes antioxidantes endógenos através da via Keap1-Nrf2, que por sua vez contribuem como importante mecanismo de defesa contra radicais livres.

Uma hipótese é que o mecanismo responsável pela falta de efeitos tóxicos induzidos pelas STXs poderia estar relacionada com a presença da P-gp na linhagem HT-22. Não existe até o momento na literatura, trabalhos que demostrem a presença de P-gp e sua atividade na extrusão de xenobióticos na linhagem hipocampal HT-22. De fato, o ensaio de viabilidade celular por MTT utilizando o verapamil (VP), um potente bloqueador da P-gp associado ao ensaio de acumulação de rodamina 123 (Rho 123), demonstraram que a P-gp está presente na linhagem hipocampal HT-22, já que na presença do bloqueador VP, foi observado uma diminuição da viabilidade nas células expostas às STXs, demonstrando assim, que a STX atua, de fato, como um substrato para a P-gp. Além disso, pode ser constatado que a interação STX+AL minimiza os efeitos gerados pelas STXs.

O ensaio de acumulação de Rho 123 fornece uma importante informação acerca dos tempos de exposição. Foi verificado que após 30 minutos de exposição as células, HT-22 expostas aos diferentes tratamentos (STX, AL e STX+AL) apresentaram acúmulo de Rho 123 elevado, sugerindo que: (1) a P-gp pode estar com seu funcionamento alterado ou (2) P-gp está ocupada com outro substrato. De fato, no caso do tratamento com o ácido lipóico, a P-gp parece estar envolvida na extrusão do solvente DMSO utilizado para dissolver o ácido lipóico e, desta maneira, favorecer um maior acúmulo de Rho 123. Após 24 horas de exposição, houve uma diminuição do acúmulo de Rho 123 nos diferentes tratamentos (STX, AL e STX+AL), e um aumento da capacidade

de extrusão foi observado, sugerindo que: (1) STX, Al e STX+AL, estão ativandoo funcionamento da P-gp, ou (2) STX e Al podem estar induzindo o aumento expressão gênica da P-gp e sua consequente síntese.

É de consenso que a P-gp desempenha um importante papel fisiológico na proteção de órgãos susceptíveis como o cérebro (SILVA et al., 2015). Os resultados in vitro de viabilidade e de extrusão de Rho 123 demonstraram que as STXs modulam a atividade da P-gp na linhagem hipocampal HT-22. Por esse motivo, o *docking* molecular foi utilizado no nosso trabalho com o objetivo confirmar a hipótese de que a atenuação dos efeitos tóxicos das STXs na linhagem hipocampal HT-22, previamente demonstrados pelos ensaios *in vitro*. A estrutura da proteína P-gp de *Mus musculus* foi obtida a partir dos bancos de dados de proteína (PDB) identificada como 4KSB, além disso, a estrutura dos ligantes STX, Neo-STX, AL foram obtidos a partir do PubChen e a interação STX+AL, foi obtida a partir dos ensaios de simulação *ab initio*. Resultados mostraram que a P-gp consiste em duas metades pseudo-simétricas, cada uma contendo um domínio de ligação a nucleótidos (NBD) e um domínio transmembranar (TMD) (WARD et al., 2013). A maioria dos ligantes foi localizada na região de TMD. Foi observada energia de ligação livre (FEB) estimada para Rho123 (-9,1 Kcal / mol) e no seu local de interação com P-gp não foi observado nenhum outro ligante de interesse. A FEB para VP (-7,6 Kcal / mol) era diferente da de AL (-5,0 Kcal / mol), embora ambos interagissem com alguns resíduos iguais de P-gp, compartilhando um sítio de ligação semelhante. Os resultados sugerem que VP e AL interagem com resíduos semelhantes ocorrendo no mesmo ponto de fixação, mas apresentam efeitos funcionais distintos: o VP age bloqueando a bomba de P-gp enquanto que AL

induz atividade de P-gp. Este resultado está de acordo com os resultados observados nos experimentos *in vitro*, nas quais o AL promoveu eficientemente a extrusão de Rho 123. Estes resultados permitem propor diferentes locais de ligação (local H) e transporte (local R) para Rho, VP e AL. Possivelmente a Rho 123 interage com resíduos de aminoácidos no local R, enquanto que VP e AL se ligam ao local H. Por conseguinte, foi possível inferir que o AL pode agir como modulador da P-gp estabelecendo dois tipos de resposta: (1) a curto prazo: Induz a ativação de P-gp e facilitando a extrusão de Rho 123; (2) a longo prazo: Induz a expressão gênica de genes associados ao sistema de defesa antioxidante, aumentando a concentração de GSH, como foi observado nos ensaios após 24 horas de exposição. Ambos os tipos de respostas podem minimizar a toxicidade STX.

Os análogos STX e Neo-STX apresentam uma toxicidade variada devido a diferença de resíduos da cadeia lateral (RAMOS et al., 2014). A presença de hidrogênio presente no radical da STX e o radical hidroxila, presente do radical de Neo-STX modifica a afinidade da toxina e consequentemente a toxicidade (O'NEILL; MUSGRAVE; HUMPAGE, 2016). Dois locais de ligação diferentes para STX e Neo-STX foram observados nos ensaios de docking, indicando que STX e Neo-STX são substrato de P-gp, assim como as interações STX+AL. Os valores de FEB para STX (-6,1 Kcal / mol) estavam próximos de STX + LA_1 (-6,5 Kcal / mol), complexo mais estável de acordo com a simulação *ab initio*, e ambos interagiram com alguns resíduos iguais De P-gp (N838, L839, L858, G842 e V861). De fato, alguns dos efeitos comentados nos ensaios *in vitro* mostraram que o tratamento de interação STX + LA reduziu os efeitos deletérios causados apenas pela STX.

Provavelmente, a presença de radical hidroxil ou hidrogênio foi determinante para o local de ligação de posição na P-gp. Em contraste, observou-se o sítio de ligação da posição oposta para NeoSTX (FEB: -6,4 Kcal / mol) que estava próximo de STX + LA_2 e STX + LA_3 (FEB: -6,2 Kcal / mol) .2) e ambos interagiram com alguns resíduos iguais de P-gp (W132, K930, D882, A879, N179) partilhando um sítio de ligação semelhante. O acoplamento molecular sugere que a P-gp está presente na linhagem de células do hipocampo HT-22 e está envolvida no sistema de defesa contra xenobióticos. De fato, a STX atua como um substrato de P-gp e o AL pode desempenhar um papel como um modulador para a P-gp. A utilização de respostas biológicas associados à técnicas de modelagem computacional fornecem uma ampla gama de evidencias e interpretações. Em ambos os trabalhos foi possível demonstrar que os resultados obtidos *in vitro* corroboram a evidência semi-empírica encontrada utilizando-se a teoria funcional da densidade de simulação *ab initio* e acoplamento molecular.

5. CONCLUSÃO GERAL

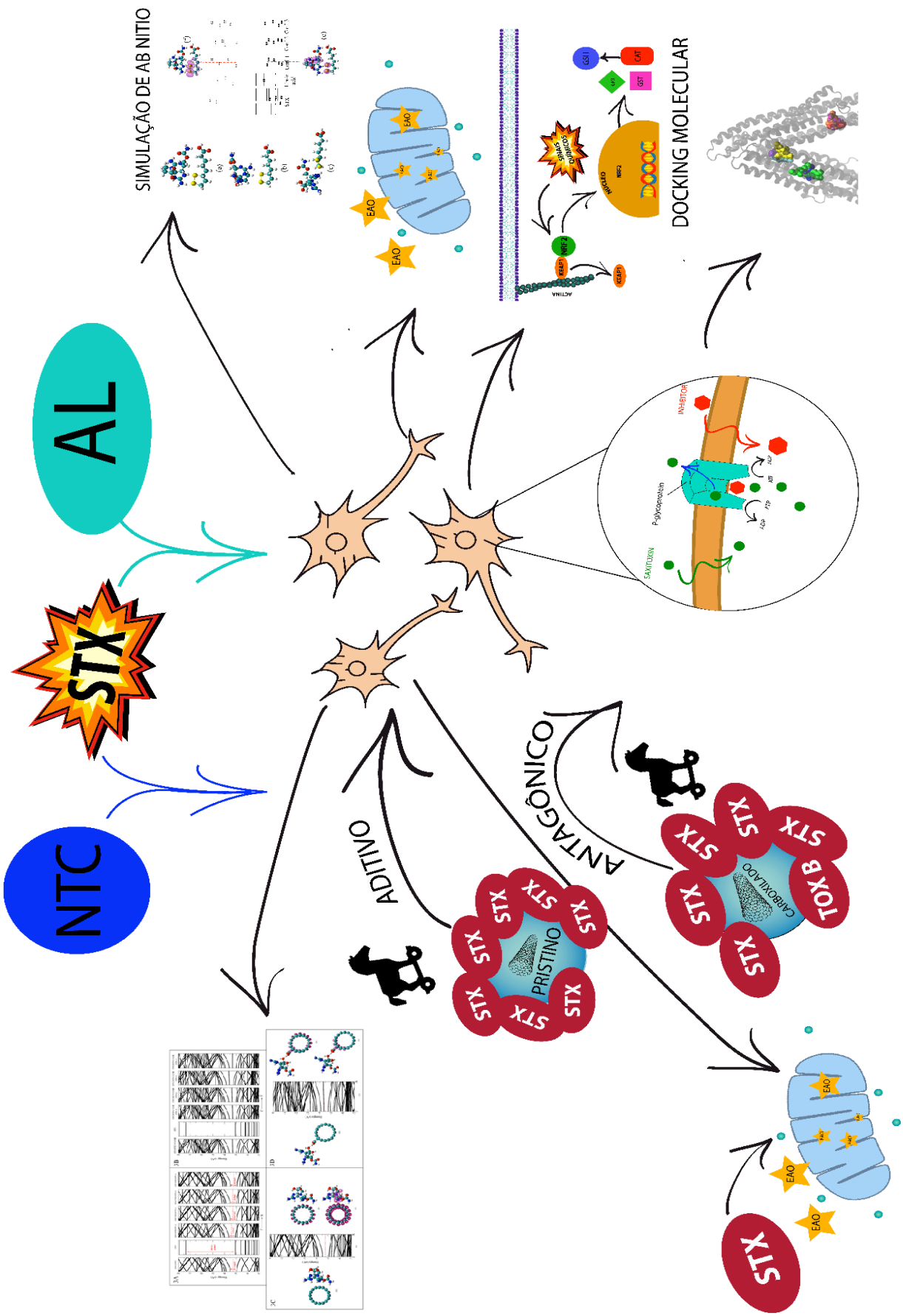

6. REFERÊNCIAS

AMADO, L. L. et al. Chemoprotection of lipoic acid against microcystin-induced toxicosis in common carp (Cyprinus carpio, Cyprinidae). **Comparative Biochemistry and Physiology Part C: Toxicology & Pharmacology**, v. 154, n. 3, p. 146–153, set. 2011.

AMADO, L. L.; MONSERRAT, J. M. Oxidative stress generation by microcystins in aquatic animals: Why and how. **Environment International**, v. 36, n. 2, p. 226–235, fev. 2010.

AMÉ, M. V. et al. Effects of microcystin–LR on the expression of P-glycoprotein in Jenynsia multidentata. **Chemosphere**, v. 74, n. 9, p. 1179–1186, mar. 2009.

APUL, O. G. et al. Adsorption of aromatic organic contaminants by graphene nanosheets: Comparison with carbon nanotubes and activated carbon. **Water Research**, v. 47, n. 4, p. 1648–1654, mar. 2013.

APUL, O. G.; KARANFIL, T. Adsorption of synthetic organic contaminants by carbon nanotubes: A critical review. **Water Research**, v. 68, p. 34–55, jan. 2015.

ARAOZ, R.; MOLGO, J.; MARSAC, N. T. DE. Toxicon Neurotoxic cyanobacterial toxins. **Toxicon**, v. 56, p. 813–828, 2010.

ARÁOZ, R.; MOLGÓ, J.; TANDEAU DE MARSAC, N. Neurotoxic cyanobacterial toxins. **Toxicon**, v. 56, n. 5, p. 813–828, out. 2010.

ASTIZ, M.; DE ALANIZ, M. J. T.; MARRA, C. A. The oxidative damage and inflammation caused by pesticides are reverted by lipoic acid in rat brain. **Neurochemistry International**, v. 61, n. 7, p. 1231–1241, dez. 2012.

AZEVEDO COSTA, C. L. et al. In vitro evaluation of co-exposure of arsenium and an organic nanomaterial (fullerene, C60) in zebrafish hepatocytes. **Comparative Biochemistry and Physiology Part C: Toxicology & Pharmacology**, v. 155, n. 2, p. 206–212, mar. 2012.

BATTIGELLI, A. et al. Endowing carbon nanotubes with biological and biomedical properties by chemical modifications. **Advanced Drug Delivery Reviews**, v. 65, n. 15, p. 1899–1920, dez. 2013.

BELYANSKAYA, L. et al. Effects of carbon nanotubes on primary neurons and glial cells. **NeuroToxicology**, v. 30, n. 4, p. 702–711, jul. 2009.

BRITTO, R. S. et al. Interaction of Carbon Nanomaterial Fullerene (C60) and

Microcystin-LR in Gills of Fish Cyprinus carpio (Teleostei: Cyprinidae) Under the Incidence of Ultraviolet Radiation. **Water, Air, & Soil Pollution**, v. 226, n. 1, p. 2215, 11 jan. 2015.

CANESI, L.; CIACCI, C.; BALBI, T. Interactive effects of nanoparticles with other contaminants in aquatic organisms: Friend or foe? **Marine Environmental Research**, v. 111, p. 128–134, out. 2015.

CERVANTES CIANCA, R. C. et al. Alterations of 3,4-dihydroxyphenylethylamine and its metabolite 3,4-dihydroxyphenylacetic produced in rat brain tissues after systemic administration of saxitoxin. **Neurochemistry International**, v. 59, n. 5, p. 643–647, out. 2011.

CHAO, T.-I. et al. Carbon nanotubes promote neuron differentiation from human embryonic stem cells. **Biochemical and Biophysical Research Communications**, v. 384, n. 4, p. 426–430, jul. 2009.

CHATZIEFTHIMIOU, A. D. et al. Cyanobacteria and cyanotoxins are present in drinking water impoundments and groundwater wells in desert environments. **Toxicon**, v. 114, p. 75–84, maio 2016.

CHENG, W.-W. et al. Single-walled carbon nanotube induction of rat aortic endothelial cell apoptosis: Reactive oxygen species are involved in the mitochondrial pathway. **The International Journal of Biochemistry & Cell Biology**, v. 43, n. 4, p. 564–572, abr. 2011.

CLEMENTE, Z. et al. Analyses of paralytic shellfish toxins and biomarkers in a southern Brazilian reservoir. **Toxicon**, v. 55, n. 2–3, p. 396–406, fev. 2010.

CORBEL, S.; MOUGIN, C.; BOUAÏCHA, N. Cyanobacterial toxins: Modes of actions, fate in aquatic and soil ecosystems, phytotoxicity and bioaccumulation in agricultural crops. **Chemosphere**, v. 96, p. 1–15, fev. 2014.

COSTA, P. M. et al. Functionalized carbon nanotubes: From intracellular uptake and cell-related toxicity to systemic brain delivery. **Journal of Controlled Release**, v. 241, p. 200–219, 2016.

COSTA, P. R. et al. Biotransformation modulation and genotoxicity in white seabream upon exposure to paralytic shellfish toxins produced by Gymnodinium catenatum. **Aquatic Toxicology**, v. 106–107, p. 42–47, jan. 2012.

D‘MELLO, F. et al. Cytotoxic Effects of Environmental Toxins on Human Glial Cells. **Neurotoxicity Research**, v. 31, n. 2, p. 245–258, fev. 2017.

DA SILVA, C. A. et al. First report about saxitoxins in freshwater fish Hoplias malabaricus through trophic exposure. **Toxicon**, v. 57, n. 1, p. 141–147, jan. 2011.

DEGORTER, M. K. et al. Drug transporters in drug efficacy and toxicity. **Annual Review of Pharmacology and Toxicoloy**, v. 52, p. 249–273, 2012.

DIEHL, F. et al. Behavioral alterations induced by repeated saxitoxin exposure in drinking water. **Journal of Venomous Animals and Toxins including Tropical Diseases**, v. 22, n. 1, p. 18, 17 dez. 2016.

DÖRSAM, B.; FAHRER, J. The disulfide compound α-lipoic acid and its derivatives: A novel class of anticancer agents targeting mitochondria. **Cancer Letters**, v. 371, n. 1, p. 12–19, fev. 2016.

EMA, M.; GAMO, M.; HONDA, K. A review of toxicity studies of single-walled carbon nanotubes in laboratory animals. **Regulatory Toxicology and Pharmacology**, v. 74, p. 42–63, fev. 2016.

ESTRADA, N. et al. Effects of the toxic dinoflagellate, Gymnodinium catenatum on hydrolytic and antioxidant enzymes, in tissues of the giant lions-paw scallop Nodipecten subnodosus. **Comparative Biochemistry and Physiology Part C: Toxicology & Pharmacology**, v. 146, n. 4, p. 502–510, nov. 2007.

ETHERIDGE, S. M. Paralytic shellfish poisoning: Seafood safety and human health perspectives. **Toxicon**, v. 56, n. 2, p. 108–122, ago. 2010.

FERRÃO-FILHO, A. D. S.; KOZLOWSKY-SUZUKI, B. Cyanotoxins: Bioaccumulation and Effects on Aquatic Animals. **Marine Drugs**, v. 9, n. 12, p. 2729–2772, 16 dez. 2011.

FERREIRA, J. L. R. et al. Co-exposure of the organic nanomaterial fullerene C60 with benzo[a]pyrene in Danio rerio (zebrafish) hepatocytes: Evidence of toxicological interactions. **Aquatic Toxicology**, v. 147, p. 76–83, fev. 2014.

FIRME, C. P.; BANDARU, P. R. Toxicity issues in the application of carbon nanotubes to biological systems. **Nanomedicine: Nanotechnology, Biology and Medicine**, v. 6, n. 2, p. 245–256, abr. 2010.

GALANO, A. Influence of Diameter, Length, and Chirality of Single-Walled Carbon Nanotubes on Their Free Radical Scavenging Capability. **The Journal of Physical Chemistry C**, v. 113, n. 43, p. 18487–18491, 29 out. 2009.

GLADE, M. J. Oxidative stress and cognitive longevity. **Nutrition**, v. 26, n. 6, p. 595–603, jun. 2010.

GOLUBIC, S. et al. Marine toxic cyanobacteria: Diversity, environmental responses and hazards. **Toxicon**, v. 56, n. 5, p. 836–841, out. 2010.

GORĄCA, A. et al. Lipoic acid – biological activity and therapeutic potential. **Pharmacological Reports**, v. 63, n. 4, p. 849–858, jul. 2011.

GRATTAN, L. M.; HOLOBAUGH, S.; MORRIS, J. G. Harmful algal blooms and public health. **Harmful Algae**, v. 57, p. 2–8, jul. 2016.

GRUBER, J. et al. Mitochondria-targeted antioxidants and metabolic modulators as pharmacological interventions to slow ageing. **Biotechnology Advances**, v. 31, n. 5, p. 563–592, set. 2013.

HAN, Y.; CHIN TAN, T. M.; LIM, L.-Y. In vitro and in vivo evaluation of the effects of piperine on P-gp function and expression. **Toxicology and Applied Pharmacology**, v. 230, n. 3, p. 283–289, 1 ago. 2008.

HANSEN, J. M.; GO, Y.; JONES, D. P. NUCLEAR AND MITOCHONDRIAL COMPARTMENTATION OF OXIDATIVE STRESS AND REDOX SIGNALING. **Annual Review of Pharmacology and Toxicology**, v. 46, n. 1, p. 215–234, fev. 2006.

HAO, J.-H. et al. An ab initio study of the size-dependent mechanical behavior of single-walled AlN nanotubes. **Solid State Sciences**, v. 45, p. 30–34, 2015.

HELLOU, J.; ROSS, N. W.; MOON, T. W. Glutathione, glutathione S-transferase, and glutathione conjugates, complementary markers of oxidative stress in aquatic biota. **Environmental Science and Pollution Research**, v. 19, n. 6, p. 2007–2023, 2012.

HILLER, S. et al. Alpha-lipoic acid supplementation protects enzymes from damage by nitrosative and oxidative stress. **Biochimica et Biophysica Acta (BBA) - General Subjects**, v. 1860, n. 1, p. 36–45, jan. 2016.

HONG, H.; LAM, P. K. .; HSIEH, D. P. . Interactions of paralytic shellfish toxins with xenobiotic-metabolizing and antioxidant enzymes in rodents. **Toxicon**, v. 42, n. 4, p. 425–431, set. 2003.

HU, X. et al. In vitro evaluation of cytotoxicity of engineered carbon nanotubes in selected human cell lines. **Science of The Total Environment**, v. 408, n. 8, p. 1812–1817, mar. 2010.

HUANG, L. et al. P-glycoprotein and its inducible expression in three bivalve species after exposure to Prorocentrum lima. **Aquatic Toxicology**, v. 169, p. 123–132, dez. 2015.

JAVADIAN, S. et al. Phase transition study of confined water molecules inside carbon nanotubes: Hierarchical multiscale method from molecular dynamics simulation to ab initio calculation. **Journal of Molecular Graphics and Modelling**, v. 38, p. 40–49, 2012.

JONES, D. P. Disruption of mitochondrial redox circuitry in oxidative stress. **Chemico-Biological Interactions**, v. 163, n. 1–2, p. 38–53, out. 2006.

KAFA, H. et al. The interaction of carbon nanotubes with an in vitro blood-brain barrier model and mouse brain in vivo. **Biomaterials**, v. 53, p. 437–452, jun. 2015.

KAISER, J.-P.; BUERKI-THURNHERR, T.; WICK, P. Influence of single walled carbon nanotubes at subtoxical concentrations on cell adhesion and other cell parameters of human epithelial cells. **Journal of King Saud University - Science**, v. 25, n. 1, p. 15–27, jan. 2013.

KESHARWANI, P.; MISHRA, V.; JAIN, N. K. Validating the anticancer potential of carbon nanotube-based therapeutics through cell line testing. **Drug Discovery Today**, v. 20, n. 9, p. 1049–1060, set. 2015.

KORIYAMA, Y. et al. Protective effect of lipoic acid against oxidative stress is mediated by Keap1/Nrf2-dependent heme oxygenase-1 induction in the RGC-5 cellline. **Brain Research**, v. 1499, p. 145–157, mar. 2013.

KUO, Y.-T. et al. Alpha-lipoic acid induces adipose triglyceride lipase expression and decreases intracellular lipid accumulation in HepG2 cells. **European Journal of Pharmacology**, v. 692, n. 1–3, p. 10–18, out. 2012.

KÜTTER, M. T. et al. Effects of dietary α-lipoic acid on growth, body composition and antioxidant status in the Plata pompano Trachinotus marginatus (Pisces, Carangidae). **Aquaculture**, v. 368–369, p. 29–35, nov. 2012.

KÜTTER, M. T. et al. Antioxidant and toxicological effects elicited by alpha-lipoic acid in aquatic organisms. **Comparative Biochemistry and Physiology Part C: Toxicology & Pharmacology**, v. 162, n. 1, p. 70–76, maio 2014.

LACHER, S. E. et al. P-Glycoprotein Transport of Neurotoxic Pesticides. **Journal of Pharmacology and Experimental Therapeutics**, v. 355, n. 1, p. 99–107, 1 set. 2015.

LANONE, S. et al. Determinants of carbon nanotube toxicity. **Advanced Drug Delivery Reviews**, v. 65, n. 15, p. 2063–2069, dez. 2013.

LAWAL, A. T. Synthesis and utilization of carbon nanotubes for fabrication of

electrochemical biosensors. **Materials Research Bulletin**, v. 73, p. 308–350, jan. 2016.

LI, J.; JAIMES, K. F.; ALLER, S. G. Refined structures of mouse P-glycoprotein. **Protein Science**, v. 23, n. 1, p. 34–46, 2014.

LI, X. et al. Transcription alterations of microRNAs, cytochrome P4501A1 and 3A65, and AhR and PXR in the liver of zebrafish exposed to crude microcystins. **Toxicon**, v. 73, p. 17–22, out. 2013.

LONGARAY-GARCIA, M. et al. Modulation of antioxidant and detoxifying capacity in fish Cyprinus carpio (Cyprinidae) after treatment with nanocapsules containing lipoic acid. **Comparative Biochemistry and Physiology Part A: Molecular & Integrative Physiology**, v. 165, n. 4, p. 468–475, ago. 2013.

MELEGARI, S. P. et al. Induction to oxidative stress by saxitoxin investigated through lipid peroxidation in Neuro 2A cells and Chlamydomonas reinhardtii alga. **Chemosphere**, v. 89, n. 1, p. 38–43, set. 2012.

MONSERRAT, J. M. et al. Modulation of antioxidant and detoxification responses mediated by lipoic acid in the fish Corydoras paleatus (Callychthyidae). **Comparative Biochemistry and Physiology Part C: Toxicology & Pharmacology**, v. 148, n. 3, p. 287–292, set. 2008.

MUKAIGASA, K. et al. Genetic Evidence of an Evolutionarily Conserved Role for Nrf2 in the Protection against Oxidative Stress. **Molecular and Cellular Biology**, v. 32, n. 21, p. 4455–4461, 1 nov. 2012.

NICOLAS, J. et al. In vitro detection of cardiotoxins or neurotoxins affecting ion channels or pumps using beating cardiomyocytes as alternative for animal testing. **Toxicology in Vitro**, v. 29, n. 2, p. 281–288, mar. 2015a.

NICOLAS, J. et al. Exploration of new functional endpoints in neuro-2a cells for the detection of the marine biotoxins saxitoxin, palytoxin and tetrodotoxin. **Toxicology in Vitro**, v. 30, n. 1, p. 341–347, dez. 2015b.

O'NEILL, K.; MUSGRAVE, I. F.; HUMPAGE, A. Low dose extended exposure to saxitoxin and its potential neurodevelopmental effects: A review. **Environmental Toxicology and Pharmacology**, v. 48, p. 7–16, 2016a.

ONDRUS, A. E. et al. Article Fluorescent Saxitoxins for Live Cell Imaging of Single Voltage-Gated Sodium Ion Channels beyond the Optical Diffraction Limit. **Chemistry & Biology**, v. 19, p. 902–912, 2012a.

ONDRUS, A. E. et al. Fluorescent Saxitoxins for Live Cell Imaging of Single

Voltage-Gated Sodium Ion Channels beyond the Optical Diffraction Limit. **Chemistry & Biology**, v. 19, n. 7, p. 902–912, jul. 2012b.

PAMPLONA, R.; COSTANTINI, D. oxidative stress in animals Molecular and structural antioxidant defenses against Molecular and structural antioxidant defenses against oxidative stress in animals. **Am J Physiol Regul Integr Comp Physiol American Journal of Physiology -Regulatory, Integrative and Comparative Physiology**, v. 301, n. July, p. 843–863, 2011a.

PAMPLONA, R.; COSTANTINI, D. Molecular and structural antioxidant defenses against oxidative stress in animals. **AJP: Regulatory, Integrative and Comparative Physiology**, v. 301, n. 4, p. R843–R863, 1 out. 2011b.

PAVAGADHI, S. et al. Removal of microcystin-LR and microcystin-RR by graphene oxide: Adsorption and kinetic experiments. **Water Research**, v. 47, n. 13, p. 4621–4629, set. 2013.

PEARSON, L. A. et al. The genetics, biosynthesis and regulation of toxic specialized metabolites of cyanobacteria. **Harmful Algae**, v. 54, p. 98–111, abr. 2016.

PI, J. et al. ROS signaling, oxidative stress and Nrf2 in pancreatic beta-cell function. **Toxicology and Applied Pharmacology**, v. 244, n. 1, p. 77–83, abr. 2010.

PICHARDO, S. et al. Oxidative stress responses to carboxylic acid functionalized single wall carbon nanotubes on the human intestinal cell line Caco-2. **Toxicology in Vitro**, v. 26, n. 5, p. 672–677, ago. 2012.

PILAR VALDECANTOS, M. et al. Essential role of Nrf2 in the protective effect of lipoic acid against lipoapoptosis in hepatocytes. **Free Radical Biology and Medicine**, v. 84, p. 263–278, jul. 2015.

QU, R. et al. Metal accumulation and antioxidant defenses in the freshwater fish Carassius auratus in response to single and combined exposure to cadmium and hydroxylated multi-walled carbon nanotubes. **Journal of Hazardous Materials**, v. 275, p. 89–98, jun. 2014.

RAMOS, P. B. et al. Oxidative stress in rats induced by consumption of saxitoxin contaminated drink water. **Harmful Algae**, v. 37, n. 2914, p. 68–74, jul. 2014.

REDDY, A. R. N. et al. Evaluation of oxidative stress and anti-oxidant status in rat serum following exposure of carbon nanotubes. **Regulatory Toxicology and Pharmacology**, v. 59, n. 2, p. 251–257, mar. 2011.

ROLDO, M.; FATOUROS, D. G. Biomedical applications of carbon nanotubes.

Annual Reports Section "C" (Physical Chemistry), v. 109, p. 10, 2013.

SAYES, C. M. et al. Functionalization density dependence of single-walled carbon nanotubes cytotoxicity in vitro. **Toxicology Letters**, v. 161, n. 2, p. 135–142, fev. 2006.

SHAY, K.; MOREAU, R.; SMITH, E. Alpha-lipoic acid as a dietary supplement: molecular mechanisms and therapeutic potential. **Biochimica et Biophysica …**, v. 1790, n. 10, p. 1149–1160, 2009.

SILVA, R. et al. Modulation of P-glycoprotein efflux pump: induction and activation as a therapeutic strategy. **Pharmacology & Therapeutics**, v. 149, p. 1–123, maio 2015.

SILVA, C. A. DA et al. Saxitoxins induce cytotoxicity, genotoxicity and oxidative stress in teleost neurons in vitro. **Toxicon**, v. 86, p. 8–15, ago. 2014.

SONG, M. et al. Study of cytotoxic effects of single-walled carbon nanotubes functionalized with different chemical groups on human MCF7 cells. **Chemosphere**, v. 92, n. 5, p. 576–582, jul. 2013.

TAKSER, L. et al. Cyanotoxins at low doses induce apoptosis and inflammatory effects in murine brain cells: Potential implications for neurodegenerative diseases. **Toxicology Reports**, v. 3, p. 180–189, 2016.

TAN, M. et al. Downregulation of Nrf2/HO-1 pathway and activation of JNK/c-Jun pathway are involved in homocysteic acid-induced cytotoxicity in HT-22 cells. **Toxicology Letters**, v. 223, n. 1, p. 1–8, out. 2013.

VALDOVINOS-FLORES, C.; GONSEBATT, M. E. The role of amino acid transporters in GSH synthesis in the blood–brain barrier and central nervous system. **Neurochemistry International**, v. 61, n. 3, p. 405–414, ago. 2012.

WANG, J. et al. Cytotoxicity of single-walled carbon nanotubes on PC12 cells. **Toxicology in Vitro**, v. 25, n. 1, p. 242–250, fev. 2011.

WANG, P.-J. et al. A review of the global ecology, genomics, and biogeography of the toxic cyanobacterium, Microcystis spp. **Harmful Algae**, v. 54, n. 1, p. 836–844, fev. 2016.

WANG, Q. et al. A novel and functional assay for pharmacological effects of marine toxins, saxitoxin and tetrodotoxin by cardiomyocyte-based impedance biosensor. **Sensors and Actuators B: Chemical**, v. 209, p. 828–837, mar. 2015.

WARD, A. B. et al. Structures of P-glycoprotein reveal its conformational flexibility

and an epitope on the nucleotide-binding domain. **Proceedings of the National Academy of Sciences**, v. 110, n. 33, p. 13386–91, 2013.

WEI, W. et al. Alpha lipoic acid inhibits neural apoptosis via a mitochondrial pathway in rats following traumatic brain injury. **Neurochemistry International**, v. 87, p. 85–91, ago. 2015.

WIESE, M. et al. Neurotoxic Alkaloids: Saxitoxin and Its Analogs. **Marine Drugs**, v. 8, n. 7, p. 2185–2211, 20 jul. 2010.

WOOD, R. Acute animal and human poisonings from cyanotoxin exposure - A review of the literature. **Environment International**, v. 91, p. 276–282, 2016.

ZABAGLO, K. et al. Environmental roles and biological activity of domoic acid: A review. **Algal Research**, v. 13, p. 94–101, jan. 2016.

ZHANG, D. et al. Zebrafish neurotoxicity from aphantoxins-cyanobacterial paralytic shellfish poisons (PSPs) from Aphanizomenon flos-aquae DC-1. **Environmental Toxicology**, v. 28, n. 5, p. 239–254, maio 2013.

ZHANG, Q. et al. A systems biology perspective on Nrf2-mediated antioxidant response. **Toxicology and Applied Pharmacology**, v. 244, n. 1, p. 84–97, abr. 2010.

ZHENG, X. et al. A saxitoxin-binding aptamer with higher affinity and inhibitory activity optimized by rational site-directed mutagenesis and truncation. **Toxicon**, v. 101, n. May, p. 41–47, jul. 2015.